Title
Facilitation of motor and bladder function after spinal cord injury via epidural stimulation and pharmacology

Author
Gad, Parag

Publication Date
2013

Peer reviewed|Thesis/dissertation

UNIVERSITY OF CALIFORNIA

Los Angeles

Facilitation of motor and bladder function

after spinal cord injury via epidural stimulation and

pharmacology

A dissertation submitted in partial satisfaction of the requirements for the degree Doctor of Philosophy in Biomedical Engineering

by

Parag Gad

2013

ABSTRACT OF THE DISSERTATION

Facilitation of motor and bladder function

after spinal cord injury via epidural stimulation and

pharmacology

by

Parag Gad

Doctor of Philosophy in Biomedical Engineering

University of California, Los Angeles

Professor V. Reggie Edgerton, Chair

A complete spinal cord transection results in loss of all supraspinal motor and bladder control below the level of the injury. The neural circuitry in the lumbosacral spinal cord, however, can generate locomotor patterns in the hindlimbs of rats and cats with the aid of motor training, epidural stimulation and/or administration of monoaminergic agonists. Gerasimenko et al., (2003) first reported the use of electrical stimulation to facilitate locomotion in chronic decerebrated cats. Ichiyama et al (2005) then demonstrated that epidural electrical stimulation of the spinal cord can induce rhythmic, alternating hindlimb locomotor activity in chronic spinal rats. Stimulation at the L2 spinal segment at frequencies between 30 and 50 Hz consistently produced successful bilateral stepping. Similar epidural stimulation at other spinal segments

were less effective, e.g., epidural stimulation at the T13 or L1 evoked rhythmic activity in only one leg and stimulation at the L3, L4, or L5 produced mainly flexion movements.

More recently, completely paralyzed (motor complete, sensory incomplete) human subjects were implanted with a commercially available spinal cord electrode array and stimulation package originally designed for pain suppression (Harkema et al., 2011). Stimulation of specific spinal segments (caudal electrodes, ~ S1 spinal level) in combination with the sensory information from the lower limbs and weeks of stand training was sufficient to generate full weight-bearing standing. These subjects also recovered some voluntary control of movements of the toe, ankle, and the entire lower limb, but only when epidural stimulation was present. Thus it appears that the epidural stimulation provided excitation of lumbosacral interneurons and motoneurons that, when combined with the weak excitatory activity of descending axons that were not otherwise detectable, achieved a level of excitation that was sufficient to activate the spinal motor circuits. These results demonstrate that some patients clinically diagnosed as having complete paralysis can use proprioceptive input combined with some synaptic input from descending motor signals, perhaps residual but functionally silent without epidural stimulation to the spinal motor circuits to generate and control a range of motor functions during epidural stimulation.

The mechanisms of pharmacological and/or epidural electrical stimulation that enable motor control (eEmc) in the spinal circuitry for locomotion are still not clearly understood. During standing, a single bipolar epidural stimulus between L2 and S1 produces three types of evoked responses, i.e., early (ER, latency 1-3 ms), middle (MR, latency 4-6 ms), and late (LRs, latency >7 ms) in the hindlimb muscles in both intact (Gerasimenko et al., 2006) and spinal (Lavrov et al., 2006) rats. Similar responses were observed during rhythmic locomotor-like EMG

activity in the hindlimb muscles of spinal rats while stepping on a motorized treadmill in the presence of epidural stimulation (40 Hz) between L2 and S1 (Lavrov et al., 2008). In addition, the time course of the re-emergence of the LRs was similar to that for the recovery of stepping after a complete spinal cord injury (SCI), indicating that LRs are a potential biomarker of functional recovery (Lavrov et al., 2006).

The results demonstrate that spinal rats can stand and step when the spinal cord is stimulated (tonic 40 Hz stimulation) by electrodes located at specific sites on the spinal cord and at specific frequencies of stimulation. The quality of stepping and standing was dependent on the location of the electrodes on the spinal cord, the specific stimulation parameters, and the orientation of the cathode and anode. spinal cord stimulation triggered evoked potentials in flexor and extensors muscles form a 'foot print' of the physiological state of the spinal cord. Chronic subthreshold stimulation enabled greater activity in completely transected rats but only with stimulation. Spinal cord stimulation at specific frequencies resulted in partial bladder control.

The dissertation of Parag Gad is approved.

Carol Newton

Vijay Gupta

Dejan Markovic

V Reggie Edgerton, Committee Chair

University of California, Los Angeles

2013

I would like to dedicate this thesis to: the SoCal Loulies; My parents, sister and Kshitij for allowing me the freedom to do whatever I wanted to and for supporting me in every insane plan. I promise you, this is just the start. To my home country India, mitti ki hain jo khusbu, woh kaise bhulayega... Tu chahe kahin jaye, Tu lautke aayega….

TABLE OF CONTENTS

LIST OF FIGURES

LIST OF TABLES

ACKNOWLEDGEMENTS

First and foremost, I would like to thank my family. It is their continual support and encouragement that have cultivated a life-long passion for learning in me. Even as a little child, they have never turned me away from a "why" question. In addition, they are always encouraged me in every crazy, insane project I opted for.

I would also like to recognize the efforts and contributions of the SoCal Loulies. They were responsible to provide me a home away from home. Vaidehi and Kartiki refer a special mention, they are my guardian angels.

I like to thank my advisor V. Reggie Edgerton. His advice and encouragement has been an invaluable asset throughout my graduate work. It is his innovative thinking and freedom to experiment that have made my research such a success.

I am especially grateful for the generous comments and collaborations from Dr. Roland Roy, Dr. Hui Zhong, Dr Yury Gerasimenko on this work. This thesis incorporates so many disciplines, it would have been nearly impossible without their expertise and facilitation. I have also benefited from the advice, teaching, collaboration and companionship of a host of memorable individuals associated with my academic career and personal life, including but not limited to Dr. Igor Lavrov, Dr. Prithvi Shah, Dr. Guillermo Garcia-Alias, Jaehoon Choe, Mrinal Rath, Maynor Herrera, Sharon Zdunowski,

I would also want to recognize an incredible team of undergraduate students, Chris Wu, Alan Bui, Sarah Kim, Jack Creagmile, Abby Imboden for all of their hard works.

Lastly, and most importantly, the author will like to thank the funding sources including the National Institute of Biomedical Imaging and Bioengineering (NIBIB) R01EB007615, the National Institute of Health (NIH) R01NS062009, Christopher and Dana Reeve Foundation, the Walkabout Foundation.

VITA

August 2nd, 1986 Born in Hubli, Karnataka, India

2008 B.E., Biomedical Engineering

D.J. Sanghvi College of Engineering

Mumbai University, India

2010 M.S. Biomedical Engineering

University of California, Los Angeles

Los Angeles, California

PUBLICATIONS AND PRESENTATIONS

1) Further Development of a High-Density Multi-Electrode Array to Facilitate Stepping and Assess Spinal Cord Function After a Spinal Cord Injury. SFN 2009 (Chicago)
2) Development of an Electronic Bridge over the Lesion between Fore and Hind-limbs to Facilitate Quadrupedal Stepping after a Complete Spinal Cord Transection. SFN 2010 (San Diego)
3) Electronic bridge: using hindlimb EMG signals to modulate the parameters of forelimb EMG triggered epidural stimulation to improve stepping in spinal rats. SFN 2011 (Washington DC)
4) Modulation of EMG components during stepping with epidural stimulation in different sensory and pharmacological conditions. SFN 2011 (Washington DC)
5) Changes in motor recruitment ability after partial and complete spinal cord injury detected by a chronically implanted flexible multielectrode array. SFN 2012 (New Orleans)
6) Development of a multi-electrode array for spinal cord epidural stimulation to facilitate stepping and standing after a complete spinal cord injury in adult rats. SFN 2012 (New Orleans)

7) Enhanced spontaneous cage activity induced by continuous low intensity spinal cord epidural stimulation in complete spinal cord transected rats. Experiment Biology 2013 (Boston)
8) Device Helps Paralyzed Rats Walk Again. Technology Review magazine by MIT. Friday December 3rd 2010.
9) Using forelimbs EMG to Control an Electronic spinal bridge to facilitate hindlimb stepping after a complete spinal cord lesion. Frontiers in Biomedical devices, Conference and exhibition. Irvine, CA, USA. Sep 2011. (Biomed 2011)
10) Forelimb EMG-based trigger to control an electronic spinal bridge to enable hindlimb stepping after a complete spinal cord lesion in rats (Journal of NeuroEngineering and Rehab, June 2012)
11) Development of a multi-electrode array or spinal cord epidural stimulation to facilitate stepping and standing after a complete spinal cord injury in adult rats. (Journal of NeuroEngineering and Rehab, Jan 2013, Special edition)

Chapter 1

Prologue

Motivation

"The *frog instantly dies when the spinal cord is pierced; and previous to this it lived without head, without heart or any bowels or intestines or skin; and here therefore it would seem lies the foundation of movement and life."* – Leonardo da Vinci.

Ancient Hindu religious literature (circa 3500-1800 BC) describes the treatment of spinal deformity rather clearly. The story is told of a woman who was "deformed in three places" and how lord Krishna straightened her back. This was accomplished by pressing down on her feet and pulling up on her chin. The orthepedic trappings of the story are unmistakable, including excellent immediate post treatment results and no long term follow-up.

Spinal cord injury (SCI) is one of the most traumatic conditions a person will have to live through, affecting every aspect of daily life, resulting in an enormous impact from psychological and social perspective (Bedbrook 1987). Spinal cord injury has an enormous economical impact as well. As of 2005, it is estimated that a person with a paraplegic spinal cord injury person will need to spend anything from $250,000 to $750,000 during the initial year of injury and more than $25,000 each subsequent year (SCIIN 2005). The estimate is even higher for tetraplegia patients.

Currently, there are between 250,000 and 400,000 Americans suffering from spinal cord injury and an additional 11,000 Americans are struck with spinal cord injury each year (NSCIA 2006). Many of these injuries are caused by accidents such as motor vehicle accidents, falls and sport injuries. As such, the demographic group most likely to suffer a spinal cord injury is men

(~80%) between 16 and 30 years old (NSCIA 2006). 36% of those who reported being paralyzed said they had "a lot of difficulty" in moving; 29% said "some difficulty"; 17% said "a little difficulty"; and 16% said they were "completely unable to move." Therefore, depending on the intensity of the injury, many of these people have to live with disability, and most likely paralysis, for the greater part of their adult life. Thus, any research that can improve their mobility and motor functions will not only greatly improve their quality of life, it will have significant impacts on the general population as a whole.

Geography is now history

The 21st century belongs to interdisciplinary fields, one of them being biomedical engineering. As the name suggests, it is an interdisciplinary field that combines biology, medicine and engineering. The synergy generated between biological sciences, medicine and engineering has resulted in developments and improvements in technologies in different areas of biomedical engineering. An area not explored to its full extent is the application of biomedical engineering techniques in understanding the finer aspects of the physiology and improvements in motor functions after a spinal cord injury and paralysis. Our objective is to develop techniques to improve locomotor function, standing and stepping as well as to gain partial volitional control after a spinal cord injury.

Objective

This thesis is a compilation of over four years of work with contributions from multiple people. Individually, this represents the maturity and clarity in thoughts that I possess and marks my coming of age. Ideas taking the shape of reality and failures acting as a motivation have been constant companions on this journey. As I write this part of my thesis, I am having a

conversation with myself and my partner in crime, Kartiki Naik. My existence in this world seems a reality now. John Rambo words echo through me, “this is what we do, this is who we are…live for nothing, die for something”, but at the business end of my academic career the feeling of individuality and personal demands seem to take greater importance than ever imagined. An attitude that has governed my life which all my peers, subordinates and bosses would subscribe to comes from the movie Armageddon. Truman tells Stamper said “…It wasn’t so much about the paper work or politics…it was all about getting the job done… ” 8 years since I first saw Armageddon but the words still drive me to perform with a 100% commitment every single day.

Thesis overview

This thesis is comprised of peer-reviewed articles from archival journals in biological science and engineering. The author is either the lead author of these articles. The organization of this thesis is meant to highlight the interdisciplinary nature of the topics at hand while providing a clear emphasis on the discipline-specific contributions of this work.

Chapter 2 will give an indepth review of spinal cord plasticity and neural control of locomotion post spinal cord injury (SCI), which is critical in understanding the significance of this thesis work. This review brings together perspectives from various disciplines to emphasize the importance of variability in neural plasticity even at the spinal cord level which is most often ignored compared to the more significant brain.

Chapter 3 will give a better understanding on the evoked potentials present select hindlimb muscles during locomotion after spinal cord injury in adult rats under the influence of spinal cord epidural stimulation. The data demonstrate, in a invivo preparation using an adult unanesthetized rat that there are unique patterns of evoked potentials having a range of delay

times relative to the stimulation pulses and predictable changes in the persistence of post-stimulation responses that seem to play a role in defining the kinematics of the stance and swing phases of the step cycle. Together these unique patterns generate predictable functional "footprints" that could be used to formulate optimal combinations of electrical and pharmacological neuromodulation of the spinal circuitry in facilitating specific motor tasks even when there is no supraspinal input to the lumbosacral spinal cord.

Chapter 4 will demonstrate a novel technique, using a high-density parylene-based multi-electrode platinum array, to selectively activate spinal neurons to facilitate standing and stepping in rats after a complete spinal cord transection at a low-thoracic level. The results demonstrate that spinal rats can stand and step when the spinal cord is stimulated (tonic 40 Hz stimulation) by electrodes located at specific sites on the spinal cord and at specific frequencies of stimulation. The quality of stepping and standing was dependent on the location of the electrodes on the spinal cord, the specific stimulation parameters, and the orientation of the cathode and anode.

Chapter 5 we show that there is a minimal amount of spontaneous activity in the sensorimotor circuits that generate and control standing and stepping after a mid-thoracic spinal cord transection in adult rats. Spinal cord epidural stimulation below the level of the lesion, however, enhanced the amount of spontaneous activity several-fold and resulted in more robust stepping-like and partial weight-bearing standing activity. In effect, this enhanced spontaneous activity results in a ‘self-training’ phenomenon. This is consistent with the observation that independent, full weight-bearing standing can be initiated “voluntarily” and sustained in humans with complete paralysis in the presence of epidural spinal cord stimulation at an intensity that, in itself, induces little or no direct motor responses

Chapter 6 we demonstrate the development of a BMSCI (Brain Machine Spinal Cord Interface) having a pattern recognition algorithm that can use EMG from the forelimb muscles to trigger the initiation and termination of the stimulation of the spinal cord below the level of a complete spinal cord injury. This algorithm detects stepping with little or no calibration and thus provides an advantage over existing systems that needs constant monitoring.

Chapter 7 we present data that demonstrates the ability to overcome detrusor-sphincter dyssynergia and facilitate efficient voiding of bladders after a complete spinal cord injury in adult female rats via epidural spinal cord stimulation.

Lastly, Chapter 8 consists of concluding remarks that will discuss relevance and contribution of this thesis. In addition, it will touch upon the future direction of this research.

Chapter 2

Background

Why does spinal cord injury result in a loss of movement control?

Movements are defined by the activation of combined motor pools in a specific order and magnitude to generate the required forces. The diminished level of movement after a spinal cord injury can be attributed to an inability to activate specific motor pools in the order and magnitude deemed necessary. Three salient issues are linked to the impaired ability to recruit appropriate ensembles of motor units in a manner that generates effective movement. First, there are functional alterations in the spinal circuitry that disrupt the coordinated activation of the appropriate motor pools. Second, the level of recruitment for a specific motor task is insufficient for some motor pools and excessive for other motor pools. Finally, the decrease in neuromuscular activation and loading associated with a spinal cord injury leads to progressive muscle atrophy. All of these impairments must be addressed to realize the maximal potential of the spinal circuitry for recovering functional movement control after a spinal cord injury.

Aberrant synapse formation leads to inappropriate muscle recruitment and poor neuromuscular co-ordination

The loss of most, if not all, descending neural control after a spinal cord injury rapidly triggers changes in the brain and spinal cord circuitries. In particular, the neural circuitries responsible for posture and locomotion undergo major reorganization (Humphrey et al., 2006). While a large number of new synapses are formed, there is overwhelming evidence that many of these are abnormal connections may misdirect neurons to inappropriate downstream motor networks. The development of such aberrant connections (between the brain and the spinal cord

for incomplete injuries, and within the spinal cord circuitry for complete injuries) generally results in poor neuromuscular coordination, unintended movements, and spasticity. This lack of specificity in synapse formation leads to co-activation of neuromuscular circuits (motor pools and muscles) that are not normally activated synchronously and this is a major challenge to overcome.

Control of locomotion: Cortical is not critical

A common, but incorrect, assumption is that control of movement occurs almost exclusively in the motor cortex. There is overwhelming evidence, however, that the details of most movements are performed routinely with little conscious or voluntary effort (Griller et al., 1973, Edgerton et al., 2004, Rossignol et al.,1998). Shik and Orlovsky (1976) described the concept of "automaticity" in movement control, suggesting that movements are executed by the spinal cord circuitry involuntarily. The phenomenon of central pattern generation (CPG) within the spinal cord (Brown 1911, Grillner et al., 1978, Edgerton et al., 2001, Rossignol et al., 1998) has magnified the importance of the concept of spinal automaticity, i.e., the ability of the spinal cord to interpret complex sensory information to make appropriate decisions without requiring millisecond to millisecond control.

There is a high predictability of the activity patterns and the kinematics patterns of the limbs during locomotion from the electromyography of a single muscle. These observations suggest that individual muscles and joints are controlled by the nervous system, not as distinct components, but as a highly interactive system with interdependent components, a concept commonly described as muscle synergies, allowing the variation of individual parameters to achieve locomotion. This greatly simplifies neural control by reducing the degrees of freedom that must be controlled to execute very complex movements.

The smart spinal cord

The idea that networks of neurons within the spinal cord can generate a cyclic motor output is centuries old, as key experiments demonstrating automaticity in the mammalian spinal cord were performed by Brown in 1911. Deliagina et al., (2008) hypothesized that each limb is modulated by supraspinal input via groups of spinal neurons that they defined as controllers. These controllers respond to a tonic drive from the brain by generating a relatively complex rhythmic pattern that activates motor pools of muscles in a coordinated pattern to generate locomotion. Shik and Orlovsky (1976) proposed a 2-level automatism control system for locomotion. One level provides nonspecific tonic input that determines the intensity of locomotion, while the other is responsible for making fine adjustments in the control of the limbs, including maintaining equilibrium. This fine control system normally interacts with sources of sensory information, such as proprioceptive and visual inputs, to execute fine adjustments in the locomotor pattern.

Treatment paradigms for restoring locomotor control after a spinal cord injury

As discussed above, two of the fundamental elements for controlling movement are (a) regulating the levels of activation of the appropriate motor pools, and (b) regulating these motor pools in a coordinated manner. Since it becomes more difficult to control these factors after a spinal cord injury, pharmacological and spinal cord stimulation strategies that increase the excitability of the locomotor circuits, as well as activity-based training techniques that reinstate functional motor pool coordination, can be highly effective in helping subjects regain locomotor function.

Pharmacological treatments

Pharmacological treatments can have an important role in restoring the chemical environment of critical locomotor circuits after a spinal cord injury. Many of the central nervous system neurotransmitters, including the monoamines, are synthesized in isolated regions of the brain (e.g., 5-HT is synthesized in the raphe nucleus) and then transported to the spinal cord. Spinal cord injuries that disrupt the descending flow of neurotransmitters can severely hinder synaptic communication caudal to the lesion, which translates into loss of motor function. The deficits associated with diminished supraspinal input are aggravated by a significant up-regulation in the inhibitory potential of spinal neurons that mediate locomotion. This results in the locomotor circuitry becoming less responsive to excitation from peripheral afferents, which normally provide important proprioceptive triggers that control many of the details of locomotion.

Despite the disruption of critical neurotransmitter systems, the spinal locomotor circuits retain the capability to respond to sensory-driven pre-synaptic excitation. Since reversing the chemical changes caused by spinal cord injury relates to increasing neurotransmitter supply rather than regenerating lost receptors, pharmacological treatments that supplement the spinal cord with an exogenous supply of neurotransmitter agonists can help regulate synaptic communication and coordinate the activation of stepping-related motor pools. A number of studies have shown that the responsiveness of the locomotor circuitry to sensory input can be readily tuned by "bathing" the lumbosacral spinal cord with various neurotransmitter agonists and antagonists (de Leon et al., 1999; Rossignol et al., 1998). The effectiveness of such blunt pharmacological presentation is quite remarkable.

Low-dose pharmacological treatments, including monoaminergic, glycinergic, and GABAergic agonists, help to supplement the neurotransmitter environment of the post-injury spinal cord and thus can partially restore synaptic communication (Parker, 2005). Treatments using quipazine (Ichiyama et al., 2008; Fong et al., 2005), clonidine (Barbeau and Rossignol, 1991), L-DOPA (Barbeau and Rossignol, 1991), and/or strychnine (de Leon et al., 1999) have been shown to facilitate locomotor recovery even after a complete spinal cord injury. The enhanced synaptic transmission generated by using these drugs potentiates other treatments, including spinal cord stimulation and locomotor training, by lowering the activation threshold of the neurons associated with locomotion resulting in higher levels of performance compared to a single intervention (Ichiyama et al., 2008, Courtine et al., 2009, Musienko et al., 2011).

Locomotor training

Locomotor training has been shown to enhance the recovery of stepping (Edgerton et al., 2001) after a spinal cord injury in mice (Fong et al., 2005), rats (Courtine et al., 2009), cats (Barbeau and Rossignol, 1998; de Leon et al., 1998, Lovely et al., 1986) and, excitingly, even human subjects (Dietz and Harkema, 2004; Harkema et al., 1997). Engaging the spinal circuitry with sensory input associated with weight-bearing stepping is essential to activating the locomotor circuitry so that effective locomotion can be regained. Using this information, the spinal cord strengthens specific pathways relevant to a particular task. Traditional manual training of human spinal cord injured patients involves supporting the subjects in a harness over a moving treadmill while a team of therapists repeatedly guides the legs through a step cycle. More recently, robotic training devices (e.g., LokoMat) have been developed to replace manual training provided by therapist. The robotic arms attached to each leg moves the various joints

through specific trajectories on a treadmill belt with a window of error to allow the spinal circuitry and legs to relearn stepping after paralysis.

In subjects with a complete spinal cord injury remarkable levels of recovery can be attained if training is provided persistently over a period of weeks to months. Experience has helped define a set of critical requirements for effective step training. First, the stepping pattern used to train must have kinematics and kinetics parameters that are stable and appropriate to the training conditions. Second, it is important for training to provide sensory stimuli that closely match normal conditions. The spinal cord circuitry is highly sensitive to proprioceptive and cutaneous inputs: "good" stimuli are processed with exquisite efficiency, whereas "bad" stimuli can lead to failure. For example, using the same stepping pattern, recovery of stepping is less robust when spinal rats are trained on an elliptical-like device that maintains continuous contact with the hindpaw than when trained on a standard treadmill where paw contact is broken during swing (Timoszyk et al., 2003). Finally, although repetitive and consistent application of training paradigms is essential to recovery, there should be a small degree of variability in the parameters that are used to train to prevent locomotor performance from becoming dependent on a single set of stimuli. A controlled amount of variability in training enables subjects to benefit from experiential learning (Cai et al., 2006, Zeigler et al., 2010).

Spinal cord stimulation

Tonically stimulating the dorsal surface of the lumbosacral spinal cord via electrodes placed epidurally can induce locomotor-like movements *in vivo* in complete spinal rats (Ichiyama et al., 2005) and cats (Gerasimenko et al., 2003) and in humans that are classified as clinically complete (Dimitrijevic et al., 1998, Harkema et al., 2011). The intensity, frequency, and site of simulation are important parameters to control in defining the nature of the locomotor

movements that are generated (Gad et al., 2013). In rats and cats, epidural stimulation alone can generate partial weight-bearing locomotor movements.

Epidural stimulation: Results from human subjects

Recently (Harkema et al., 2011 & Angeli et al., 2012 SFN 2012 abstract), three completely paralyzed human subjects were implanted with a commercially available spinal cord electrode array and stimulation package originally designed for pain suppression. With an epidurally implanted electrode array, they modulated the physiological state of the spinal circuitry to enable full weight-bearing standing in the very first attempt in a patient with a chronic clinically motor complete SCI (Harkema et al., 2011). Epidural stimulation did not induce standing by directly activating motor pools, but enabled motor function by stimulating afferent fibers in the dorsal root and engaging populations of interneurons that integrated load-bearing related proprioceptive input to coordinate motor pool activity. Dynamic changes in position during standing were observed and were accompanied by motor patterns needed to maintain upright posture without changing the epidural stimulation parameters. Intensive task-specific training combined with epidural stimulation extended the duration of periods of full weight-bearing standing). In addition, these subjects regained some voluntary control of specific hindlimb movements when under the influence of epidural stimulation.

Phase-dependent modulation of proprioceptive input during stepping

A clear example of the dynamic ability of the spinal locomotor circuitry to process and adapt to sensory information is the enhanced activation of flexor motor pools in response to a mechanical tripping stimulus. When an obstacle is placed in front of the paw of a spinal cat during the swing phase of stepping, there is enhanced flexion of the tripped limb (Forssberg,

1979). If this same mechanical stimulus is applied during the stance phase, however, there is an enhanced excitation of the ipsilateral extensor motor pools. In other words, the same stimulus results in opposite effects depending on the phase of the step cycle. The functional importance of phase-dependent modulation of sensory input to the spinal cord has been reinforced by recent experiments demonstrating a very predictable suppression or potentiation of monosynaptic and polysynaptic responses when electrically evoked stimuli are applied to the dorsum of the spinal cord . The amplitudes of these responses are increased during the normal active bursting phases of a given muscle and suppressed during the inter-burst intervals. During the stance phase, the net effect of sensory input is potentiated in the extensor musculature, while during the swing phase the sensory input is potentiated in the flexor musculature. This type of modulation occurs in uninjured and complete spinal rats, cats, and humans (Gerasimenko et al., 2007; Lavrov et al., 2006, 2008). A similar modulation of responses has been reported in uninjured human subjects during treadmill locomotion (Courtine et al., 2007). From these data, it is clear that the spinal circuitry processes sensory information in a strongly cyclic, phase-dependent manner whether or not the spinal cord is injured.

Although the mechanisms for these dynamic responses are unknown, the results reflect a level of "smartness" and decision making capability of the spinal cord circuitry, and provide some insight into how sensory information combines with central pattern generation to generate remarkably effective locomotion after a spinal cord injury. For instance, these observations make it obvious that phase-dependent processing of proprioceptive input provides a remarkable means of coordinating massive amounts of dynamic sensory information projecting to the motor pools that generate stepping.

Adaptive mechanisms of the spinal cord to process afferent information to modulate motor output

Musienko et al., (2011) demonstrated that during epidural stimulation of a decerebrated cat the spinal cord possesses the ability to dynamically process ongoing somatosenry input and dynamically update the motor commands required to sustain weight-bearing locomotion with adequate balance and posture. They also reported that when perturbed with a lateral force, the animal was able to modulate the EMG patterns to accommodate the perturbation and continue to step consistently. The stance phase was prolonged on the side ipsilateral to the perturbation whereas the swing phase was prolonged on the contralateral side. Zhong et al., (2012) reported that spinal cats responded to a single instantaneous perturbation (being tripped during locomotion and thus inducing a dynamic variation of afferent information) during a complex motor task, i.e., stepping with a newly adopted neural control strategy with an elongation of the ipsilateral swing and a contralateral stance phase during the phase of perturbation reinforcing our hypothesis of the ability of the spinal cord being a center for afferent information processing and a 'driving force' for locomotion.

Integrating neuro-engineering and biological concepts to regain posture and locomotion

Based on the successful recovery that has been attained using spinal cord stimulation, pharmacological, and/or activity-based motor training interventions, the potential for enhancing locomotor recovery by aggressively pursuing complementary and synergistic strategies is clear and represents a logical direction for translating some of the basic biological concepts to the clinical setting. While it cannot be assumed that multiple interventions

always will be complementary (Maier et al., 2009), careful consideration of the interactive effects of multi-intervention approaches appear to be obvious solutions staring us in the face (Fong et al.,2005).

We already have observed significant positive interaction when multiple modes of treatment are combined. Optimal recovery of locomotion requires two important factors: the damaged spinal cord must be provided with adequate information that it can use to relearn to step. This explains why the recovery of locomotion using robotically assisted training, which provides information on functional stepping patterns, is significantly enhanced by co-administration of pharmacological agonists that improve synaptic signaling. In mice, e.g., while robotic training restores gross stepping function, pharmacological modulation with quipazine further improves locomotion by facilitating the recovery of movements that are difficult to access with training alone, e.g., activation of the distal extensor muscles during weight-bearing stance (Fong et al., 2005). We also have observed substantial recovery in rats from a combination of locomotor training, two serotonergic drugs, and multiple-site epidural stimulation, and have shown that selective combinations of these treatments lead to very different locomotor effects (van den Brand et al., 2007). The next step is to optimize the combination treatment parameters to maximize the synergies between the constituent interventions. All evidence suggests that engaging complementary approaches may result in the greatest functional gains.

Combinations of paradigms can be effective when each component treatment focuses on repairing a different aspect of motor function loss. Continued technological advancement in pharmacological treatment, spinal cord stimulation, and activity-based training, machine learning based stimulation protocols, enhance activity based offers great potential. Pharmacological

therapies will improve with the arrival of sophisticated drug delivery systems that enable treatment of focal regions of the spinal cord. Spinal cord stimulation will continue to progress with electrode array development.

Activity-based treatments will advance in conjunction with the development of learning algorithms that will help define optimal training protocols that adapt dynamically with the constantly evolving state of the recovering spinal circuitry. With the aggressive pursuit of the combination therapies "staring us in the face," the expectations for recovery of locomotion are now significantly higher for individuals with spinal cord injury, their family, friends, therapists, and physicians.

Chapter 3

Neuromodulation of motor-evoked potentials in spinal rats

Abstract

The rat spinal cord isolated from supraspinal control via a complete low- to mid-thoracic spinal cord transection produces locomotor-like patterns in the hindlimbs when facilitated pharmacologically and/or by epidural electrical stimulation. To evaluate the role of epidural electrical stimulation in enabling motor control (eEmc) for locomotion and posture, we recorded potentials evoked by epidural spinal cord stimulation in selected hindlimb muscles during stepping and standing in adult spinal rats. We hypothesized that the temporal details of the phase-dependent modulation of these evoked potentials in selected hindlimb muscles while performing a motor task in the unanesthetized state would be predictive of the potential of the spinal circuitries to generate stepping. To test this hypothesis we characterized soleus and TA muscle responses as middle response (MR, 4-6 ms) or late responses (LRs, >7ms) during stepping with eEmc. We then compared these responses to the stepping parameters with and without a serotoninergic agonist (quipazine) or a glycinergic blocker (strychnine). Quipazine inhibited the MRs induced by eEmc during non-weight-bearing standing, but facilitated locomotion and increased the amplitude and number of LRs induced by eEmc during stepping. Strychnine facilitated stepping and reorganized the LRs pattern in the soleus. The LRs in the TA remained relatively stable at varying loads and speeds during locomotion, whereas the LRs in the soleus were strongly modulated by both these variables. These data suggest that LRs facilitated

via electrically and/or pharmacologically are not time locked to the stimulation pulse but are highly correlated to the stepping patterns of spinal rats.

Introduction

The lumbosacral spinal circuitry can generate partial weight-bearing stepping of the hindlimbs in rats spinalized as adults when facilitated pharmacologically and/or with epidural electrical stimulation (Gerasimenko et al., 2007; Courtine et al., 2009; Musienko et al., 2011). The mechanisms of pharmacological and/or epidural electrical stimulation that enable motor control (eEmc; Gad et al., 2012) in the spinal circuitry for locomotion are still not clearly understood. During standing, a single bipolar epidural stimulus between L2 and S1 produces three types of evoked responses, i.e., early (ER, latency 1-3 ms), middle (MR, latency 4-6 ms), and late (LRs, latency >7 ms) in the hindlimb muscles in both intact (Gerasimenko et al., 2006) and spinal (Lavrov et al., 2006) rats. Similar responses were observed during rhythmic locomotor-like EMG activity in the hindlimb muscles of spinal rats while stepping on a motorized treadmill in the presence of epidural stimulation (40 Hz) between L2 and S1 (Lavrov et al., 2008). In addition, the time course of the re-emergence of the LRs was similar to that for the recovery of stepping after a complete spinal cord injury (SCI), indicating that LRs are a potential biomarker of functional recovery (Lavrov et al., 2006).

We hypothesized that the pattern of pharmacological neuromodulation of evoked potentials as generated *in vivo* when performing a specific motor task can be used as a biomarker for the prediction of locomotor characteristics. Presently we know few details as to which components of the spinal sensorimotor networks are dynamically facilitated or depressed in a phase-dependent pattern during a well-defined postural and/or locomotor task when it is being modulated pharmacologically. Understanding the nature of the electrically and/or pharmacologically evoked responses and their modulation *in vivo* may provide the insight

needed to design optimal rehabilitation paradigms to enable postural control and stepping after a SCI.

Thus, the purpose of the present study was to define the epidurally motor-evoked responses in hindlimb muscles of spinal rats when the spinal circuitries are modulated by eEmc during stepping with and without strychnine and quipazine under different treadmill speed and loading conditions. We hypothesized that 1) the improvement in weight-bearing stepping by modulating the excitability of glycinergic and serotoninergic receptors will be related to the facilitation of MR and LR neuronal circuitries associated with extensor muscles, and 2) the manner in which the MR and LRs are facilitated or depressed during locomotion will be dependent on the patterns of afferent input to the spinal cord.

MATERIALS AND METHODS

Animals and animal care

Data were obtained from 5 adult female Sprague Dawley rats (270-300 g body weight). Pre- and post-surgical animal care procedures have been described in detail previously (Roy et al., 1992). The rats were housed individually with food and water provided *ad libitum*. All survival surgical procedures were conducted under aseptic conditions with the rats deeply anesthetized with isoflurane gas administered via facemask as needed. All procedures described below are in accordance with the National Institute of Health Guide for the Care and Use of Laboratory Animals and were approved by the Animal Research Committee at UCLA.

Head connector and intramuscular EMG electrode implantation

A small incision was made at the midline of the skull. The muscles and fascia were retracted laterally, small grooves were made in the skull with a scalpel, and the skull was dried thoroughly. Two amphenol head connectors with Teflon-coated stainless steel wires (AS632, Cooner Wire, Chatsworth CA) were securely attached to the skull with screws and dental cement as described previously (Roy et al., 1992; Ichiyama et al., 2005). Selected hindlimb muscles, i.e., the tibialis anterior (TA) and soleus (Sol), were implanted bilaterally with intramuscular EMG recording electrodes as described by Roy et al. (1991). Skin and fascial incisions were made to expose the belly of each muscle. Two wires extending from the skull-mounted connector were routed subcutaneously to each muscle. The wires were inserted into the muscle belly using a 23-gauge needle and a small notch (~0.5-1.0 mm) was removed from the insulation of each wire to expose the conductor and form the electrodes. The wires were secured in the belly of the muscle via a suture on the wire at its entrance into and exit from the muscle belly. The proper placement

of the electrodes was verified during the surgery by stimulating through the head connector and post-mortem via dissection.

Spinal cord transection, epidural electrode implantation, and post-surgical animal care procedures

A partial laminectomy was performed at the T8-T9 vertebral level and a longitudinal cut was made in the dura to expose the spinal cord. A complete spinal cord transection to include the dura was performed at approximately the T8 spinal level using microscissors. Two surgeons verified the completeness of the transection by lifting the cut ends of the spinal cord and passing a glass probe through the lesion site. Gel foam was inserted into the gap created by the transection as a coagulant and to separate the cut ends of the spinal cord.

For epidural electrode implantation, partial laminectomies were performed to expose the spinal cord at spinal levels L2 and S1. Two Teflon-coated stainless steel wires from the head connector were passed under the spinous processes and above the dura mater of the remaining vertebrae between the partial laminectomy sites. After removing a small portion (~1 mm notch) of the Teflon coating and exposing the conductor on the surface facing the spinal cord, the electrodes were sutured to the dura mater at the midline of the spinal cord above and below the electrode sites using 8.0 Ethilon suture (Ethicon, New Brunswick, NJ). Two common ground (indifferent EMG and stimulation grounds) wires (~1 cm of the Teflon removed distally) were inserted subcutaneously in the mid-back region. All wires (for both EMG and epidural stimulation) were coiled in the back region to provide stress relief.

All incision areas were irrigated liberally with warm, sterile saline. All surgical sites were closed in layers using 5.0 Vicryl (Ethicon, New Brunswick, NJ) for all muscle and

connective tissue layers and for the skin incisions in the hindlimbs and 5.0 Ethilon for the back skin incision. All closed incision sites were cleansed thoroughly with saline solution. Analgesia was provided by buprenex (0.5–1.0 mg/kg, s.c. 3 times/day). The analgesics were initiated before completion of the surgery and continued for a minimum of 2 days. The rats were allowed to fully recover from anesthesia in an incubator. The rats were housed individually in cages that had ample CareFresh bedding, and the bladders of the spinal rats were expressed manually 3 times daily for the first 2 weeks after surgery and 2 times daily thereafter. The hindlimbs of the spinal rats were moved passively through a full range of motion once per day to maintain joint mobility. All of these procedures have been described in detail previously (Courtine et al., 2009).

Stimulation and testing procedures

Bipolar epidural stimulation between L2 and S1 was used to evoke potentials in the hindlimb muscles during standing (1 and 40 Hz) and stepping (40 Hz) (Lavrov et al., 2006; Gerasimenko et al., 2008; Ichiyama et al., 2008; Courtine et al., 2009). The rats were stepped bipedally on a specially designed motor-driven rodent treadmill using a body weight support system (de Leon et al., 2002). The rats were stepped under three conditions: 1) weight-bearing stepping during which there was complete foot contact while stepping; 2) toe stepping when only the toes were in contact with the treadmill; and 3) air stepping when there was no foot contact with the treadmill. The evoked potentials and locomotor performance induced by epidural stimulation were determined before and after administration of quipazine (Quip, 0.3 mg/kg; Ichiyama et al., 2008) or strychnine (Strych, 1 mg/kg; de Leon et al., 1999) intraperitoneally.

Kinematics recording parameters

A four-camera system was calibrated and then used to track reflective markers placed on bony landmarks on the iliac crest, greater trochanter, lateral condyle, lateral malleolus, the distal end of the fifth metatarsal of both hindlimbs. The video footage was processed using SIMI Motion analysis software (SIMI, Unterschleissheim, Germany) to produce the 3-D reconstruction of the hindlimb and forelimb movements, as well as the 2-D ball-and-stick diagrams and hindlimb trajectory plots (Courtine et al., 2009). The 3-D coordinates for a given marker were calculated using a triangulation procedure that partially accounts for the movement of the skin. The 3-D coordinates then were used to estimate the joint angles. This is a technique that has been used successfully and implemented in many labs and has the precision necessary for the present study.

Data analysis

EMG recordings from the hindlimb muscles were band-pass filtered (1 Hz to 5 KHz), amplified using an A-M Systems Model 1700 differential AC amplifier (A-M Systems, Carlsborg, WA), and sampled at a frequency of 10 KHz using a custom data acquisition program written in the LabView development environment (National Instruments, Austin, TX) as described previously (Courtine et al., 2009). Evoked potentials were identified using a custom script written in MATLAB (Mathworks). Peaks were detected using a moving window differentiation technique (Vivó-Truyols et al., 2005) by locating the point at which the slope was zero (identified as either a peak or a valley) for peaks above a set threshold, i.e., three times the standard deviation of the individual trace (Vivó-Truyols et al., 2005). Figure 3B shows an example of a single trace for MRs and LRs (circles) that were detected along with smaller

responses (crosses) that did not qualify as peaks. With a singe pulse, the ER was estimated in the window of 1-3 ms, the MR in the window of 4-6 ms, and LRs in the window of >7ms. At the higher frequency of stimulation (40 Hz), the LRs were estimated as responses with 7-25 ms delay. The response latencies were determined from the onset of the stimulation pulse to the identified peak. These criteria scales are based on previously published data (Gerasimenko et al., 2003, 2006; Lavrov et al., 2006, 2008). The integral in the EMG signal was calculated by estimating the area under the curve after rectification of the raw EMG to account for any oscillations in baseline activity as previously described (Whiting et al., 1984, Roy et al., 1991). The LR/MR ratio was calculated as the integral of the LR region to the integral of the MR region. The cumulative integral was calculated by summing the integral from each stimulation pulse across the entire step cycle. The step cycle was determined by analyzing kinematics data using Virtual Dubmod (open source video processing, GPL). The step cycle was initiated at the start of the swing phase i.e., when the toe lost contact with the treadmill, and ended with the start of the next swing phase.

Statistical analyses

All data are reported as mean ± SEM. Statistically significant differences were determined using a one-way repeated measures analysis of variance (ANOVA). The criterion level for the determination of a statistical difference was set at $P < 0.05$ for all computations.

RESULTS

Characteristics of motor-evoked responses to epidural stimulation at different frequencies during bipedal standing

Stimulation at a low frequency evoked responses within three general time frames in the TA and soleus when the rat was not bearing weight, i.e., an ER (1-3 ms latency), MR (4-6 ms latency), and LR (>7 ms latency) (Fig. 1, top panel) as demonstrated previously (Gerasimenko et al., 2003, 2006; Lavrov et al., 2006, 2008). Epidural stimulation at 40 Hz facilitated tonic EMG activity in both the TA and soleus muscles during bipedal standing while the rat was partially weight bearing (Fig. 1, bottom traces). The average latency for these responses in both muscles was between 4 to 6 ms, i.e., a latency corresponding to a MR (Gerasimenko et al., 2006; Lavrov et al., 2006). Note the higher amplitudes at the lower frequency reflecting a depression in the evoked potentials at 40 Hz. There was a large MR in the soleus during partial weight bearing (Fig. 1, bottom traces), whereas there was no or minimal ER, MR, and LR in the absence of weight bearing in either muscle (Fig. 1, middle traces).

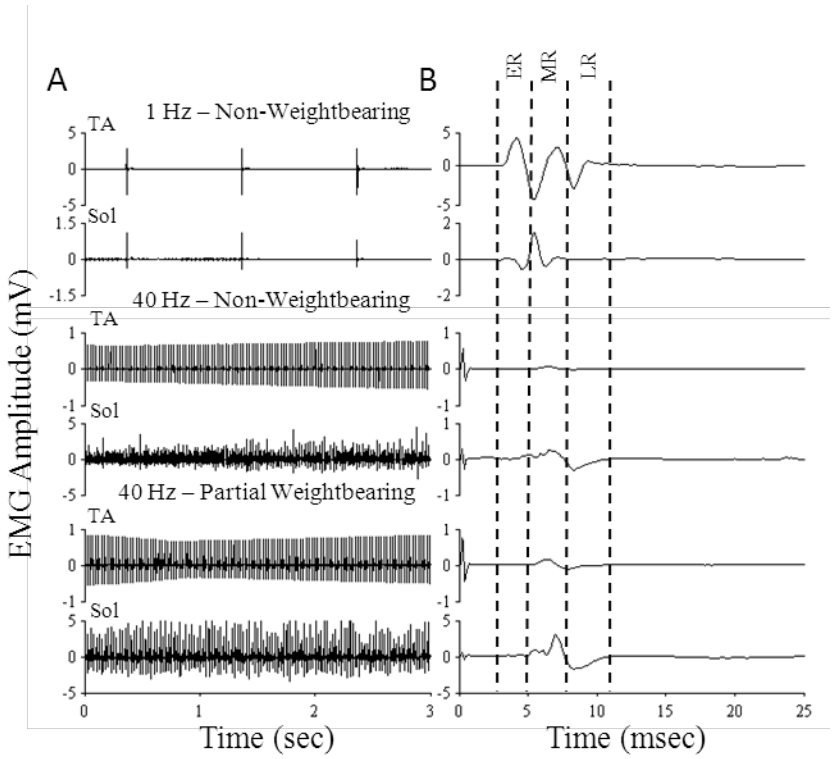

Figure 3.1: Evoked potentials during standing under different loading conditions

(A) Tibialis anterior (TA) and soleus (Sol) EMG amplitudes during epidural stimulation eEmc (ES) (1 Hz, between L2 and S1) with the rat standing bipedally and supporting none of its body weight and during eEmc ES (40 Hz, between L2 and S1) with the rat standing bipedally but not supporting any body weight (middle panel) and with partial weight support (bottom panel). (B) Average of the motor-evoked potentials during the 3 sec of recordings shown in (A), identifying the early (ER, latency 1-3 ms), middle (MR, latency 4-6 ms), and late (LR, latency 7-9 ms) responses. The range of latencies for each response is based on previous observations (Gerasimenko et al., 2006; Lavrov et al., 2008). Note the different scales for EMG amplitudes based on the weight supported by the animal.

Characteristics of motor-evoked responses to ES during stepping

The latencies and amplitudes of the evoked potentials to epidural stimulation were modulated in a phase-dependent manner during bipedal stepping on a treadmill. These patterns were modulated to a large extent based on the presence or absence of an EMG burst (see light and dark gray shaded areas in Fig. 2A). Averages of all responses during (intraburst) and between (interburst) EMG bursts of the TA and soleus are shown in Figure 2B. The amplitudes of the responses are 5-10-fold higher during than between bursts. In addition the number of LRs is greater during compared to between bursts. The evoked responses, however, are further modulated as a function of whether they are induced in the early vs. late phase of the flexor (TA) or extensor (soleus) EMG (see orange and green in Fig. 2C). The latency of the MR is slightly longer in the TA than the soleus throughout the burst, and in the later phase of the soleus burst there are little or no LRs.

Stepping under different levels of body weight support modulates the sensory information received by the spinal cord. To begin to better understand the unique changing "footprints" reflected in the responses to different load bearing conditions, we examined the latencies of the responses throughout the step cycle to each evoked stimulus administered tonically at 40 Hz. In this way we could observe the response to each stimulus during consecutive 25 ms epochs throughout the flexor and extensor phases of the step cycle (Fig. 3A). The start of each 25 ms epoch was synchronized with each stimulation pulse with the initial epoch plotted at the bottom of the Figure and beginning with the initiation of the swing phase of the step cycle. The LRs in the TA tended to persist for more consecutive 25 ms epochs during air stepping compared to weight-bearing stepping. Clear variations in the MR and LRs related to the

early and late phases of soleus activation were observed (similar to Fig. 2). The MR in the soleus is prominent and relatively consistent in amplitude and latency throughout the extension phase of the step cycle during air stepping and toe stepping. During weight bearing stepping, however, there was a progressive decrease in the amplitude of the MR during the stance phase. This finding is consistent with a concomitant decrease in proprioception related to load bearing during the stance phase of the step. A reduction in the duration of the LRs in the soleus (i.e., in the number of 25 ms epochs and the duration of responses within a given epoch) occurred with load bearing (see red boxes highlighting the occurrence of LRs).

Varying the speed of stepping largely affects the EMG burst duration of ankle extensors but not flexors in intact (Roy et al. 1991) and spinal (Courtine et al., 2009) rats. We examined the behavior of motor-evoked potentials in flexor and extensor muscles during stepping at different treadmill speeds. Plotting the evoked responses to consecutive 25 ms epochs between stimuli for a single step cycle at different speeds demonstrates different patterns of changes in the amplitudes and durations for the LRs compared to the MR (Fig. 4A). Increased treadmill speed resulted in a decrease in the number of epochs during the stance phase, but no change in the number of epochs during the swing phase. The amplitude of the MR in the TA increased with speed of stepping, while the LRs were small and occurred randomly during the swing phase at all speeds tested. In the soleus, a prominent MR was present and it occurred only during the stance phase. The largest MR amplitudes generally occurred at the beginning of stance and progressively decreased throughout the remainder of the stance phase. The LRs in the soleus also were present only during the stance phase. At the initiation of stance LRs were sustained throughout each 25 ms epoch but with succeeding epochs the initiation of the LRs had a progressively longer delay following each stimulus (areas outlined in red in Fig. 4A). The

amplitudes of the individual LR did not seem to vary consistently across the speeds tested. Another feature of the LRs in the soleus was the inverse relationship between the speed of stepping and the number of 25 ms epochs in which LRs occurred (Fig. 4A and B).

The total amount of activation for the TA within the LRs vs. MR (LR/MR integral) remained constant as a function of speed (Fig. 4B). In contrast, the relative activation of the LRs vs. MR progressively decreased with increasing speed in the soleus. The relative rate of cumulative integral for the TA or the soleus was not remarkably different across the three speeds studied (Fig. 4C). The absolute rate of accumulation, however, was approximately 5-fold greater in the soleus than TA. The total cumulative integral for the soleus, but not the TA, decreased with increasing treadmill speed.

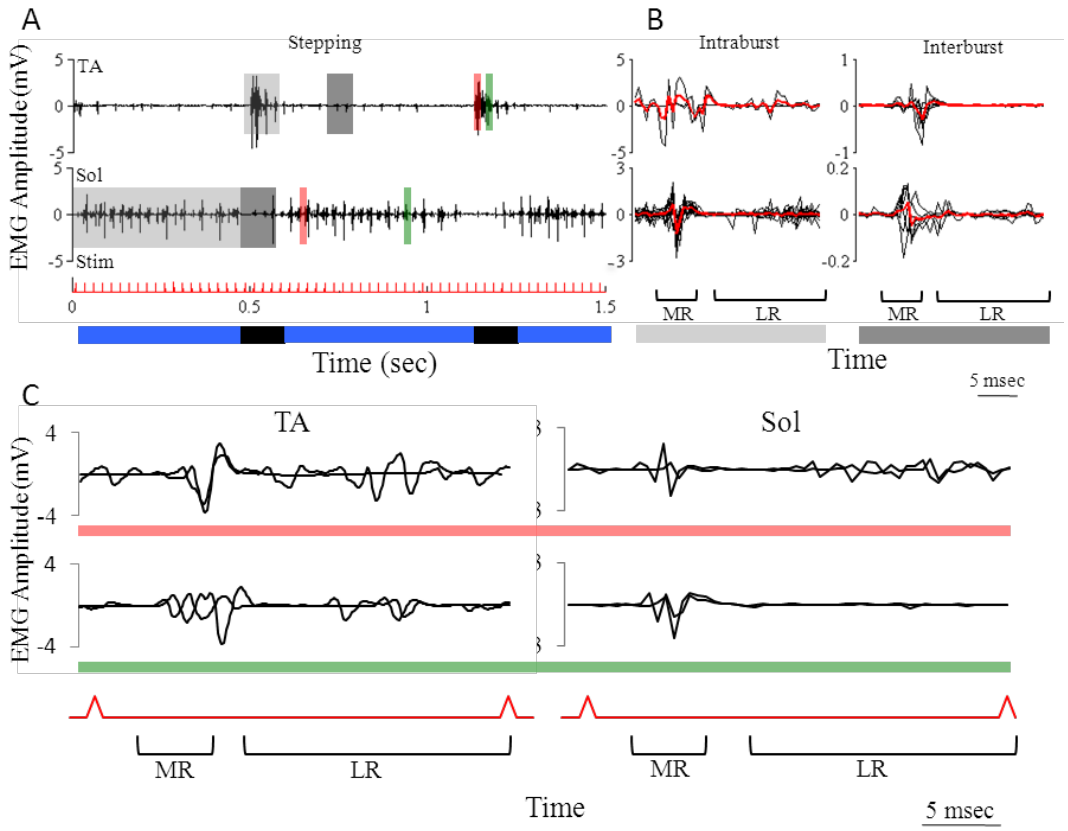

Figure 3.2: Modulation of eEmc ES evoked potentials during stepping

(A) TA and Sol EMG during the stance (blue) and swing (black) phases of stepping on a treadmill at 13.5 cm/s with partial weight bearing under the influence of eEmc ES (40 Hz, between L2 and S1). Light gray highlight, during intraburst interval; dark gray highlight, during interburst interval; red and green highlights, early and late phases of the EMG burst, respectively; Stim, eEmc ES pulse. (B) The MR and LRs for all motor-evoked potentials during the intraburst interval (left plots for the areas highlighted in light gray in (A)) and during the interburst interval (right plots for the areas highlighted in dark gray in (A)) are shown as black traces and the red bold line shows the average of all potentials. (C) Zoomed in view of the early (top traces) and late (bottom traces) phases of the TA and Sol EMG bursts highlighted in (A).

Note the presence of both an MR and LRs during both phases of the EMG burst in the TA and for the early phase in the Sol, but only an MR for the later phase in the Sol.

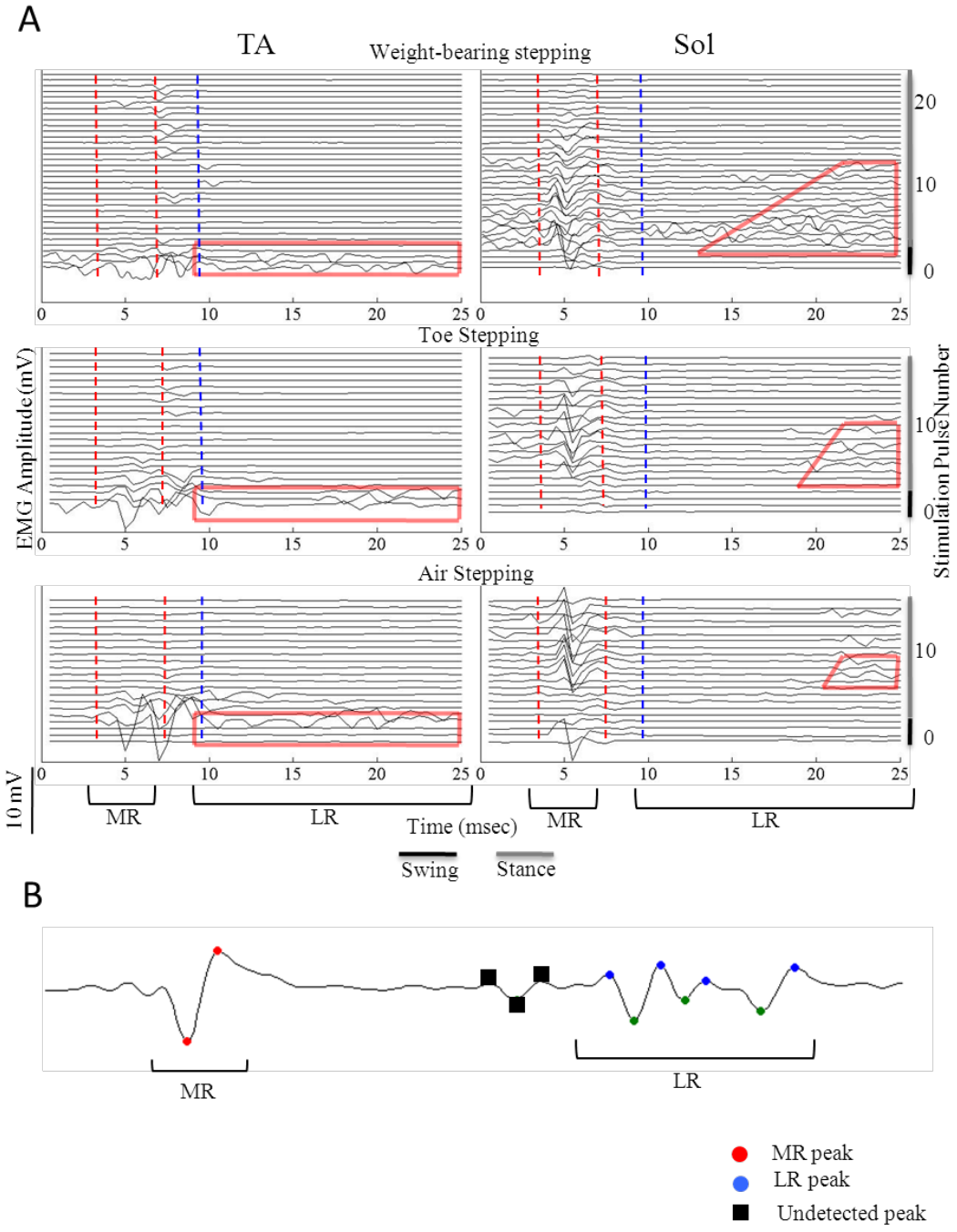

Figure 3.3: Modulation of ES evoked potentials during stepping under different loading conditions

The effect of load on the modulation of evoked potentials generated for each stimulation pulse in the TA and Sol muscles for a single cycle during weight bearing, toe, and air stepping. The start of each trace is synchronized with the initiation of eEmc ES. Each trace is 25 ms, i.e., the time between successive eEmc ES pulses. The red vertical dashed lines denote the MR window. The vertical dashed blue line denotes the beginning of the window for the LRs. The areas outlined by solid red lines denote the LR duration during the swing phase for the TA and during the stance phase for the Sol.

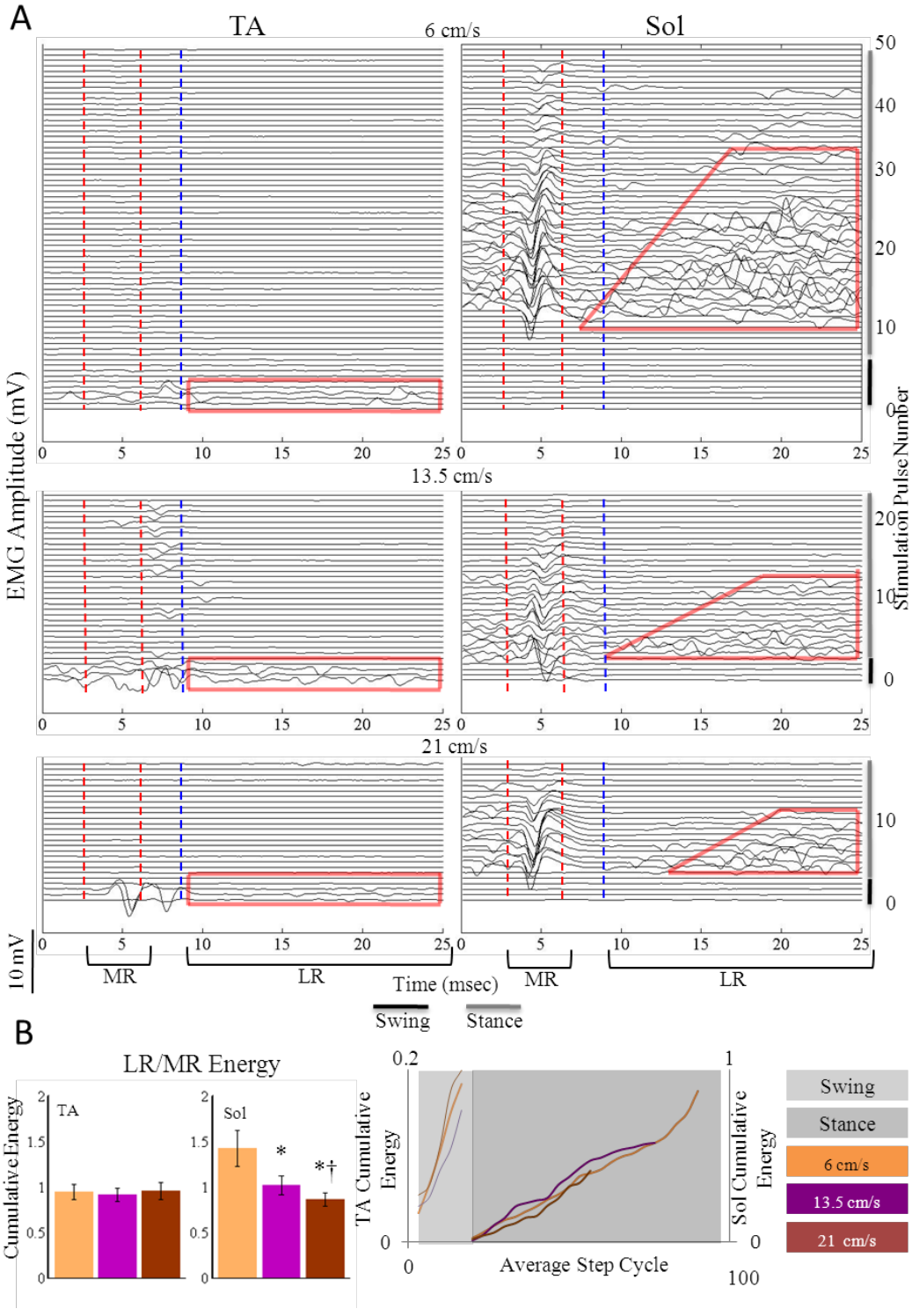

Figure 3.4: eEmcES evoked potentials during stepping at different treadmill speeds

The effect of treadmill speed on the modulation of evoked potentials generated for each stimulation pulse in the TA and Sol muscles for a single step cycle. (A) The layout is similar to that in Figure 3. (B) The average (n = 5 rats, 10 steps/rat) LR/MR ratio of the cumulative energy in the TA and Sol when stepping at 6, 13.5, and 21 cm/s. (C) The cumulative levels of activation over consecutive 25 ms epochs during the swing and stance phases are shown for each of the three speeds. * and †, significantly different from 6 and 13.5 cm/s, respectively, at $P > 0.05$.

Pharmacological modulation of motor-evoked potentials during non weight-bearing standing and stepping

eEmc (1 Hz) at a supra-threshold intensity (> 4 V) when the limbs were non weight bearing elicited an ER, MR, and LR in the TA and an ER and MR in the soleus (Fig. 5, similar to Fig. 1, top traces). In the presence of eEmc, Strych (a glycinergic antagonist) facilitated the MR in the TA, whereas Quip (a serotoninergic agonist) reduced the MR in both muscles. The addition of Strych or Quip in concert with eEmc modulated the stepping pattern of the spinal rats (Fig. 6 and Supplemental Video 1). eEmc+Strych modestly increased the prominence of the MR in the TA, while markedly increasing the LRs in the soleus during the stance phase. The number and duration of LRs in the soleus were higher with eEmc+Strych than with eEmc alone (Fig. 6, compare red outlined box for eEmc vs. eEmc+Strych), suggesting that blocking glycinergic receptors resulted in disinhibition of the neural networks and facilitated stepping.

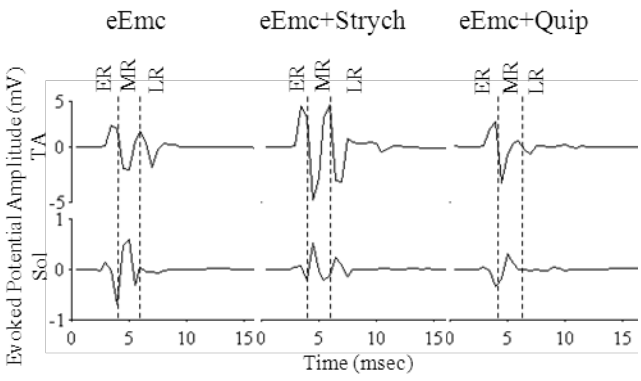

Figure 3.5: Evoked potentials during standing under the influence of eEmc ES with and without strychnine or quipazine

Average amplitude (10 responses) of the evoked potentials induced by eEmc ES (1 Hz) from the Sol and TA with the rat under non weight-bearing conditions with and without quipazine (Quip) or strychnine (Strych) administration.

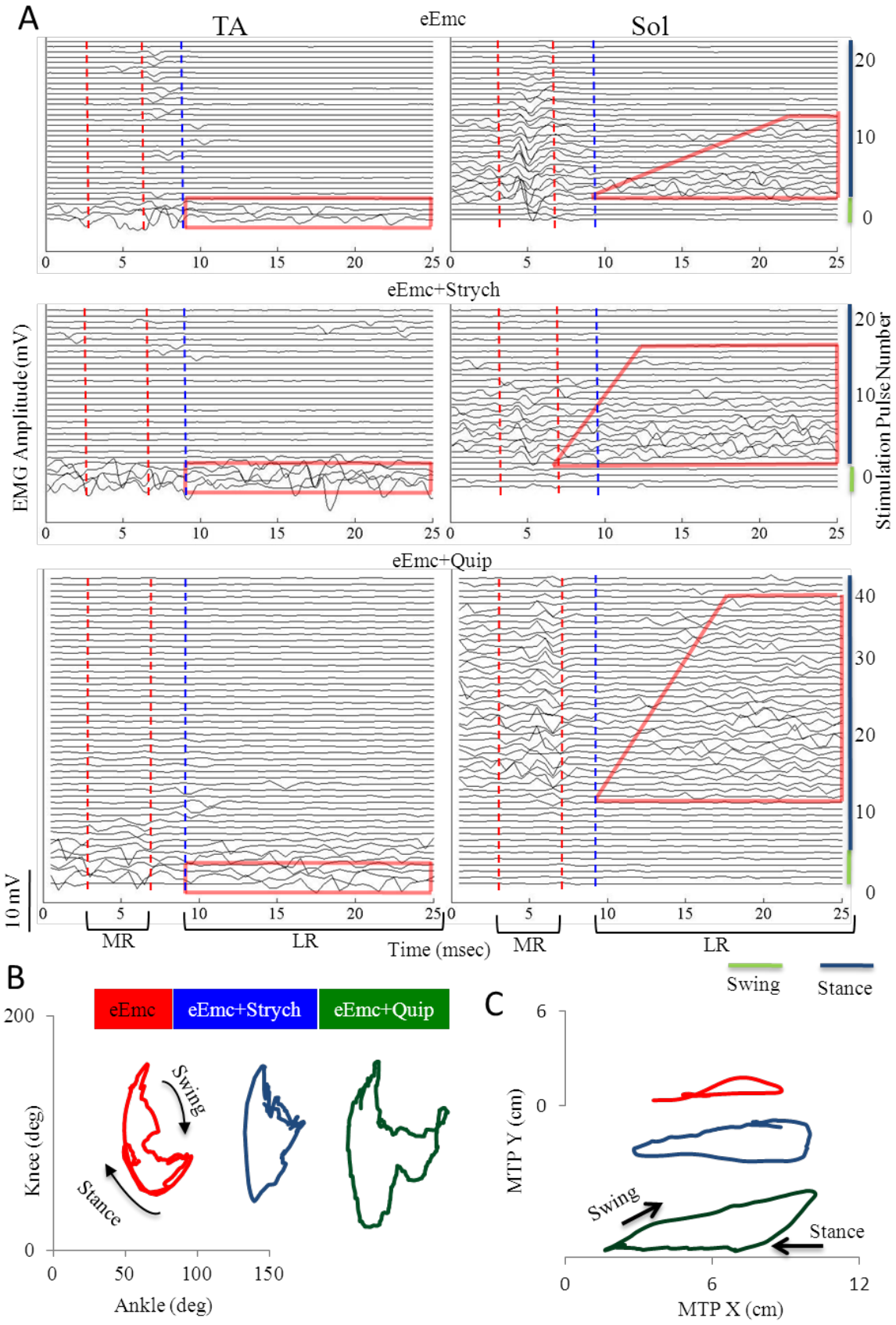
A
TA
eEmc
Sol
eEmc+Strych
eEmc+Quip
EMG Amplitude (mV)
Stimulation Pulse Number
10 mV
MR
LR
Time (msec)
Swing
Stance
B
eEmc
eEmc+Strych
eEmc+Quip
Knee (deg)
Ankle (deg)
C
MTP Y (cm)
MTP X (cm)

Figure 3.6: Evoked potentials during stepping under the influence of eEmc with or without strychnine or quipazine

(A) Modulation of the evoked potentials generated by each stimulation pulse with eEmc alone and after Quip or Strych administration with eEmc. The layout is similar to that in Figure 3. (B) Angle-angle plots (knee vs. ankle) for a single step cycle with eEmc alone and after Quip or Strych administration with eEmc. (C) X-Y plots representing the trajectory of the foot marker (metatarsophalangeal, MTP) during a single step cycle with eEmc alone and after Quip or Strych administration with eEmc.

The MR and LRs were more prominent under eEmc+Quip relative to eEmc alone corresponding to a more prolonged stance phase. The effects of Quip on the pattern of the evoked potentials throughout the step cycle differed in several ways from that of Strych. For example, there was significantly longer duration of LRs and a more prominent MR occurring throughout the stance phase with eEmc+Quip compared to eEmc+Strych in the soleus. The differences in the pattern of stepping are demonstrated in Figure 6B. The angle-angle plots with eEmc alone demonstrate the smaller excursions in the ankle and knee angles during a single step cycle compared to eEmc+Quip and eEmc+Strych. Administration of Strych or Quip increased the excursion at both the knee and ankle joints, more so with Quip than Strych. The foot (metatarsophalangeal, MTP) trajectory in the X-Y plane also demonstrates the differences in the pattern of stepping with eEmc alone compared to eEmc+Quip and eEmc+Strych (Fig. 6C). The administration of Quip with eEmc resulted in a higher foot position during the swing phase than with eEmc+Strych and eEmc alone. Similar patterns of evoked potentials were observed across several animals (Fig. 7).

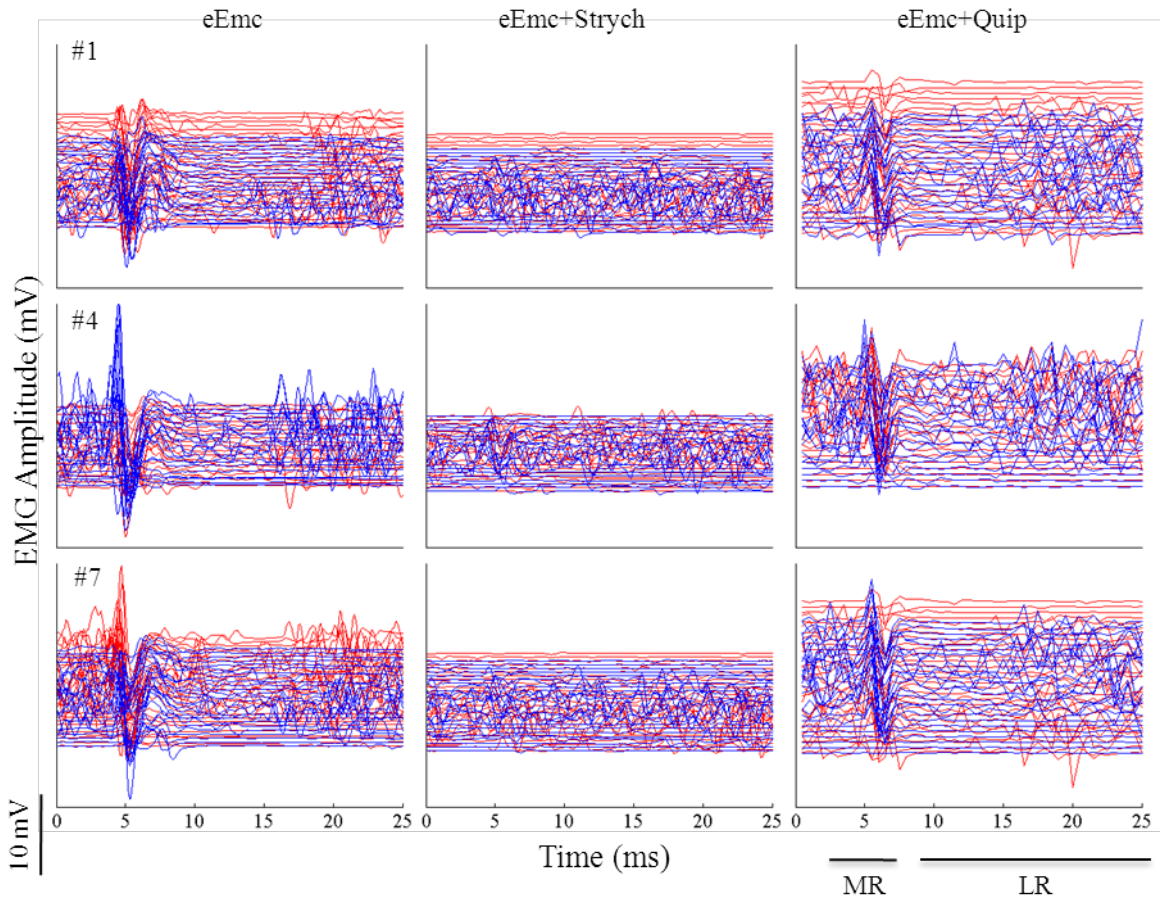

Figure 3.7: Evoked potentials during stepping under the influence of eEmc with or without strychnine or quipazine from multiple animals

Modulation of evoked potentials generated by each stimulation pulse with eEmc alone and after Strych and Quip administration for 2 steps (red, blue) from each of three animals (#1, #4, and #7). The layout is similar to that in Figure 3.

The net activation of the soleus and TA based on the EMG responses was measured to determine the relative importance of the modulation of the MR and LR components during the flexor and extensor phases of the step cycle. To do this we determined the area under the rectified EMG burst (integrated area of the rectified EMG burst) during the MR region and the LR region after each stimulation pulse (Fig. 8A). For the total step cycle, the integral of both the MR and LRs and the total integral in the TA were higher with eEmc+Quip and eEmc+Strych than eEmc alone and lower with eEmc+Strych than with eEmc+Quip. Similar increases in the integral for the LRs and the total integral were observed with eEmc+Quip and eEmc+Strych relative to eEmc alone in the soleus. The overall effect of eEmc+Strych or eEmc+Quip relative to eEmc alone was similar, i.e., dominated by the LRs in both the TA and soleus.

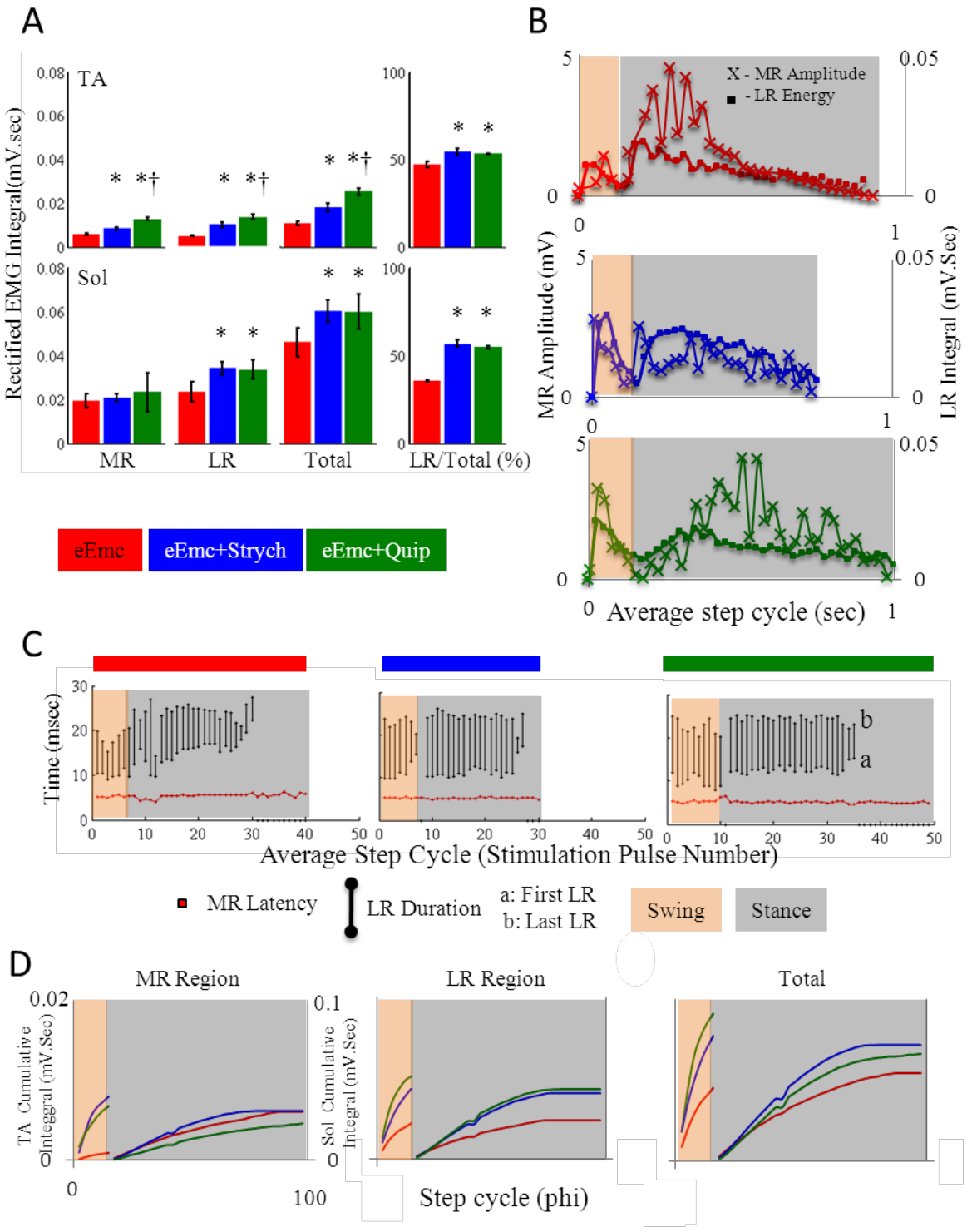

Figure 3.8: Average evoked potentials during stepping under the influence of eEmc with or without strychnine or quipazine

(A) Average integral levels in the TA (top panel) and Sol (bottom panel) EMG in the MR, LR, and total regions and the relative percentage of the LR (LR/Total) during stepping (13.5 cm/s) with eEmc alone (red), eEmc+Strych (blue), and eEmc+Quip (green). * and †: significantly different from eEmc and eEmc+Strych, respectively, at $P > 0.05$. (B) The average MR amplitude and latency for each stimulus pulse are shown for the eEmc alone (red), eEmc+Strych (blue), and eEmc+Quip (green) conditions. (C) Plots showing the average MR latency (red line) and LR duration (vertical lines; a, first LR; b, last LR) for each stimulation pulse within a step cycle. (D) Average cumulative integral curves for the TA and Sol EMG during the swing and stance phases for all step cycles for the MR, LR, and total regions under the three conditions tested. Values are mean ± SEM for 5 rats, 10 steps/rat.

More unique features of the effects of Strych and Quip became apparent when comparing the time course of the changes in the MR within the flexor and extensor phases of the step cycle (Fig. 8B and 9A). For example, the peak level of activation in the soleus during stance was higher with eEmc alone than with eEmc+Quip or eEmc+Strych (Fig. 8B). The amplitude of the MR in response to eEmc+Strych was more modest but at the same time persisted at a more constant level throughout the stance phase. Note also that eEmc+Quip resulted in a more prolonged stance phase compared to eEmc alone or eEmc+Strych (the results were similar for the LRs). The impact of the enhancement of the swing and stance phases attributable to Strych and Quip was made apparent by the more prolonged activation within each 25 ms epoch (Fig. 8C). The net effect of the stimulation pulse on the LR integral relative to the MR integral was greatest for the eEmc+Strych condition and smallest with eEmc alone during the stance phase (Fig. 9A).

To further examine the dynamics of this activation pattern relative to the phase of the step cycle, we calculated the cumulative integrated EMG attributable to the MR and LRs (Fig. 8D). The importance of this cumulative effect, theoretically, would be related to the speed of movement occurring throughout the step cycle as well as to the duration of the flexor and extensor phases of the step cycle. This rationale is based on the assumption that a higher and longer level of activation (increased MR and LR amplitude) results in higher muscle forces attributable to more muscle fibers being activated or the muscle fibers being activated at a higher frequency. Given this interpretation the results predict that under the conditions of the present experiment the level of activation attributable to the MR is consistently higher than that attributable to the LRs in response to eEmc alone (Fig. 8B and 9A). The opposite tends to occur in response to eEmc+Strych. eEmc+Quip also enhances the LRs relative to the MR during the stance phase compared to eEmc alone, has a unique effect in prolonging the duration of this enhancement, and probably contributes significantly to a longer stance phase (Fig. 8B).

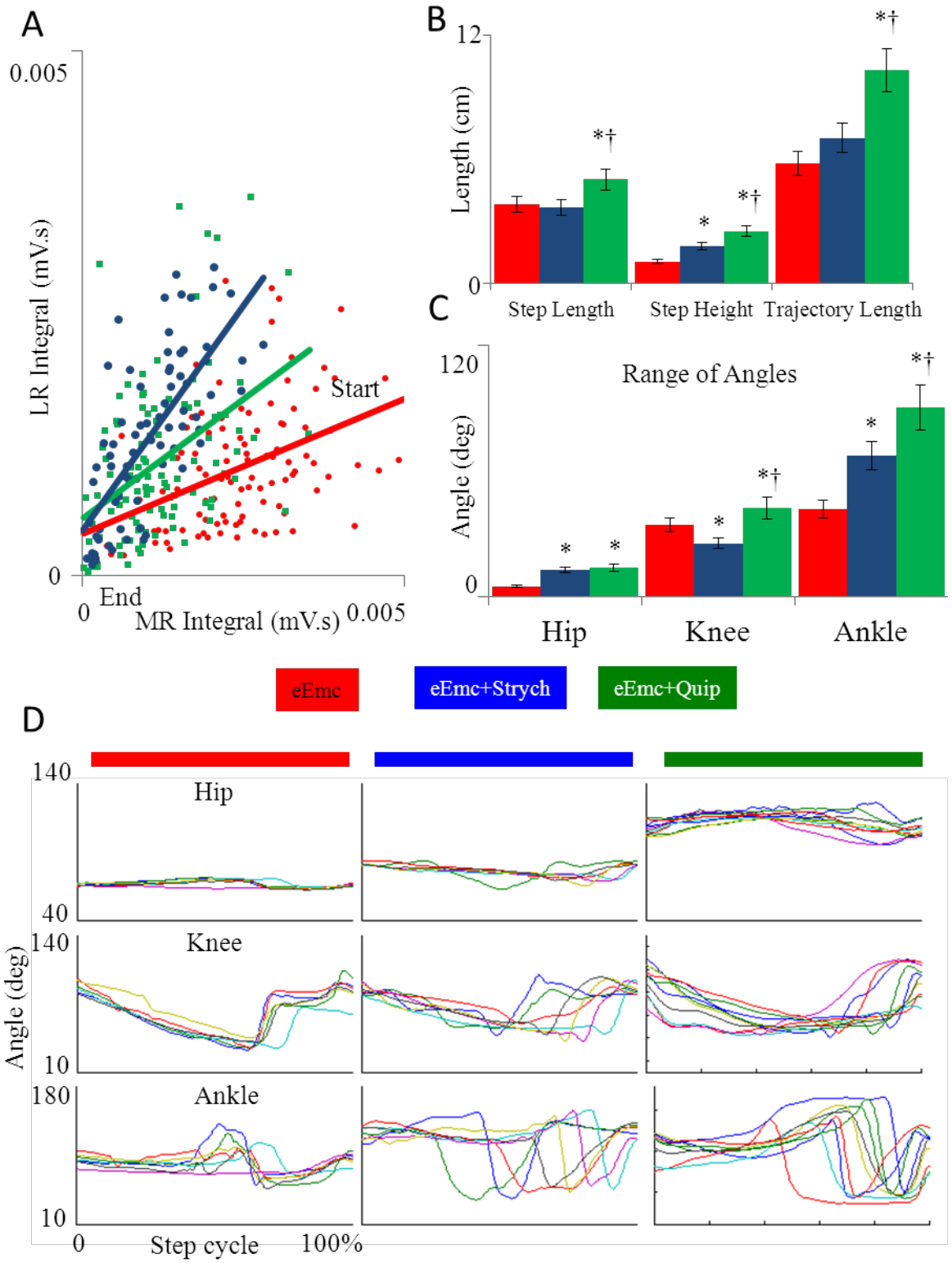

Figure 3.9: Evoked potentials and kinematics characteristics during stepping under the influence of eEmc with and without strychnine or quipazine

(A) Each dot represents the MR and LR integral from a single eEmc pulse from the start to the end of the stance phase (n = 3 rats, 5 steps per rat). (B) The average step length, step height, and trajectory length are shown for the eEmc alone (red), eEmc+Strych (blue), and eEmc+Quip (green) conditions (n = 5 rats, 5 steps per rat). (C) Average range of angle excursions during a step cycle for the eEmc alone (red), eEmc+Strych (blue), and eEmc+Quip (green) conditions (n = 5 rats, 5 steps per rat). D) Hip, knee, and ankle angles from normalized step cycles for each condition (n = 3 rats, 3 steps per rat). * and † in (B) and (C): significantly different from eEmc and eEmc+Strych, respectively, at $P > 0.05$.

Compared to eEmc alone, eEmc+Strych increased step height during treadmill locomotion (Fig. 9B). In addition, the excursion at the hip and ankle joints was greater and that at the hip smaller at the knee with eEmc+Strych than eEmc alone (Fig. 9C and D). eEmc+Quip had a more robust effect on the step kinematics increasing step length, step height, and trajectory length compared to both eEmc alone and eEmc+Strych (Fig. 9B). With eEmc+Strych the excursion at all joints was greater than with eEmc alone and greater at the knee and ankle than with eEmc+Strych (Fig. 9C and D).

DISCUSSION

We recently demonstrated progressive post-lesion changes in the MR and LRs in the extensor muscles during standing (Lavrov et al., 2006) and phase-dependent modulation during stepping in control rats (Gerasimenko et al., 2006) and humans (Courtine et al., 2007) and in spinal rats (Lavrov et al., 2008) and SCI patients (Dy et al., 2010). As observed previously (Gerasimenko et al., 2007; de Leon et al., 1999), locomotion was facilitated by eEmc and by Quip or Strych in spinal animals. The present data demonstrate in an adult *in vivo* preparation using an unanesthetized rat that there are unique patterns of evoked potentials having a range of delay times relative to the stimulation pulses and predictable changes in the persistence of post-stimulation responses that appear to play a role in defining the kinematics of the stance and swing phases of the step cycle. These unique patterns generate predictable functional "footprints" that could be used to formulate optimal combinations of electrical and pharmacological neuromodulation of the spinal circuitry in facilitating specific motor tasks even when there is no supraspinal input to the lumbosacral spinal cord.

What are the MR and LRs in the EMG bursts?

Although the MR have some properties consistent with spinal cord monosynaptic circuits (Lavrov et al., 2006, 2008) and their latency is similar to the responses recorded with magnetic spinal cord stimulation in normal and spinal rats (Chiba et al., 2003), there is no compelling reason to assume that this response can be attributed solely to the classical monosynaptic reflex when stimulating Ia afferents. As the MR is a single response with a relatively constant latency after the stimulation pulse, it may represent a simple mechanism involving a few spinal networks that could facilitate the generation of the locomotor pattern. The

latency of the first component of the LRs, on the other hand, as recorded during standing probably results from more than one synaptic delay (Lavrov et al., 2006). Some combination of eEmc and afferent input derived from the moving hindlimbs appears to facilitate multiple spikes within the LR region of the EMG burst. We speculate that the multiple peaks of the LRs reflect primarily variable numbers of synaptic events within the constantly changing neural networks involved at any given phase of the step cycle rather than a synchronized reflex responses being generated with a similar delay. Among the neural networks that control the extensor muscles, we speculate that there could be multiple parallel, as well as in series, networks that generate the LRs that are not strictly time-linked to individual stimuli.

Multiple LRs of varying amplitudes and latencies reflect the dynamic proprioception associated with the moving hindlimbs and suggest that the origin of these evoked responses is due to activation of a complex interneuronal network modulated pharmacologically, electrically, and through proprioception. These responses cannot be classified as stereotypical reflex responses generated by activation of specific fibers and/or pathways.

The lack of LRs in both the soleus and TA during the interburst period (Fig. 2B) could be attributed to presynaptic inhibition between antagonistic muscles. The mechanism for the systematic and progressive delay of about 2 ms with successive stimuli within the stance phase of the step cycle is not clear. Intuitively it seems unlikely to be only attributable to a progressively increasing complexity, i.e., number of synapses, of the network. Given that the evoked potentials were recorded in the muscles, there could be several simpler mechanisms to explain the systematic delay of LRs during stance. There could be a progressive change in the neuronal excitability in response to successive stimuli, a property that theoretically could be at the level of the neuromuscular junction, the motoneurons, or the interneuronal networks driving

the motoneurons. Given that this phenomenon is not evident in the MR, the most logical site for this effect would seem to be the interneuronal networks that drive and coordinate the motoneurons.

Step cycle dependent mechanisms for stepping

The formation of the EMG bursts in the soleus and TA involved the modulation of both the MR and LRs, but the modulation of the LRs was phase dependent only in the soleus (Figs. 2 and 3). In contrast, EMG activity in both the flexor and extensor muscles showed only MR during the interburst interval (Fig. 2). Thus, it appears that the neural networks responsible for the genesis of the EMG pattern for extensor muscles during stepping are mediated by the modulation of MR, whereas this process is associated with a switching from MR to LR pathways in the flexor muscles (Gerasimenko et al., 2006). LRs were present during the entire TA burst of the swing phase and during the first portion of the soleus burst that is related to foot placement on the treadmill during the initial portion of the stance phase. The later portion of the soleus burst contains only an MR and is related to the supportive and extension reactions during the later portion of the stance phase. Thus the interval of the step cycle where LRs were observed requires precise movement and control.

Based on these findings LRs probably reflect the activation of spinal networks involved in complex motor programs, such as coordination of precise movements during stepping. These networks could be responsible for planning and executing the next step. During the swing phase, these networks may be planning the position of the foot for the next stance phase based on afferent information received during the previous step and from the contralateral hindlimb. During the beginning of the stance phase when the foot touches the treadmill, it seems

likely that the afferent information processed in the spinal cord helps in maintaining balance, posture, coordination of different hindlimb muscles, and the ability to make appropriate adjustments (Musienko et al., 2012; Zhong et al., 2012). During the later portion of the stance phase these circuits are normally "disconnected" to provide only supportive reactions. We speculate that during this 'disconnected' state the neural networks also are dedicated to modulating the MR and LRs of the contralateral limb.

The role of afferent input on the effect of eEmc in facilitating stepping

In the absence of any supraspinal influence the sensory input from hindlimb receptors determines the formation of adaptive motor patterns in spinal rats during stepping facilitated by epidural stimulation (Lavrov et al., 2008). In fact, the spinal rats can perform forward, sideward, and backward stepping depending on the direction of the treadmill movement (Courtine et al., 2009, Shah et al., 2012). In addition, during bilateral stepping facilitated by eEmc of spinal rats with a unilateral deafferentation, each limb is dependent on the afferent information from the ipsilateral side (Lavrov et al., 2008). As the animal recovers, there is a reorganization of the spinal circuitry to adapt for the lack of afferent information from the deafferented side.

In this study we demonstrate a direct relationship between the LRs in the soleus and the afferent information being processed in the spinal cord (Fig. 6). The number of LRs increases significantly during weight-bearing stepping compared to toe stepping or air stepping (Fig. 3). In addition we show that with increasing treadmill speeds, the number of LRs in the soleus decreases, whereas the MR remains consistent (Fig. 4). Thus, the number of LRs is associated with the duration of foot contact and loading with the treadmill. Combined, these findings demonstrate a very close link between stepping and the presence of LRs in spinal animals

(present data and Lavrov et al., 2008) and that there is an important role of afferent information in shaping the LRs.

Mechanisms of neuropharmacological modulation and activation of spinal networks

de Leon et al. (1999) demonstrated that the ability of spinal cats to step can be dramatically and rapidly enhanced by inhibiting the glycinergic pathways. They also reported a prolonged EMG burst duration during step testing in cats that were trained to stand. In contrast to the lengthened stance phase of the step cycle based on the EMG burst duration of the soleus, in the presence of eEmc+Strych the stance duration was reduced compared to eEmc alone (Fig. 8B). Our data suggest that the modulation of the step cycle by strychnine could be attributed to enhanced LRs and MR, but with a relatively greater effect on the LRs during both the swing and stance phases of the step cycle (Fig. 8B and C).

A wide range of studies demonstrates the importance of 5-HT-mediated neuromodulation of locomotion (Rossignol et al., 1998; Jacobs and Fornal, 1993). These studies have reported 5-HT-mediated increases in cycle period, primarily during the stance phase, in spinal animals. In the present study, we show that the effects of Quip on the step cycle differ in several ways from that of Strych. Relative to eEmc alone, eEmc+Quip increased the MR and LRs in the TA to a greater extent than that observed with eEmc+Strych. The largest qualitative difference in the soleus between eEmc+Quip and eEmc+Strych was the greater prominence of the MR relative to the LR with eEmc+Quip. In addition, the MR and LRs occurred over a more prolonged period during eEmc+Quip compared to eEmc+Strych resulting in a significantly longer stance phase with eEmc+Quip (Fig. 8B and C). Based on these comparisons, one might predict that the

combined effects of these two drugs could be complementary or even synergistic given that their mechanisms of neuromodulation of the locomotor networks have fundamentally different characteristics. These pharmacological interventions neuromodulate the physiological state of the spinal networks so that they will process the ensemble of sensory information associated with the kinetics and kinematics of stepping. This processing, in turn, generates a predictable efferent pattern from the relevant motor pools. In essence the combination of the physiological state and the sensory ensemble that it reads generates a unique, predictable footprint.

Can the functionality of the spinal circuitry be embedded in the dynamic patterns of the MR and LRs during stepping in spinal rats?

The present data demonstrate distinct differences in the temporal dynamics of the modulation of the MR and LRs throughout the stance phase of a step. In the presence of Strych the physiological state of the circuitry seems to be modulated in a way that results in markedly enhanced LRs and MR immediately upon placement of the paw during the second phase of extension (Forssberg et al., 1980) resulting in a significantly greater stiffness, i.e., less yield, in the early phase of stance (Fig. 8B). The physiological state generated by Quip, on the other hand, results in a considerably more moderate response to foot placement in the LRs and MR and consequently results in less stiffness and a greater yield. Another feature of Quip is a prolongation of both the LRs and MR resulting in a longer stance phase (Fig. 8B and C). These two contrasting pharmacological effects on the stance phase demonstrate dramatically different pharmacological footprints on the spinal circuitry and how it responds to proprioception (Fig. 8B & 9B). These results also demonstrate the temporal dynamics of both the LRs and MR and can potentially serve as important biomarkers for understanding the relationship between

pharmacological treatments and the kinetics and kinematics of stepping (Fig. 9C & 9D).

Chapter 4

Development of a multi-electrode array for spinal cord epidural stimulation to facilitate stepping and standing after a complete spinal cord injury in adult rats

Abstract

Stimulation of the spinal cord has been shown to have great potential for improving function after motor deficits caused by injury or pathological conditions. Using a wide range of animal models, many studies have shown that stimulation applied to the neural networks intrinsic to the spinal cord can result in a dramatic improvement of motor ability, even allowing an animal to step and stand after a complete spinal cord transection. Clinical use of this technology, however, has been slow to develop due to the invasive nature of the implantation procedures, the lack of versatility in conventional stimulation technology, and the difficulty of ascertaining specific sites of stimulation that would provide optimal amelioration of the motor deficits. Moreover, the development of tools available to control precise stimulation chronically via biocompatible electrodes has been limited. In this chapter, we outline the development of this technology and its use in the spinal rat model, demonstrating the ability to identify and stimulate specific sites of the spinal cord to produce discrete motor behaviors in spinal rats using this array.

We have designed a chronically implantable, rapidly switchable, high-density platinum based multi-electrode array that can be used to stimulate at 1-100 Hz and 1-10 V in both

monopolar and bipolar configurations to examine the electrophysiological and behavioral effects of spinal cord epidural stimulation in complete spinal cord transected rats. In this chapter, we have demonstrated the effectiveness of using high-resolution stimulation parameters in the context of improving motor recovery after a spinal cord injury. We observed that rats whose hindlimbs were paralyzed can stand and step when specific sets of electrodes of the array are stimulated tonically (40 Hz). Distinct patterns of stepping and standing were produced by stimulation of different combinations of electrodes on the array located at specific spinal cord levels and by specific stimulation parameters, i.e., stimulation frequency and intensity, and cathode/anode orientation. The array also was used to assess functional connectivity between the cord dorsum to interneuronal circuits and specific motor pools via evoked potentials induced at 1 Hz stimulation in the absence of any anesthesia.

Therefore the high density electrode array allows high spatial resolution and the ability to selectively activate different neural pathways within the lumbosacral region of the spinal cord to facilitate standing and stepping in adult spinal rats and provides the capability to evoke motor potentials and thus a means for assessing connectivity between sensory circuits and specific motor pools and muscles.

Introduction

It is well established that the spinal cord contains intricate computing units capable of performing rapid ongoing motor processing of complex proprioceptive and cutaneous input during coordinated motor behaviors such as standing and stepping (Grillner 1975). Neural networks in the lumbosacral spinal cord (i.e., central pattern generators (CPG)) can function autonomously (without any brain control) to produce the characteristic alternating motor patterns of gait and to compensate for errors and obstacles (Edgerton et al.,2004, Hodgson et al.,1994) using only sensory information from the limbs (Fossberg 1979, Harkema et al.,1997, Musienko et al.,2007, Lavrov et al.,2008). More recently it has become recognized that these networks have the ability to process complex sensory ensembles that can serve as the controller of posture and locomotion [Musienko et al.,2007, Harkema et al.,2011, Musienko et al.,2011)

The rat or cat spinal cord isolated from supraspinal control via a complete low- to mid-thoracic spinal cord transection produces locomotor-like patterns in the hindlimbs when facilitated pharmacologically and/or by epidural spinal cord stimulation ([9,11Gerasimenko et al.,2003, 2007)]. Thus, locomotor-like patterns can be modulated by stimulation of the networks intrinsic to the spinal cord without the contribution of descending signals. To take advantage of these properties, a more thorough knowledge of the mechanisms of spinal cord stimulation, along with a more detailed understanding about specific sites and parameters of stimulation and their corresponding motor output is needed.

Ichiyama et al (2005) reported that epidural electrical stimulation of the spinal cord can induce rhythmic, alternating hindlimb locomotor activity in chronic spinal rats. Stimulation at the L2 spinal segment at frequencies between 30 and 50 Hz consistently produced successful bilateral stepping. Similar epidural stimulation at other spinal segments were less effective, e.g.,

epidural stimulation at the T13 or L1 evoked rhythmic activity in only one leg and stimulation at the L3, L4, or L5 produced mainly flexion movements.

More recently, completely paralyzed (motor complete, sensory incomplete) human subjects were implanted with a commercially available spinal cord electrode array and stimulation package originally designed for pain suppression (Harkema et al.,2011). Stimulation of specific spinal segments (caudal electrodes, ~ S1 spinal level) in combination with the sensory information from the lower limbs and weeks of stand training was sufficient to generate full weight-bearing standing. These subjects also recovered some voluntary control of movements of the toe, ankle, and the entire lower limb, but only when epidural stimulation was present. Thus it appears that the epidural stimulation provided excitation of lumbosacral interneurons and motoneurons that, when combined with the weak excitatory activity of descending axons that were not otherwise detectable, achieved a level of excitation that was sufficient to activate the spinal motor circuits. These results demonstrate that some patients clinically diagnosed as having complete paralysis can use proprioceptive input combined with some synaptic input from descending motor signals, perhaps residual but functionally silent without epidural stimulation to the spinal motor circuits to generate and control a range of motor functions during epidural stimulation.

These studies suggest that the intrinsic circuits of the spinal cord, if intact, are desirable targets for stimulus-based therapies and strategies. Secondly, the specific stimulation parameters are highly critical to the pattern and quality of functional motor output. The technological hurdles to reach these targets are non-trivial. We have designed an electrode array capable of selectively stimulating specific segments of the rat spinal cord to generate discrete motor responses using a high-density grid of epidural electrodes embedded within a thin-film

flexible substrate (Nandra et al.,2011, Rodger et al.,2005). Although stimulation occurs at the surface level, miniaturization of the electrode contacts and the use of materials specific to our design restrict the effective field of stimulation to a smaller area as compared with conventional wire surface electrodes.

The specificity and high-density features of the electrode array enable us to capitalize on two key features of the spinal cord circuitries that are believed to be essential for rehabilitating posture and locomotion after spinal cord injury (SCI). Firstly, the spinal circuitry can be neuromodulated and the stimulation can be carefully delimited to affect only relevant areas of the spinal cord, thus optimizing the motor outcome. Secondly, as locomotor circuitries are highly plastic and adapt when provided with sensory cues during motor training (Edgerton et al., 2004), the density and versatility of the multi-electrode array allows for rapid adjustments of stimulation protocols and adaptations to physiological changes that may occur in the spinal cord over time after injury.

Several design features were taken into account including the flexibility of the array, biocompatibility of the base, and stability of the electrodes for a chronic implant. Parylene C has emerged as an ideal electrode array substrate due to its biocompatibility, insulative properties, flexibility, and tear resistance (Wolgemuth 2000). The tear resistance of parylene C is large, making the arrays robust to surgical manipulation, as well as to stresses produced in a moving animal (Rodger et al., 2007). The techniques needed to manufacture these multi-electrode devices are not unprecedented. This is the first time, however that this technology has been adapted for the express purpose of controlling stimulation at specific sites of the spinal cord in a chronic preparation. Given these basic principles and the results observed in the animal models with conventional wire electrodes (Gerasimenko et al., 2003, Ichiyama et al., 2008) and from the

human subjects with commercially available electrode arrays (Harkema et al.,2011), it seems likely that use of a high-density electrode array could greatly improve the quality of standing and stepping after paralysis.

Rather than attempting to impose exogenous motor commands, this strategy will capitalize on the intrinsic neural control mechanisms of the spinal cord that remain functional post-SCI, enabling the spinal circuits to process sensory input and to serve as the primary source of control. Using this technology, we can selectively and differentially activate distinct neuronal groups distributed throughout the spinal cord, allowing stimulation of specific electrodes on the array to modulate the physiological state of the spinal circuitry so that sensory input can control various hindlimb motor outputs. To examine the potential capabilities of this stimulation system, we used this novel, flexible, high-density stimulating electrode array during the recovery of standing and stepping in adult rats after a complete mid-thoracic spinal cord transection.

Methods

Data were obtained from adult female Sprague Dawley rats (270-300 g body weight). Pre- and post-surgical animal care procedures have been described in detail previously (Roy et al., 1992). The rats were housed individually with food and water provided ad libitum. All survival surgical procedures were conducted under aseptic conditions and with the rats deeply anesthetized (isoflurane gas administered via facemask as needed). All procedures described below are in accordance with the National Institute of Health Guide for the Care and Use of Laboratory Animals and were approved by the Animal Research Committee at UCLA.

Five rats were implanted and tested for the biocompatibility of the implant and stability of the spinal electrodes and stable EMG responses. Once we were satisfied with the stability of the design, a stable array was implanted in one animal to collect chronic physiological data. Due to the complex nature of the fabrication, implantation, and experimentation processes, a limitation of the study is that the standing and stepping data presented in this manuscript are from one animal chronically implanted for 5 weeks. These data will be used as a stepping-stone for future experiments and design modifications.

Implant fabrication

The electrode array is fabricated with a sandwich structure of parylene-metal-parylene. Parylene-C is a USP class VI biocompatible material and its mechanical properties provide the necessary flexibility to make good epidural contact with the spinal cord. The micro-fabrication process begins with an optional layer of sacrificial photoresist being spun onto a wafer followed by a deposition of 10-μm thick parylene-C. It is patterned to form a structural frame around the outside of the electrode array and is followed by another layer of 5-μm thick parylene-C. The

metal layer, patterned using liftoff, was deposited using e-beam evaporation and was composed of a titanium adhesion layer of 100Å followed by 2000Å of platinum. The top layer of parylene-C is also 5-μm thick. Openings to expose the metal, formation of the frame, and overall device outline were achieved with oxygen plasma etching. The completed devices were released from the wafer using acetone or water and annealed in a vacuum oven at 200°C for 48 hours. The full micro-fabricated device is 59 mm x 3 mm and has a 9 x 3 array of electrodes which are 200 x 500 μm with a parylene grid structure to help prevent delamination (Figs. 4.1 & 4.12).

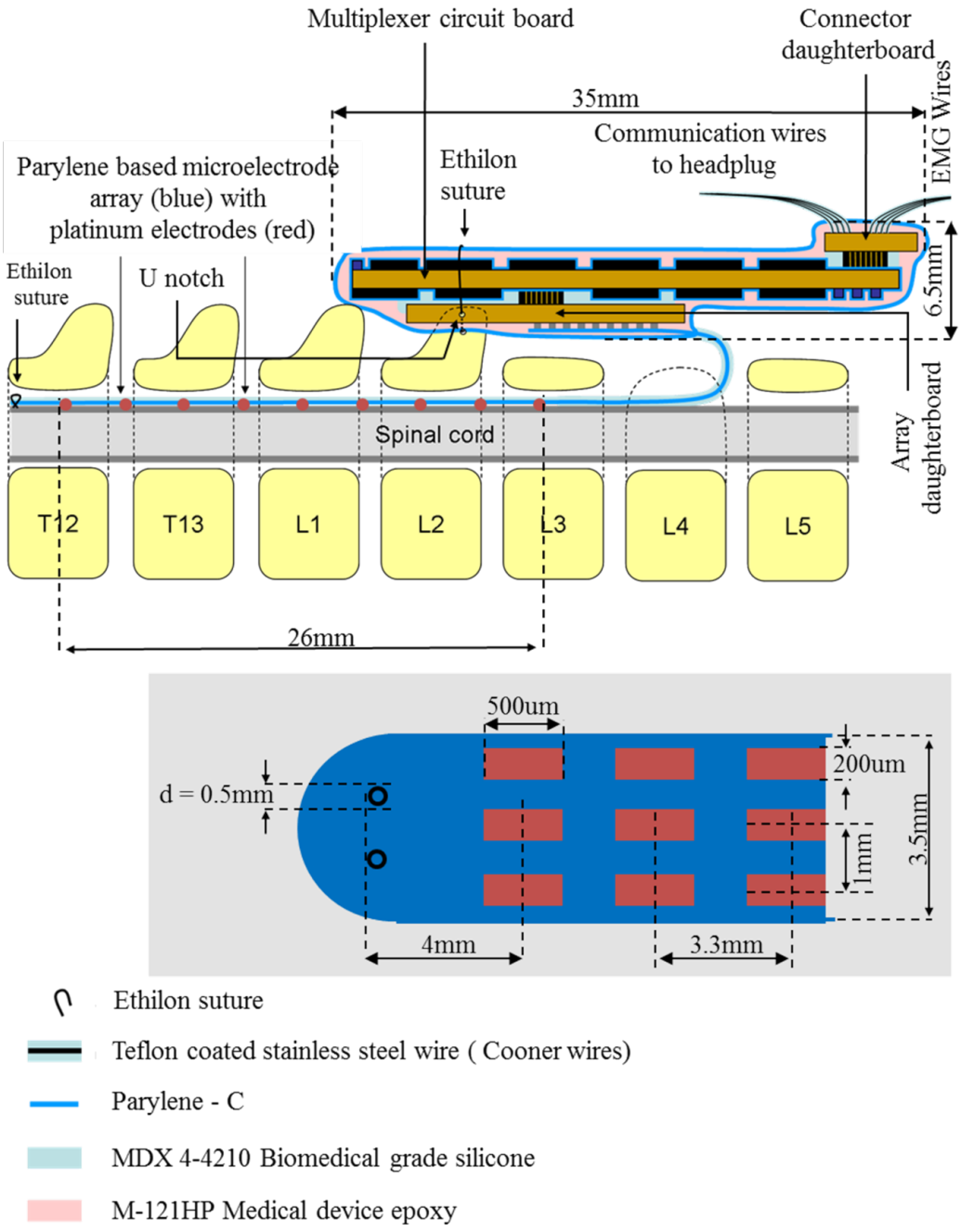

Figure 4.1: Parylene based electrode array with multiplexer control and its position and layout with respect to the spinal cord when implanted in the rat. Inset shows the dimensions and design of the platinum electrodes.

The complete implant consists of this electrode array, a multiplexer circuit, various wires, and a headplug (Fig. 4.1). The multiplexer circuit routes connections and performs pre-ampification to reduce the total number of headplug wires needed from 37, for a passive implant as seen in prior work by our group (Nandra et al.,2011), to just 12 wires. This design reduces surgery complications and also serves as a stepping-stone for a fully wireless design. The electrode array is interfaced to the multiplexer board with conductive epoxy. The implant then is sealed with 20 μm of parylene, biocompatible silicone (MDX 4-4210), biocompatible epoxy (Loctite M-121HP), and another 20 μm of parylene.

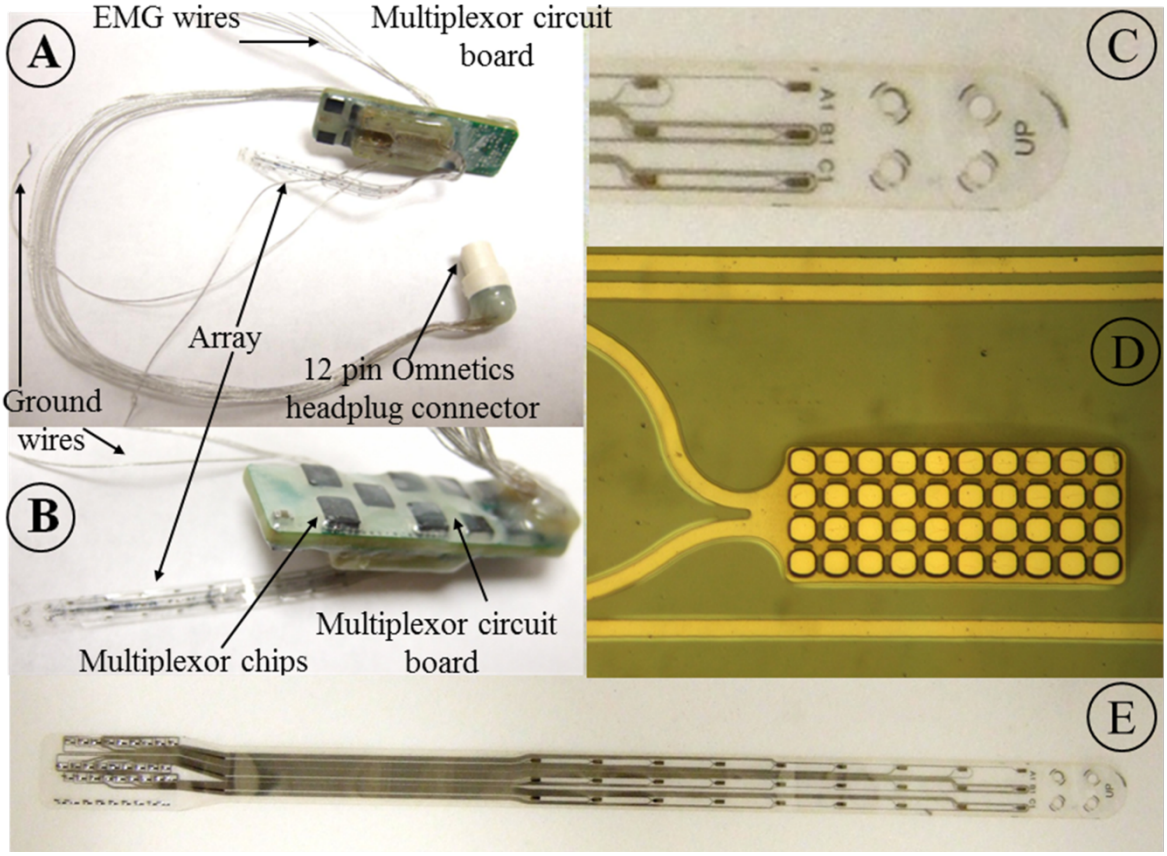

Figure 4.2: A) Ventral view of the implant system: external omnetics connector that is secured to the skull (headplug connector), Teflon coated stainless steel wires from the connector to the circuit board (control wires), electrode array, EMG wires, and ground wires. B) Dorsal surface of the implant. C) Zoomed in view of the multi-electrode array: note the plantinum electrodes, platinum traces, and the holes used to thread the array during implantation. D) Zoomed in view of a single electrode along with the platinum traces. Note the grid-like pattern formed by the parylene on the electrode used to prevent delamination. E) Expanded view of the parylene-based array with platinum electrodes.

Control box and multiplexer circuit board description

The overall system block diagram is illustrated in Figure 3. The stimulation host computer has a software interface to choose the electrodes to be stimulated along with the stimulation intensity (specified by pulse voltage or current), pulse duration, and pulse frequency. The software generates a 5 MHz signal stream to be output by an ADC/DIO card (National Instruments PXI-6123) and fed to the control box. This signal stream consists of the *EN*, *Clock*, and *Data* signals (Figs. 4.3 & 4.4) to control the multiplexer circuit in the implant, *PWM* (pulse-width modulation) and *Mode* signals for stimulation, and a *Sync* signal to synchronize EMG recordings. The control box has an op-amp circuit (Fig. 4.5) to generate the stimulation signal. The *PWM* signal is passed through an RC filter and creates any required analog waveform at V_{in} (0-2.5 V, ~5 μs effective pulse rise time). When *Mode* is low, the op-amp circuit is transformed to that of a positive gain voltage amplifier ($V_{Stim+} = 25(V_{in} - 0.86V)$); otherwise, it becomes a voltage controlled current amplifier ($I_{Stim+} = (V_{in} - 1.92V)/667\Omega$). This circuit generates the *Stim+* signal to be fed into the implant's multiplexer circuit along with the control signals and power lines. The *Stim+* signal also is fed back to the NI ADC for voltage monitoring along with the *CurrSense+* and *CurrSense-* signals for current monitoring. The pre-amplifier signals *A1-A4* from the implant pass through a voltage divider (adjustable) and then are output to the EMG amplifier (AM Systems Model 1700). The stimulation signals (*Stim+* and *Stim-)* are fed into the multiplexer circuit that is designed to operate in 4 modes to meet the experimental requirements (both current and future). Current generations: 1) stimulation between almost any two sets of spinal electrodes (bipolar and monopolar) or EMG wires (needed to check position of EMG implants during surgery), and 2) recording from 4 EMG wire pairs. Future generations: 1) recording between multiple pairs of electrodes on the spinal cord, and 2) recording from 4

electrodes in the same column with relative to a fifth electrode in the same column (e.g., A1-A9, A3-A9, A5-A9, and A7-A9).

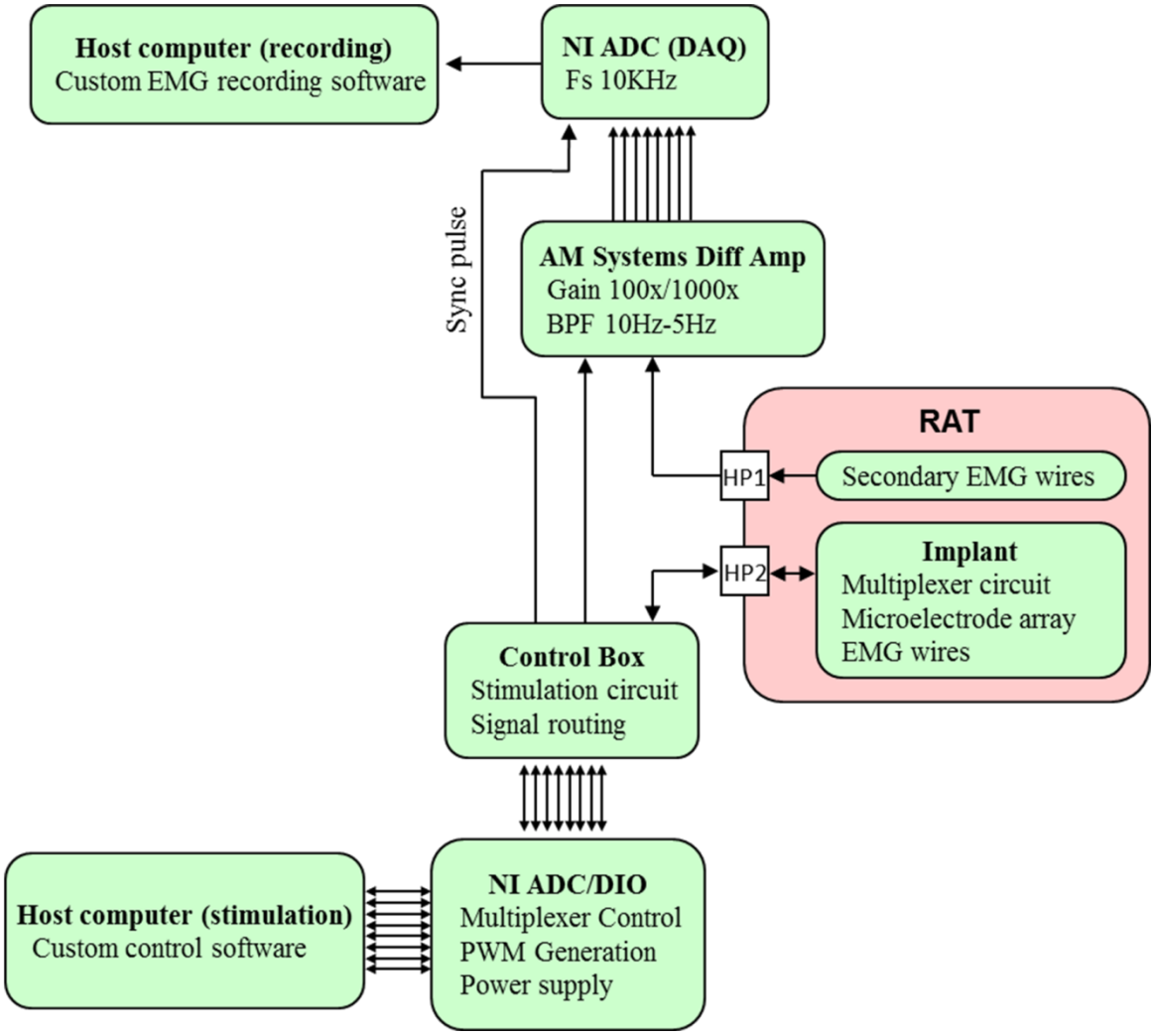

Figure 4.3: Block diagram showing the experimental setup of the stimulation and recording system. The arrows indicate the direction of the flow of the signals.

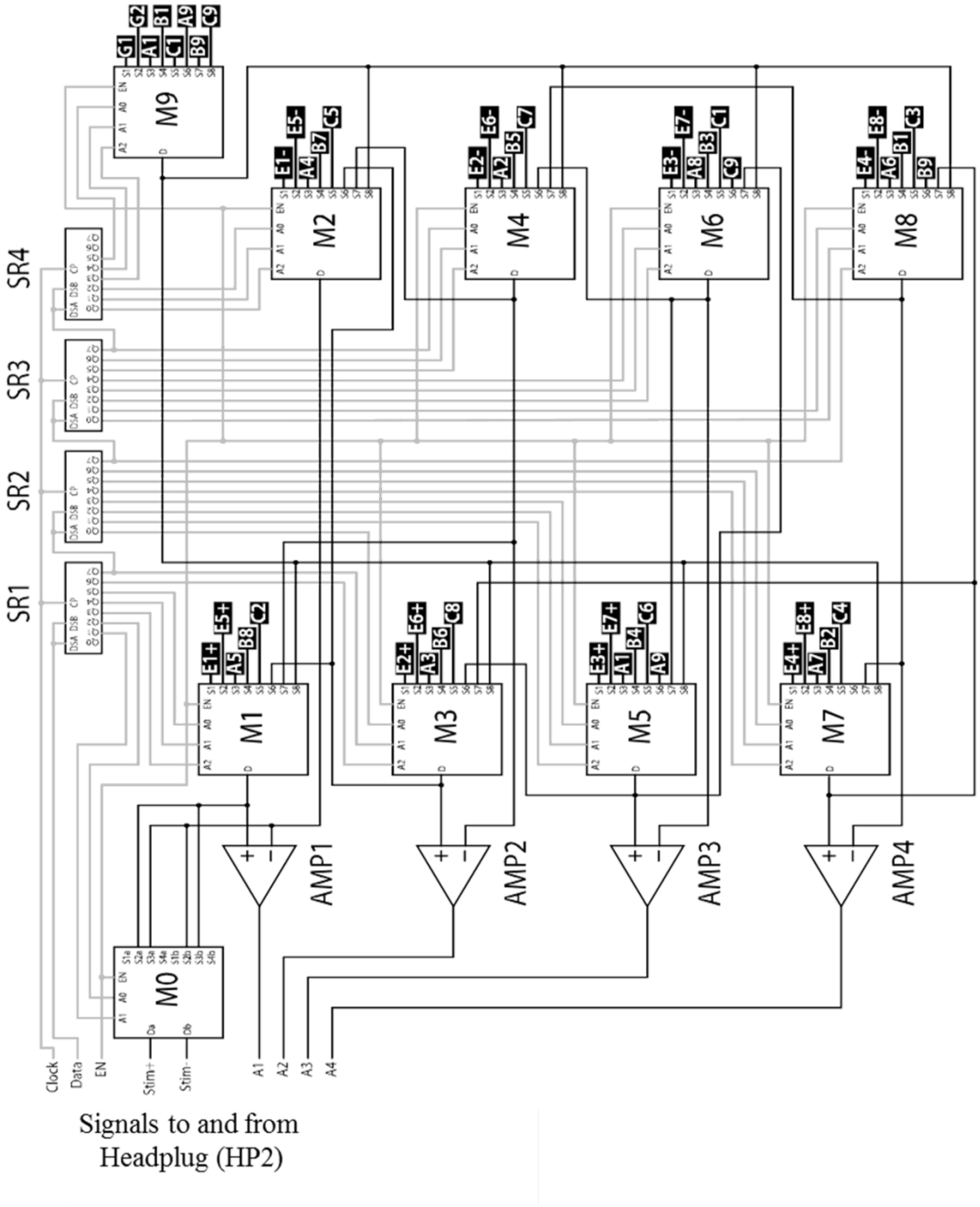

Figure 4.4: Multiplexer circuit schematic. The 9 lines on the left along with the 3 power lines (12 V, 5 V, and Gnd, not shown) represent the 12 control lines used to interface the array and EMG wires with the external electronics. Black tags represent the spinal cord electrodes and EMG wire pairs.

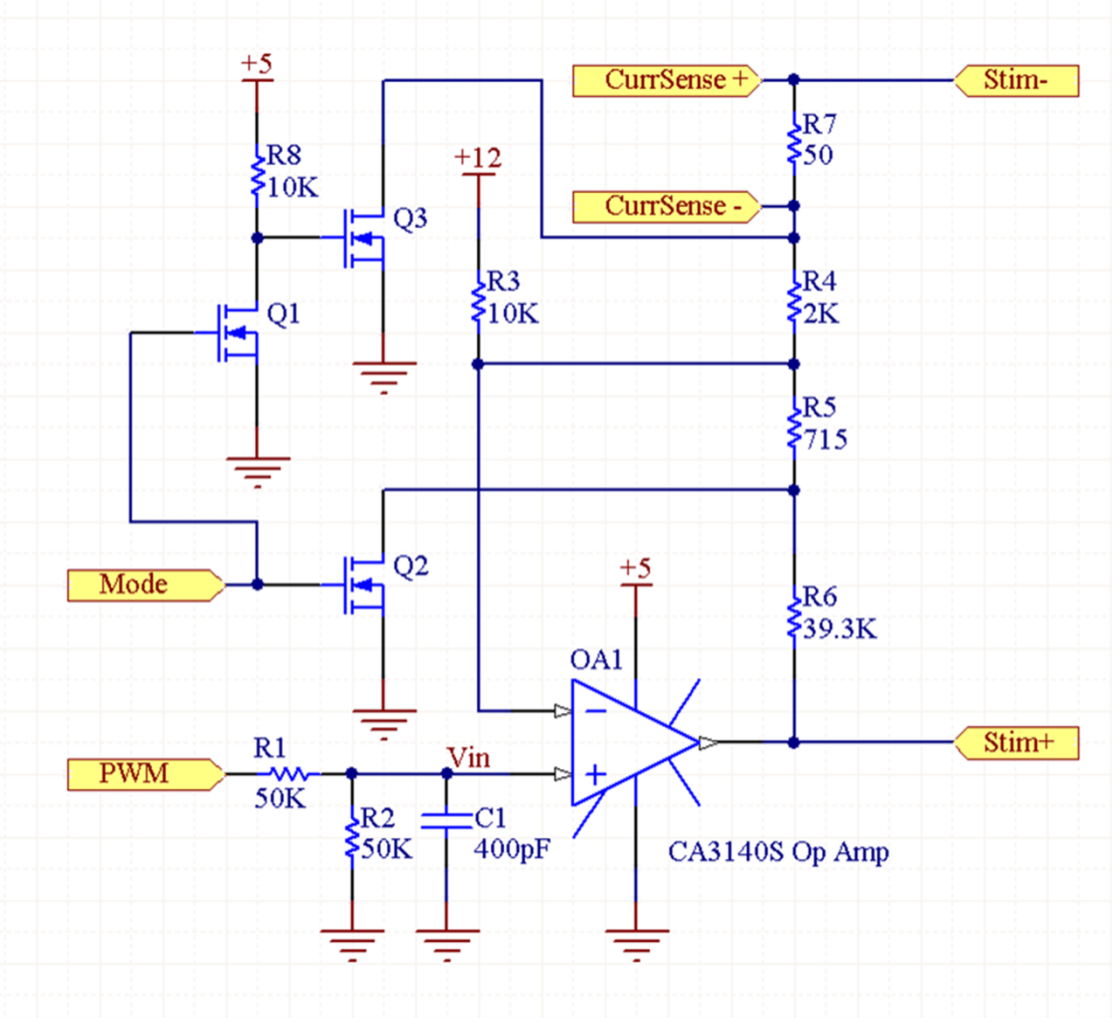

Figure 4.5: Stimulator circuit used describing the use of the Pulse Width Modulation (PWM) to generate the required voltage between *Stim+* and *Stim-*. *Mode* controls current mode vs. voltage mode, and the *CurrSense* signals allow the stimulating host computer to measure the drawn current.

In the multiplexer circuit schematic (Fig. 4.4), the black tag refers to the connection to the spinal electrode. En+, En- refers to an EMG wire pair. A3 refers to a spinal electrode in column A and row 3. G1 and G2 are reference wires (implanted on either side of the back of the animal).

Three power lines are present that are used to power up the system: 12 V, 5 V, and ground (not shown in Fig. 4.4). The desired operating mode of the circuit is configured by sending a 30-bit serial data stream (6 μs configuration time) through *Clock* and *Data* that feed into the shift registers SR1-SR4 (NXP Semiconductors 74HC164). These shift registers, in turn, configure the 10 analog multiplexer chips (M0 to M9) and *EN* enables them. M0 (Analog Devices ADG1209) and M1-M9 (Analog Devices ADG1209) are interconnected such that after configuration the desired electrodes or EMG wires are routed either to *Stim+* and *Stim-* during stimulation or to pre-amplifiers AMP1-AMP4 (Analog devices AD8224) during recording. The pre-amplifiers are differential instrumentation amplifiers set to a gain of 200 and send outputs to *A1-A4*. The circuit board uses four copper layers and measures 10.3 mm by 33.2 mm.

Head connector and intramuscular EMG electrode implantation

A small incision was made at the midline of the skull. The muscles and fascia were retracted laterally, small grooves were made in the skull with a scalpel, and the skull was dried thoroughly. Two amphenol head connectors with Teflon-coated stainless steel wires (AS632, Cooner Wire, Chatsworth CA) were securely attached to the skull with screws and dental cement as described previously (Roy et al., 1992, Ichiyama et al., 2005). The medial gastrocnemius (MG), tibialis anterior (TA), and soleus (Sol) muscles were implanted bilaterally with EMG recording electrodes as described by Roy et al. (Roy et al., 1991). Skin and fascial incisions were made to expose the belly of each muscle. Two wires extending from the multiplexer circuit board (Fig. 1) were routed subcutaneously to each muscle. The wires were inserted into the muscle belly using a 23-gauge needle and a small notch (~0.5-1.0 mm) was removed from the insulation of each wire to expose the conductor and form the electrodes. The wires were secured in the

belly of the muscle via a suture on the wire at its entrance into and exit from the muscle belly. The wires were looped at the entrance site to provide stress relief. The proper placement of the electrodes was verified 1) during the surgery by stimulating through the stimulator in the control box (Figs. 4.1-4.4) and by selecting the correct channels on the multiplexer circuit board and, 2) post-surgery by dissection.

Spinal cord transection and array implantation

A partial laminectomy was performed at the T8-T9 vertebral level and a complete spinal cord transection to include the dura was performed at ~T8 spinal level using microscissors. Two surgeons verified the completeness of the transection by lifting the cut ends of the spinal cord and passing a glass probe through the lesion site. Gel foam was inserted into the gap created by the transection as a coagulant and to separate the cut ends of the spinal cord.

To implant the array, the spinous processes and portions of the dorsal and lateral aspects of the vertebrae of T11, and the rostral portions of T12 and L4 were removed. A suture (4.0 Ethilon) was inserted through the opening at T11 and passed down to the opening at L4. This suture then was threaded into holes at the most rostral end of the electrode array (Fig. 1 inset) and used to gently pull the array rostrally between the dura and the vertebral column. The most rostral row of electrodes was placed at the middle of the T12 vertebrae. Once the array was positioned satisfactorily over the dorsal surface of the spinal cord, the rostral end of the array was sutured (8.0 Ethilon) to the dura to secure it in position. The L3 spinous process was removed to form a flat surface. The multiplexer circuit board then was placed on the vertebral column over L3. A U notch on the ventral surface of the implant (Fig. 4.1) was secured into the L2 spinous process via a suture (4.0 Ethilon) threaded through the hole on the circuit board and

tied around the L2 spinous process. A schematic diagram of the electrode placement and approximate location of the motor pools for the MG, TA, and Sol muscles are shown in Figure 5.

All incision areas were irrigated liberally with warm, sterile saline. All surgical sites were closed in layers, i.e., muscle and connective tissue layers with 5.0 Vicryl (Ethicon, New Brunswick, NJ) and the skin incisions on the back and the limbs with 5.0 Ethilon. All closed incision sites were cleansed thoroughly with warm saline solution. Analgesia was provided by buprenex (0.5–1.0 mg/kg, 3 times/day s.c.). The analgesics were initiated before the completion of the surgery and continued for a minimum of 2 days post-surgery. The rats were allowed to fully recover from anesthesia in an incubator. The spinal rats were housed individually in cages that had ample CareFresh bedding and their bladders were expressed manually 3 times/day for the first 2 weeks after surgery and 2 times per day thereafter. The hindlimbs of the spinal rats were moved passively through a full range of motion once per day to maintain joint mobility.

Stimulation and testing procedures

Two stimulation protocols were used for testing (Figs. 4.3 & 4.4). A monopolar configuration where the cathode was chosen from one of the 27 electrodes on the array and the anode placed subcutaneously on the side of the body (ground wire, Figs. 4.1-4.4). On the testing day, the cathode was selected sequentially among all electrodes on the array to systematically cover the entire surface of the array and was used to record evoked potentials from the MG, TA, and Sol muscles bilterally. Evoked potentials were recorded from the muscles implanted with EMG electrodes by stimulating the spinal cord at a low frequency (1 Hz) and voltage sweep from 1-8 V (1 V increments) with the rat suspended in a jacket with its hindpaws in contact with a stationary treadmill (bipedal standing position). A bipolar configuration where both the cathode

and anode were selected from the set of 27 electrodes on the array was used to facilitate the standing and stepping ability of the spinal rats. Sub-sets of bipolar configurations were tested on different test days. For both the bipolar configurations, the stimulation frequency was based on previously reported values (Lavrov et al.,2008, Gerasimenko et a.,2003, Courtine et al.,2009, Lavrov et al., 2006) and the stimulation intensity was varied (range from 1-8 V) to optimize the standing and stepping ability of the spinal rats. EMG was recorded from the MG, TA, and Sol bilaterally while the rats stepped bipedally on a specially designed motor-driven rodent treadmill at 13.5 cm/s (de Leon et al., 2002). The treadmill belt had an anti-slip material that minimized slipping while stepping. The rats were placed in a body weight support system that allowed the rat to support the maximum amount of its body weight while stepping with plantar placement (de Leon et al., 2002).

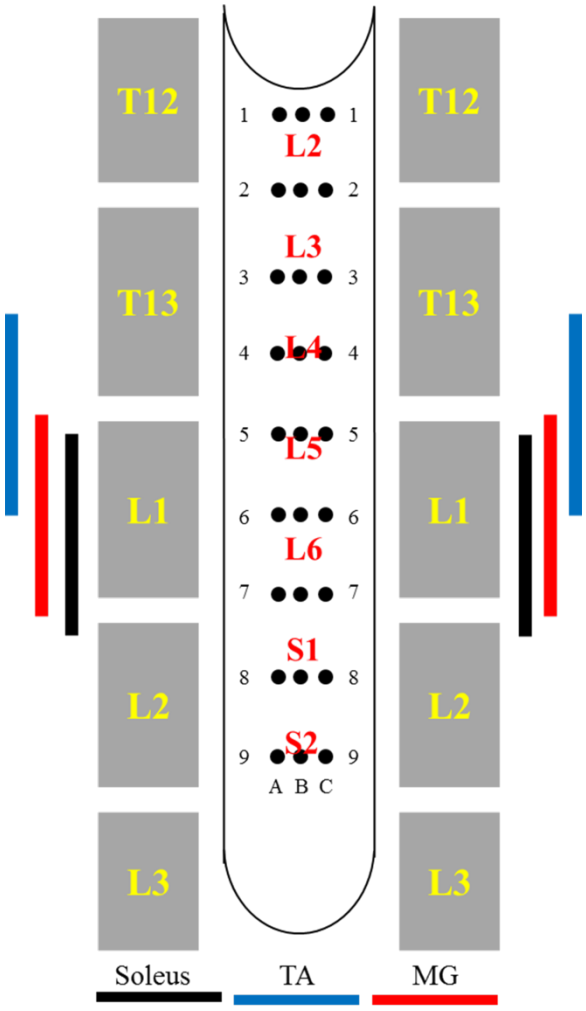

Figure 4.6: Vertebral (yellow) and spinal cord (red) levels with respect to the 27 electrodes on the array (black circles) and the location of the motor pools of an ankle flexor (TA, tibialis anterior) and two ankle extensor (MG, medial gastrocnemius, and Soleus) muscles.

Data collection and analysis

EMG recordings from the hindlimb muscles were pre-amplified by the multiplexer circuit board and an external control box before being sent to a band-pass filter (1 Hz to 5 KHz), externally amplified (A-M Systems Model 1700 differential AC amplifier: A-M Systems, Carlsborg, WA), and sampled at a frequency of 10 KHz using a custom data acquisition program written in the LabView development environment (National Instruments, Austin, TX) as described previously (Courtine et al., 2009). Evoked potentials during standing with low frequency stimulation (1 Hz) were analyzed as described previously (Gerasimenko et al., 2003, Lavrov et al., 2006). The responses were divided into 20 ms windows using the stimulation pulse as the trigger. These windows were averaged over 10 evoked responses and the peak response was detected using custom MATLAB code. These peaks then were binned into early (ER, 1-3 ms latency), middle (MR, 4-6 ms latency), and late (LR, 7-10 ms) responses. The mean amplitudes and latencies for the ER, MR, and LR for both the MG and TA at different intensities of stimulation for each electrode on the array were determined. The EMG signals during weight-bearing standing under epidural stimulation at higher frequencies were analyzed using a custom script written in MATLAB to estimate the MR (latency 4-6 ms) and LR (latency 10-25 ms). The raw EMG signals during bipedal stepping on the treadmill were rectified and then sent through a low pass filter to form a linear envelope to assess the stepping patterns as previously described (Vejsada et al., 1980).

Impedance measurement

A 400 mV sinusoidal wave (10 KHz with a 10 KΩ resistor in series with the spinal electrode and the indifferent ground) was used to test electrode impedance. The voltage across

the electrode on the spinal cord and the ground placed subcutaneously in the back region was used to measure the electrode impedance. The electrode impedance was inversely related to the ability of the electrode to stimulate the spinal cord.

Results

Facilitation of standing with epidural stimulation

Stimulation of rostral pairs of electrodes at low frequencies (10-15 Hz) produced vibratory movements in both hindlimbs, but did not facilitate standing (Supplemental Video 1). Stimulation at higher frequencies (80-100 Hz) resulted in over-activation of the neuronal circuits and produced some non-specific movements in both hindlimbs with no interlimb coordination during standing. In contrast, stimulation between 40-60 Hz resulted in activation of the extensor muscles in both hindlimbs leading to partial weight-bearing standing (Fig. 4.7, Supplemental Video 1). Thus, distinct motor responses were induced by stimulation of the rostral electrodes at different frequencies. An example of the motor responses produced by stimulation between electrodes A1 (cathode) and C5 (anode) at 40 Hz is shown in Fig. 4.7 and Supplemental Video 1. There is an initial flexion (increased activation of the TA) of the left hindlimb and extension (increased activation of Sol and MG) of the right hindlimb (Fig. 4.7A). Following this immediate response there is a gradual increase in the level of excitation of the extensors. The intermittent bursting shown in the RMG, RSol, and LSol illustrate the activation of circuitries presumably representing significant levels of polysynaptic activity that are not time-linked to the 40 Hz stimuli (Fig. 4.7B). Supplemental Video 1 demonstrates that the right hindlimb initially is bearing greater weight than the left hindlimb. The average evoked responses in selected muscles for 20 stimulations during full weight-bearing standing are shown in Figure 4.7C. MRs with similar latencies (~5 ms), but varying amplitudes, were observed consistently in all muscles. The RMG shows a higher degree of long latency responses (LR) that may be correlated with the relatively high weight bearing by the right limb.

In contrast to stimulation of rostral electrode pairs, bipolar stimulation of caudal electrode pairs at any frequency failed to facilitate weight-bearing standing. This difference between stimulation of rostral vs. caudal electrode pairs clearly demonstrates the importance of the location of the electrodes and the frequency of stimulation in tuning the neural circuits to generate a specific motor response.

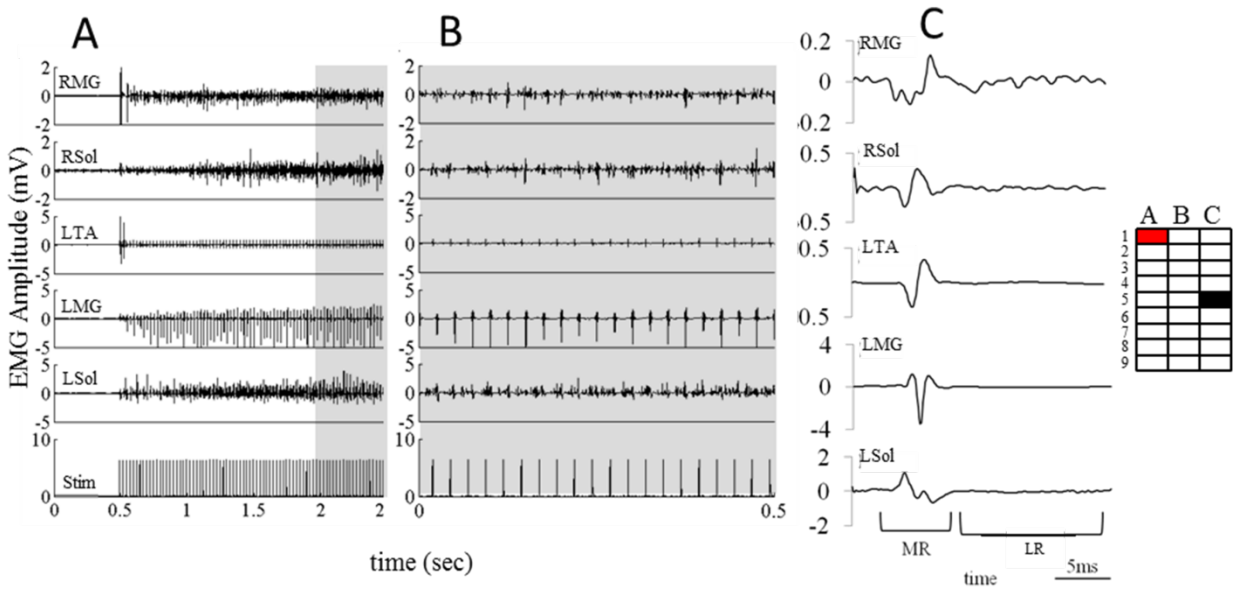

Figure 4.7: A) EMG from ankle flexor and extensor muscles bilaterally while the spinal rat transitions from a crouched to a standing position facilitated by epidural stimulation (40 Hz). B) EMG from the right (R) and/or left (L) MG, Sol, and TA muscles during standing under the influence of epidural stimulation (highlighted region in A). C) Average responses of 20 evoked potentials during full weight-bearing standing under the influence of epidural stimulation. MR represents the monosynaptic response and the LR represents the long latency polysynaptic response. Note the different amplitude scales for each muscle.

Facilitation of stepping via epidural stimulation

The ability of the spinal rats to step with weight support on a treadmill at 13.5 cm/s was tested by stimulating (40 Hz, pulse width of 0.2 ms, and 3-4 V) different pairs of electrodes on the array. The results using 6 different bipolar combinations are shown in Figure 8. Two combinations with the cathode rostral to the anode resulted in coordinated bilateral stepping with good body weight support and interlimb coordination (Fig. 4.8A & B, Supplemental Video 2). Two other combinations with the cathode rostral to the anode also produced good bilateral stepping with interlimb coordination, but at a lower body weight support (Fig. 4.8C & D). Thus, stimulation with these 4 combinations of electrodes produced bilateral stepping with good interlimb coordination although the rats had varying weight-bearing capability based on the position of the anode and cathode. In a case where the cathode was placed caudal to the anode and both electrodes were at the caudal portion of the electrode array, the rat was unable to generate weight-bearing stepping (Fig. 4.8E). In another case where the cathode and the anode were placed adjacent on the same column of the electrode array with the cathode placed more rostrally than the anode, the rat was able to generate step-like movements, but with little or no body weight support (Fig. 4.8F and Supplemental Video 3).

Combined, these results highlight the importance of the position of the cathode and anode on the spinal cord to facilitate stepping after injury and that the ability to choose between specific sites of stimulation is critical for modulating the types of motor output produced by the epidural stimulation.

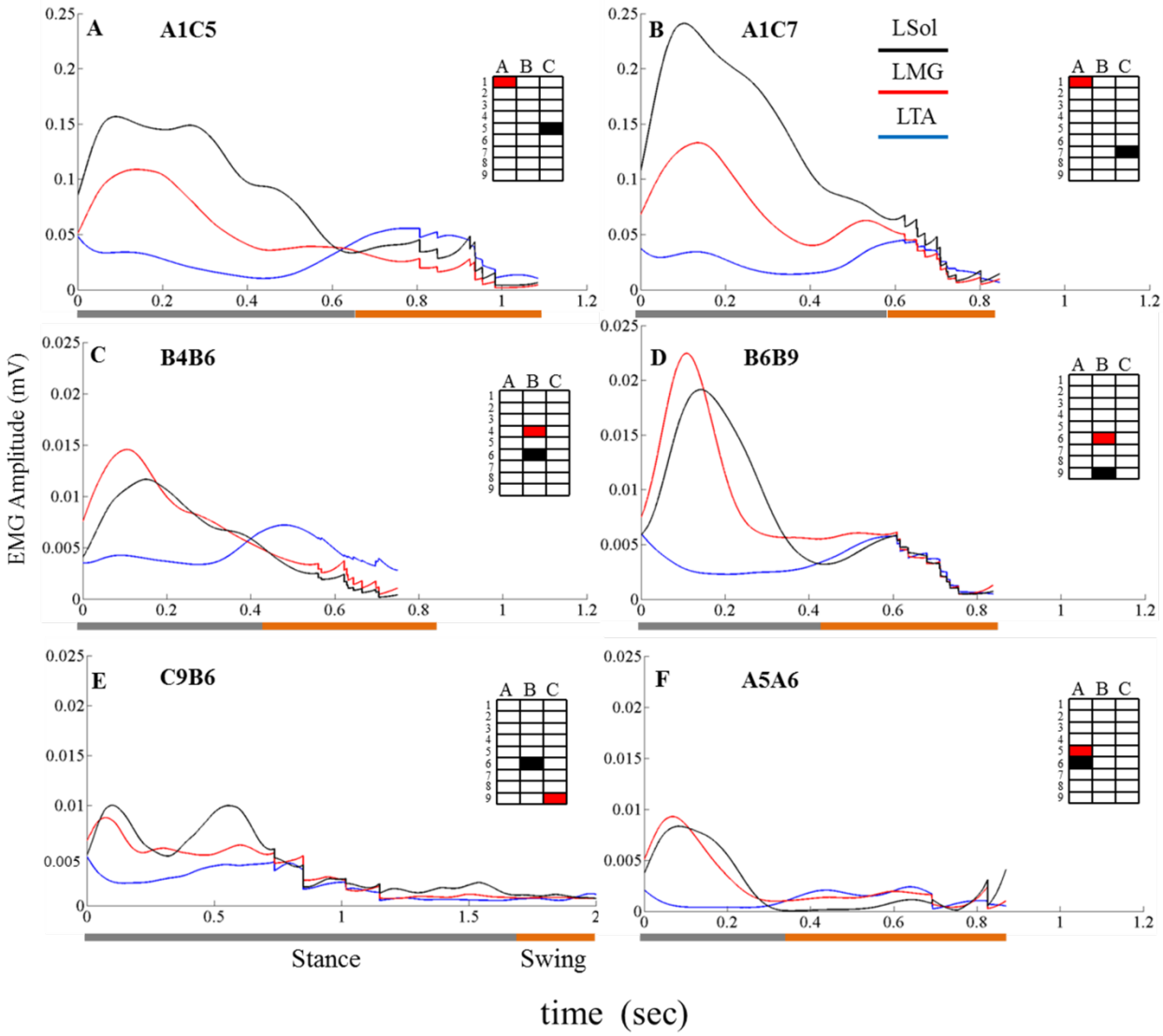

Figure 4.8: Average (10 consecutive steps) rectified EMG (linear envelope) for an ankle flexor (TA) and two ankle extensors (Sol and MG) during stimulation (at 40 Hz, pulse width 0.2 ms, and 3-4 V) using different electrode combinations. A and B: coordinated bilateral stepping with good body weight support. C and D: bilateral stepping with lower body weight support compared to A and B. A, B, C, and D: cases demonstrating good rhythmic bilateral stepping ability with varying degrees of body weight support depending on the position of the cathode and anode on the spinal cord. E: Uncoordinated and non-rhythmic stepping during stimulation with the cathode

positioned more caudal than the anode demonstrating the importance of having the cathode at a more rostral segment compared to the anode. Note that the time scale for E is the longest due to extended periods of dragging. F: rhythmic stepping movements with very low (near zero) body weight support, demonstrating the need to position the cathode and anode at different columns to facilitate stepping with good body weight support. Note the EMG amplitude scale in A and B are an order of magnitude higher than in C-F.

Modulation of evoked potentials based on electrode position

The mean amplitudes and latencies for the ER, MR, and LR for both the MG and TA at different intensities of stimulation for each electrode on the array are shown in Figures 9, 10, and 11, respectively. In general, the ER initially appears around rows 4-6 (Fig. 9). Rows 4 and 5 correspond to the beginning of the motor pools for the TA, MG, and Sol muscles (Fig. 9), suggesting that the ER may be a direct response to stimulation of afferents without any synaptic delay. As the intensity of stimulation increases, a similar ER (with latency ~3 ms) was observed in rows 1-3 even though these electrodes were not directly over the motor pools of the ankle flexor and extensor muscles. Responses with these short latencies were generally independent of their relative position to the motor pools. The ER amplitudes increased with increased stimulation intensity, consistent with previous results using wire electrodes (Lavrov et al., 2006, Gerasimenko et al., 2003). The increased spatial resolution of the microelectrodes, however, also shows variability across the array, a feature that is not apparent when using wire electrodes.

Similar to the ER, the MR begins around rows 4 and 5 and generally increases in amplitude with increasing stimulation intensity (Fig. 4.10). Unlike the ER, however, the latency

of the MR in the TA remains constant from rows 4 to 9 across the stimulation intensities and the latencies in the MG decrease in the more caudal electrodes for any given intensity of stimulation. The MR from stimulation of the most rostral sets of electrodes (rows 1, 2, and 3) shows a much higher latency (~7 ms) compared to the MR from rows 4, 5, and 6 (4-6 ms), i.e., the start of the motor pools of the ankle flexors and extensors, suggesting that there could be an additional synapse for the evoked potential from the rostral region of the spinal cord before the signal reaches the muscles (Fig. 4.10 – e.g., RMG 4V). The MR in the muscles are higher in the right limb in both the TA and MG at any given voltage (Fig. 4.10 – e.g., TA and MG at 5 V) through the C, or right side, column of electrodes located ipsilateral to the muscles. Thus, it appears that these evoked responses may be highly dependent on the spatial location of the stimulation. These results highlight the importance of the ability to stimulate specific sites from a therapeutic and device standpoint.

The LR are very general with no real pattern in the observed latencies or amplitudes, suggesting that the LR is a result of activation of various spinal interneuronal circuits that eventually filter down to the muscles. Stimulation at all intensities generates an LR at all electrodes. Several investigators have shown the importance of the presence of an LR to the stepping ability in spinal rats (Lavrov et a., 2006, Lavrov et al., 2008). While the specific interaction of the interneurons and the possible structure of these network circuitries are beyond the scope of this chapter, it is nonetheless important to identify the diversity of the signals evoked at this level. These results provide important insight into the highly crucial nature of the finite spatial resolution of the stimuli. In addition, the above data indicate that the LR is far less electrode specific than the ER and MR. The functional significance of these observations needs further study.

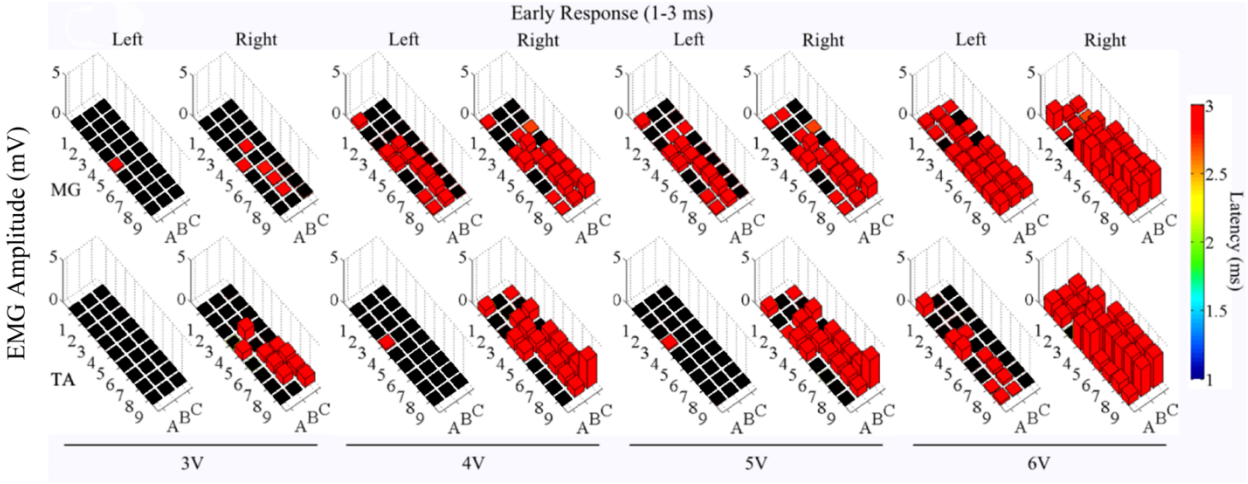

Figure 4.9: Early responses (1-3 ms latency) recorded in the MG (top row) and TA (bottom row) bilaterally during low frequency (1 Hz) monopolar stimulation (3-6 V) at each electrode on the array. The height of each bar indicates the amplitude and the color indicates the latency of the response. The black box indicates a case where no response was recorded for that particular window.

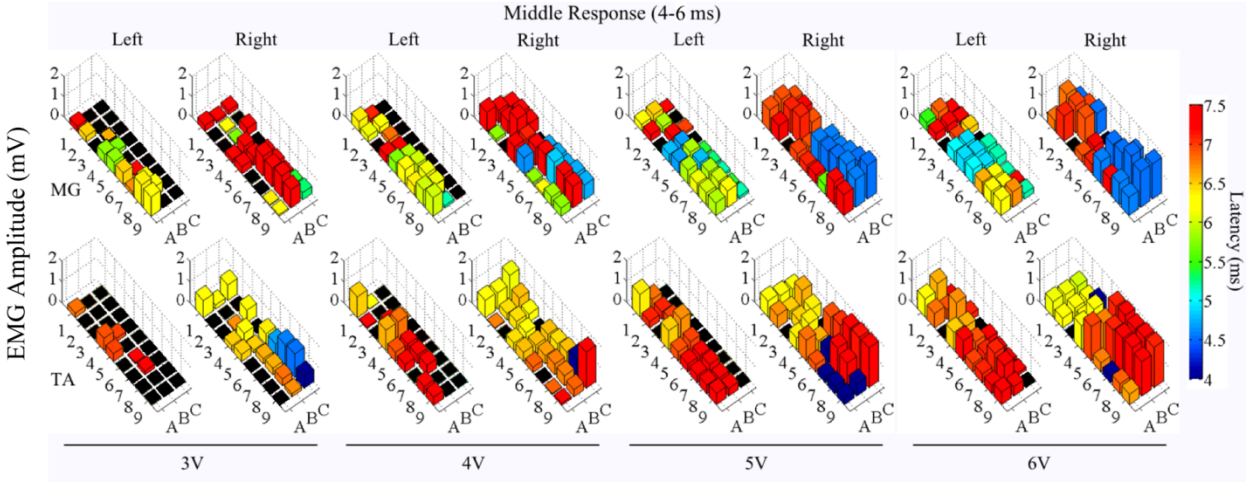

Figure 4.10: Middle responses (4-6 ms latency) recorded in the MG (top row) and TA (bottom row) bilaterally during low frequency (1 Hz) monopolar stimulation (3-6 V) at each electrode on the array. The height of each bar indicates the amplitude and the color indicates the latency of the response. The black box indicates a case where no response was recorded for that particular window.

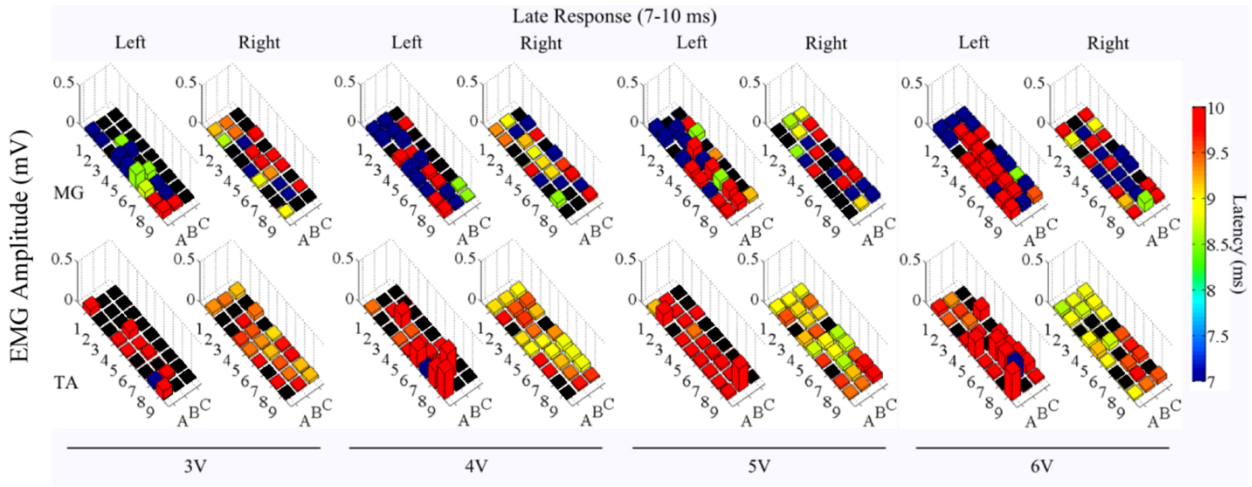

Figure 4.11: Late responses (7-10 ms latency) recorded in the MG (top row) and TA (bottom row) bilaterally during low frequency (1 Hz) monopolar stimulation (3-6 V) at each electrode on the array. The height of each bar indicates the amplitude and the color indicates the latency of the response. The black box indicates a case where no response was recorded for that particular window.

The LR are very general with no real pattern in the observed latencies or amplitudes, suggesting that the LR is a result of activation of various spinal interneuronal circuits that eventually filter down to the muscles. Stimulation at all intensities generates an LR at all electrodes. Several investigators have shown the importance of the presence of an LR to the stepping ability in spinal rats (Musienko et al., 2007, Lavrov et al., 2008, Harkema et al., 2011). While the specific interaction of the interneurons and the possible structure of these network circuitries are beyond the scope of this paper, it is nonetheless important to identify the diversity of the signals evoked at this level. These results provide important insight into the highly crucial nature of the finite spatial resolution of the stimuli. In addition, the above data indicate that the LR is far less electrode specific than the ER and MR. The functional significance of these observations needs further study.

Biocompatibility and durability of the chronic multi-electrode array

Electrode impedances were measured daily to assess their reliability and to determine the potential for the array to be implanted chronically. At 5 weeks post-implantation only 2-4/27 electrodes were non-functional due to high impedances. Table 1 shows the average impedance from 5 animals at 1, 3, and 5 weeks post-implantation. Electrodes with higher impedances needed a higher threshold to generate any motor response. We observed that two electrodes (C4 and B5) had very high impedance and were nonfunctional at 3 and 5 weeks post-implantation. Electrode impedances at 7 days post implantation were similar to impedances recorded invitro (in saline) prior to implantation. Stimulation via these electrodes neither generated any evoked potentials nor facilitated standing or stepping during monopolar/bipolar stimulation. Even though the C4 electrode showed high impedance (shown as a black dot in Figs. 4.9-4.11), it did not

affect the functional ability of neighboring electrodes, i.e., C3, C5, or B4. The spinal cord morphology was assessed (in all five rats) after explanting the array at 5 weeks post-implantation. Neither the array nor the rest of the implant compressed the spinal cord and no signs of infection were observed around the implant. The hindlimb muscles were inspected visually and showed no signs of damage or atrophy beyond that expected after a complete spinal cord transection.

Table 1: Average impedances for each electrode in chronically implanted arrays

		Days Post-Implantation								
		7			**21**			**35**		
		Array Columns								
		A	**B**	**C**	**A**	**B**	**C**	**A**	**B**	**C**
Array Rows	**1**	4.8	5.6	5.9	8.5	11.1	12.8	4.8	13.9	17.0
	2	6.6	5.3	8.2	9.2	5.4	9.8	5.2	13.9	17.0
	3	8.0	6.7	8.7	5.3	5.0	6.5	3.9	6.8	5.6
	4	4.1	9.4	4.0	4.9	6.3	25.9	5.1	18.0	50.0
	5	4.1	3.8	6.7	7.7	7.0	7.1	4.4	36.0	7.0
	6	5.6	11.5	6.4	4.1	11.6	5.4	4.4	13.0	6.0
	7	7.2	4.9	8.9	7.3	6.7	7.4	4.1	8.0	9.8
	8	5.8	5.1	4.3	5.2	6.5	6.0	11.2	8.0	7.0
	9	5.3	6.1	6.2	7.5	5.8	6.2	9.2	7.0	7.0

Table 4.1: Values (kΩ) are the average (n = 5) electrode impedances at 7, 21, and 35 days post-implantation. Increased impedance resulted in higher stimulation intensities needed to evoke a functional motor response. Impedances at 7 days post-implantation were similar to impedances recorded prior to implantation.

Discussion

We have demonstrated a novel technique, using a high-density parylene-based multi-electrode platinum array, to selectively activate spinal neurons to facilitate standing and stepping in rats after a complete spinal cord transection at a low-thoracic level. The results demonstrate that spinal rats can stand and step when the spinal cord is stimulated (tonic 40 Hz stimulation) by electrodes located at specific sites on the spinal cord and at specific frequencies of stimulation. The quality of stepping and standing was dependent on the location of the electrodes on the spinal cord, the specific stimulation parameters, and the orientation of the cathode and anode. In addition, the amplitude and latency of evoked potentials were determined in non-anesthetized spinal rats during standing to assess the efficacy of selected spinal circuits. The evoked potentials are critical tools to study selective activation of interneuronal circuits via responses of varying latencies.

Critical features of the stimulation parameters for facilitating standing and stepping

Based on the results, we can generalize that combinations of stimulation with the cathode at the rostral end of the spinal cord results in better stepping ability as compared to combinations with the cathode at the caudal electrodes. This suggests that neurons and neuronal circuits at the rostral end of the spinal cord respond more effectively to the cathode as compared to the caudal sets of electrodes that respond more effectively to the anode. The best results were observed with the cathode and anode located in different rows of the electrode array and the cathode and anode in different columns of the electrode array. The present data also suggest that the more effective

standing and stepping can be obtained with bipolar compared to monopolar stimulation. This issue, however, needs to be examined more thoroughly. While the specific composition of the neuronal circuitry and aggregate networks of the spinal cord must be studied further, it is clear that modulating the stimulation protocol and targeting specific, anatomical sites of the spinal cord lead to variable motor outputs distinct from one another, with unique functional effects.

Modulation of specific motor pools using the multi-electrode array

The evoked potentials from specific muscles during monopolar stimulation at different intensities allowed us to assess the activation of the motor pools of the ankle flexor and extensors in the spinal cord as shown previously (Manzano et al., 1988, Rivero-Melián et al., 1996). Evoked potentials from monopolar stimulation reflect the activation of specific neuronal circuits as demonstrated by the responses shown in Figures 4.9-4.11. Additionally, the higher amplitudes of the MR on the ipsilateral compared to contralateral side demonstrate the ability to selectively activate different circuitries and to stimulate specific anatomical areas and combinations of motor pools. Different levels of inhibition vs. excitation of spinal circuitries also could be induced selectively. This potential to selectively activate specific combinations of motor pools and levels of inhibition and excitation translates into the unique capability of electrode arrays to control motor behavior.

Importance of the multiplexer for chronic implantation with wireless capability in small animals

When the durability of an implant is a requirement, the size and biocompatibility of the device are crucial factors in successfully collecting data. Our animal experiments currently rely upon wire bundles to connect the electrode arrays to external computers and electronics. As the number of required connections and the complexity of the device increases, the size of the wire bundle increases as well, reducing the probability of success of the implant due to potential tissue damage and infections caused by the wire bundles. We have partially addressed this problem in our original design by employing a multiplexer (Fig. 4.4) to reduce the number of required connections and changing the form factor of the electrode package into a more easily implantable design. We now plan to develop a relatively generic implantable wireless multi-channel stimulating/recording engine that can be scaled to different species, e.g., rat, cat, or human. This will make the electrode array more useful in a number of ways. For example, the elimination of the wire bundle will increase the biocompatibility of the implant and reduce chances of infection and tissue damage. Additionally, because the wireless system will be a general device designed to have a variety of applications, the transition from animal to human studies will likely be simplified since the fundamental basis of the device will remain consistent.

Early recovery of stepping and standing after SCI facilitated by epidural stimulation

Several investigators have shown that epidural stimulation at L2 and/or S1 using wire electrodes in combination with motor training can facilitate stepping within 3-4 weeks after a complete spinal cord transaction (Ichiyama et al., 2005, Lavrov et al., 2006). Using the parylene-based platinum electrode arrays described herein we have been successful in facilitating weight-bearing standing and stepping within 8-10 days post-transection. Thus use of the electrode array allows us to tap into the spinal networks to enable stepping sooner after injury as compared to using conventional wire electrodes. Future directions to improve this technology will be to 1) develop computational and mathematical means to detect patterns, determine relationships using evoked potentials, and predict functional outputs, 2) record spinal-evoked potentials during stepping, and 3) combine pharmacological interventions with multi-electrode epidural stimulation as a therapeutic rehabilitation strategy.

Mathematical modeling to characterize motor responses using learning algorithms

The development of mathematical and computational infrastructures to better characterize motor outputs of stimulation will be crucial to the further development of this neuromodulatory technology. The sheer numbers of involved electrodes, the wide range of stimulation parameters, and the number of functional outcome measures represent a matrix of inputs and outputs that creates a bottleneck to accurately analyze all results. Therefore, it will

become necessary to develop tools such as machine-learning algorithms and classification schemes to automate the processing. This is not only important from the perspective of experimental efficiency or basic scientific goals, but particularly from the point of transitioning this technology to clinical therapeutic paradigms. Using a highly differentiated electrode array, it becomes crucial to determine the holistic differences between the smallest variations in the stimulation properties and locations to modulate the networks and produce ordered, desired behavioral outputs. To achieve this, we must develop the means to process and interpret the voluminous information recorded from high-density electrode arrays.

Need for the ability to record evoked potentials from the spinal cord

The full potential for the use of high-density epidural electrode arrays in clinical and basic scientific studies cannot yet be realized due to limitations in currently available implantable stimulating electronics. The stimulators currently FDA-approved for human studies are too limited in the types of stimulation that they can generate and have no capability to record evoked potentials. Currently, we are unable to detect dynamic changes in intra-spinal cord network interactions during stimulation. The importance of the afferent information to motor command and control cannot be overestimated, yet we have little to no information about the ascending signals that form a significant component of the CPG's input data. Adding the ability to record from intrinsic networks of the spinal cord could reveal a great deal about the feedback mechanisms that form the foundation for locomotor pattern generation. This will require that the technology for the electrodes be refined to provide optimal characteristics for both stimulation and recording.

Potential for neuromodulation of the spinal cord and facilitation of specific responses using pharmacological interventions combined with the electrode array

An important aspect of facilitating stepping after SCI is the administration of pharmacological interventions. Although the pharmacological effects are transient, concurrent application of other treatments seems to supplement pharmacologically induced activity (Courtine et al., 2009). These pharmacological treatments appear to raise the excitability of the spinal locomotor circuits by lowering their threshold for activation, and thereby facilitating the effects of multi-electrode epidural stimulation. Specific activation of neuronal networks through the use of an electrode array after administration of pharmacological interventions will allow us to selectively activate specific motor pools for the control of fine movements as well as stepping patterns. Examination of these altered physiological states have the potential to reveal more information about the underlying circuitry of the spinal cord by further delimiting the inhibitory and excitatory components of the circuits responsible for motor behavior, ultimately allowing for the identification and characterization of the neuronal populations responsible for the recruitment of specific motor pools.

Neurophysiological mechanisms and specific sensorimotor integration impacting motor function via the electrode array after SCI

Given the range of motor behaviors that can be generated with modest levels of stimulation, i.e., primarily sub-motor threshold levels, of different combinations of electrodes and at different frequencies, it is evident that the threshold for excitation of different spinal interneuronal networks are being modulated. Conceptually our strategy for facilitating these motor behaviors is to achieve a physiological state that enables the proprioceptive input derived from stepping and standing to serve as the source of control. That is, the "sub-threshold" intensity of stimulation that modulates the spinal circuitry associated with stepping and standing may not, and actually preferably does not, induce action potentials among the pathways extending from sensory afferents to all of the motor pools. Thus, rather than imposing a specific motor response by stimulating at high intensities, and thus precluding proprioceptive modulation, the activated pathways are determined by the ensemble of sensory information being projected in real time to the spinal circuitry. Regarding the degree of selectivity of specific pathways that could be modulated, it is important to recognize that the extensive divergence of a single Ia fiber from each spindle has extensive synaptic connectivity to not only the homonymous motor pools, but also to synergists and indirectly to antagonistic motor pools through Ia inhibitory interneurons (Nelson and Mendell 1978). In addition, robust intersegmental connectivity among the lumbar segments via ascending projections from the sacral segments has recently been reported (Etlin et al., 2010). Combined, these observations are consistent with the interpretation that epidural stimulation combined with pharmacological modulation is impacting many

different pathways simultaneously but in different degrees and proportions based on the stimulation parameters described in the present chapter .

Conclusions

The high density electrode array described in this chapter 1) allows high spatial resolution and the ability to selectively activate different neural pathways within the lumbosacral region of the spinal cord to facilitate standing and stepping in adult spinal rats, and 2) provides the capability to evoke motor potentials and thus a means for assessing connectivity between sensory circuits and specific motor pools and muscles. Our initial data underscore the importance of electrode location and anode-cathode orientation and stimulation properties, especially with respect to future therapeutic devices and modulatory "tuning" of epidural stimulation patterns, to provide optimal stimulation for motor function restoration after SCI in animals and humans. Further revisions and additions to this system, including wireless transmission of data, greater software control of the stimulation properties, and increasingly sophisticated data analysis techniques will allow us to further our work/results and gain insights into the neural circuits responsible for specific functional motor responses.

Chapter 5

Sub-threshold spinal cord stimulation facilitate spontaneous standing and voluntary locomotor-like activity in paralyzed rats

Abstract

We have used epidural stimulation of the spinal cord to enable motor control (electrical enabling motor control, eEmc) after a complete mid-thoracic spinal cord transection in adult rats. The effect of eEmc in paralyzed rats was accomplished using a sub-threshold intensity of stimulation with load-bearing proprioception providing the supra-threshold excitation needed to generate and control hindlimb stepping and standing. In the present study, we hypothesized that eEmc during spontaneous cage activity would greatly increase the activation of the locomotor circuits in paralyzed rats and enhance their motor function. The spinal rats initially were very lethargic in their cages showing little movement. Without eEmc, the rats remained rather inactive with the torso rarely being elevated from the cage floor. When the rats used their forelimbs to move, the hindlimbs were extended and dragged behind with little or no flexion. In contrast, with eEmc the rats were highly active and the hindlimbs showed robust alternating flexion and extension resulting in step-like movements during forelimb-facilitated locomotion and often would stand using the sides of the cages as support. The mean and summed integrated EMG levels in both the flexor and extensor muscles were higher with than without eEmc. These data suggest that eEmc, in combination with the associated proprioceptive input can modulate the

spinal networks to significantly amplify the amount and robustness of spontaneous motor activity in paralyzed rats.

Introduction

A wide range of animal spinal cord injury models and species have shown that stimulation applied to spinal neural networks can dramatically improve motor ability, i.e., enhance the ability to stand and step on a treadmill with partial body weight support (Iwahara et al., 1991, Gerasimenko et al., 2003, Ichiyama et al., 2005, Gerasimenko et al., 2008, Courtine et al., 2009). More recently (Harkema et al., 2011 & Angeli et al., 2012 SFN 2012 abstract) three completely paralyzed human subjects (one classified as ASIA A and two as ASIA B) were implanted with a commercially available spinal cord electrode array and stimulation package originally designed for pain suppression. Epidural stimulation of specific spinal segments (caudal electrodes, ~ S1 spinal level), in combination with the sensory information from the lower limbs and weeks of stand training, was sufficient to generate full weight-bearing standing. These subjects also recovered some voluntary control of movements of the toe, ankle, and the entire lower limb, but only when electrical enabling motor control (eEmc) was present. Thus, one possibility is that modulation of the excitability of the lumbosacral region of the spinal cord via eEmc, combined with the weak excitatory activity of descending axons that were not otherwise detectable, could volitionally achieve a level of excitation that was sufficient to activate the spinal motor circuits above the motor thresholds of a significant number of motoneurons among synergistic motor pools. These results demonstrate that some patients clinically diagnosed as having complete paralysis can use proprioceptive input combined with some input from descending motor signals (perhaps residual but functionally silent without eEmc) to activate spinal motor circuits, thus generating and controlling a range of motor functions via eEmc.

There can be significant levels of spontaneous activity in the paralyzed muscles after a complete mid-thoracic spinal cord transection. For example, in spinal cats during a 24-hr period,

the total amount of integrated EMG activity in the soleus and lateral gastrocnemius muscles was ~25% and ~33% respectively of that occurring in uninjured cats (Alaimo et al., 1984). The present experiment was designed to determine the feasibility of enhancing the amount of spontaneous activity of the paralyzed muscles using modest intensities of stimulation via chronically implanted epidural electrodes placed over the lumbosacral spinal cord in adult spinal rats were put through a rehabilitation process to step on a treadmill for 6 weeks under the influence of eEmc. Therefore, we determined the activity levels and patterns of the hindlimbs of rats having a complete spinal cord transection at a low thoracic level while in their home cages during 6-hour periods with and without continuous eEmc (40 Hz). We hypothesized that eEmc would modulate the spinal locomotor circuits such that the hindlimbs would be more active during periods with than without eEmc. If so this could provide a means of more frequently engaging those neural networks that control the routine, spontaneous postural and locomotor functions that are critical in defining the level of functionality after severe paralysis. In general, the results are consistent with this hypothesis.

Methods

Animal care procedures

Data were obtained from 4 adult female Sprague Dawley rats (270-300 g body weight). Pre- and post-surgical animal care procedures have been described in detail previously (Roy et al., 1992). The rats were housed individually with food and water provided *ad libitum*. All survival surgical procedures were conducted under aseptic conditions and with the rats deeply anesthetized with isoflurane gas administered via facemask as needed. All procedures described below are in accordance with the National Institute of Health Guide for the Care and Use of Laboratory Animals and were approved by the Animal Research Committee at UCLA.

Head connector and intramuscular EMG electrode implantation

A small incision was made at the midline of the skull. The muscles and fascia were retracted laterally, small grooves were made in the skull with a scalpel, and the skull was dried thoroughly. Two amphenol head connectors with Teflon-coated stainless steel wires (AS632, Cooner Wire, Chatsworth CA) were securely attached to the skull with screws and dental cement as described previously (Roy et al., 1992; Ichiyama et al., 2005). Selected hindlimb muscles, i.e., the tibialis anterior (TA) and soleus (Sol), were implanted bilaterally with EMG recording electrodes as described by Roy et al. (1991). Skin and fascial incisions were made to expose the belly of each muscle. Two wires extending from the skull-mounted connector were routed subcutaneously to each muscle. The wires were inserted into the muscle belly using a 23-gauge needle and a small notch (~0.5-1.0 mm) was removed from the insulation of each wire to expose the conductor and form the electrodes. The wires were secured in the belly of the muscle via a suture on the wire at its entrance into and exit from the muscle belly. The proper placement of

the electrodes was verified during the surgery by stimulating through the head connector and post-mortem via dissection.

Spinal cord transection and eEmc electrode implantation procedures and post-surgical animal care

A partial laminectomy was performed at the T8-T9 vertebral level. A complete spinal cord transection to include the dura was performed at approximately the T8 spinal level using microscissors. Two surgeons verified the completeness of the transection by lifting the cut ends of the spinal cord and passing a glass probe through the lesion site. Gel foam was inserted into the gap created by the transection as a coagulant and to separate the cut ends of the spinal cord.

For eEmc electrode implantation, partial laminectomies were performed to expose the spinal cord at spinal levels L2 and S1. Two Teflon-coated stainless steel wires from the head connector were passed under the spinous processes and above the dura mater of the remaining vertebrae between the partial laminectomy sites. After removing a small portion (~1 mm notch) of the Teflon coating and exposing the conductor on the surface facing the spinal cord, the electrodes were sutured to the dura mater at the midline of the spinal cord above and below the electrode sites using 8.0 Ethilon suture **(**Ethicon, New Brunswick, NJ**)**. Two common ground (indifferent EMG and stimulation grounds) wires (~1 cm of the Teflon removed distally) were inserted subcutaneously in the mid-back region. All wires (for both EMG and eEmc) were coiled in the back region to provide stress relief.

All incision areas were irrigated liberally with warm, sterile saline. All surgical sites were closed in layers using 5.0 Vicryl (Ethicon, New Brunswick, NJ) for all muscle and connective tissue layers and for the skin incisions in the hindlimbs and 5.0 Ethilon for the back skin incision.

All closed incision sites were cleansed thoroughly with saline solution. Analgesia was provided by buprenex (0.5–1.0 mg/kg, s.c. 3 times/day). The analgesics were initiated before completion of the surgery and continued for a minimum of 3 days. The rats were allowed to fully recover from anesthesia in an incubator. The rats were housed individually in cages that had ample CareFresh bedding, and the bladders of the spinal rats were expressed manually 3 times daily for the first 2 weeks after surgery and 2 times daily thereafter. The hindlimbs of the spinal rats were moved passively through a full range of motion once per day to maintain joint mobility. All of these procedures have been described in detail previously (Courtine et al., 2009).

Stimulation and testing procedures

The rats went through a rehabilitation process for 6 weeks and were tested to step bipedally on a specially designed motor-driven rodent treadmill using a body weight support system (de Leon et al., 2002) under the influence of eEmc at 40 Hz between L2 and S1 at the end of 6 weeks (Lavrov et al., 2006; Gerasimenko et al., 2008; Ichiyama et al., 2008; Courtine et al., 2009)

Chronic training engages and reinforces the locomotor networks that would potentially be activated during spontaneous cage activity. The spontaneous activity levels of the spinal rats were determined six weeks post-injury in a cage with sufficient care fresh bedding similar to their normal housing environment using a swivel attached to the head connector to allow them to move freely in their home cage. The head connector was connected to a set of amplifiers and a stimulator. Food (pellets, pieces of fruit, and fruit loops) was distributed throughout the cage floor to encourage movement and exploration. Video data were recorded using a camcorder with a series of IR LEDs to enable recording in the dark, i.e., the active period for the rats. EMG data

were amplified and recorded using custom LabView-based data acquisition software with a sampling frequency of 10 kHz. Data were recorded for 6 continuous hours starting at 8pm and ending at 2am. EMG recordings from the hindlimb muscles were band-pass filtered (1 Hz to 5 KHz), amplified using an A-M Systems Model 1700 differential AC amplifier (A-M Systems, Carlsborg, WA), and sampled at a frequency of 10 KHz using a custom data acquisition program written in the LabView development environment (National Instruments, Austin, TX) as described previously (Courtine et al., 2009). The energy in the EMG signal was calculated by estimating the area under the curve after rectification of the raw EMG as previously described (Viitasalo and Komi1977, Whiting et al., 1984, Roy et al., 1991).

Statistical analyses

All data are reported as mean ± SEM (unless otherwise indicated). Statistically significant differences were determined using paired t-tests. The criterion level for the determination of a statistical difference was set at $P< 0.05$ for all computations (unless otherwise indicated).

Results

Evidence of enabling vs. inducement of neuromuscular activity

We carefully examined the relationship between the absence or presence of eEmc and the amount and pattern of spontaneous cage activity. In the absence of eEmc there were periods of spontaneous activity when the rats remained in a sitting posture (Fig. 5.1A) and on some occasions when it appeared that they were attempting to stand (Fig. 5.1B). EMG activity increased, particularly in the soleus, during incidences of apparent attempted standing (Fig. 5.1B). The most common observed position was for the rats to have their hindlimbs completely extended often showing little or no movement except some spastic-like reactions. Even during movement propelled by the forelimbs, the upper body remained low with the head close to the floor of the cage.

A sub-motor threshold intensity of eEmc is evident by the absence of any time-linked evoked muscle responses (Fig. 5.1C). In the presence of eEmc the forelimbs were used to move around in the cage more often than in its absence. During this activity the hindlimbs usually dragged behind showing some bursting in both the flexor and extensor muscles (Fig. 5.1E) and the upper body was maintained at a greater height compared with that seen without eEmc. The rats often would stand on the hindlimbs with partial weight bearing using the sides of the cage as support (Fig. 5.1D), a behavior hardly observed without eEmc.

We compared the level of activity that was generated spontaneously in the cage (Fig. 5.1E) to when the rat was stepping on a treadmill with a body weight support system (Fig. 5.1F) with eEmc. Note that the stimuli imposed did not induce synchronized motor responses with

each individual stimulus, but was sufficient to enable a higher level of activity within the TA and soleus and the motor responses were more asynchronous as occurs normally (Fig. 5.1F). Also note that there is a greater level of synchronous activity during treadmill stepping than spontaneous cage activity at the same stimulation intensity.

The total amount of time that the rats were active during these recordings was ~5-fold higher in the presence compared to the absence of eEmc, i.e., ~2500 sec or ~12% of the time vs. ~500 sec or ~2.5% of the time (Fig. 5.2). The mean integrated EMG (Fig. 5.3B) and summed integrated EMG (Fig. 5.3C) for both the TA and soleus muscles during the 6-hr recording periods of spontaneous cage activity were significantly higher in the presence than the absence of eEmc. To provide some point of reference regarding these increases in EMG activity with stimulation, Figure 5.3A shows the large differences in integrated EMG in both muscles studied with and without eEmc when the rats were stepping on a treadmill. Furthermore, the amount of activity during six hours of spontaneous activity was equivalent to ~33 minutes of stepping on the treadmill with eEmc compared to ~15 minutes without stimulation.

There was a larger number of 1-min bins with relatively high levels of integrated EMG activity with than without eEmc distributed across the 6-hr recording period in both the TA and soleus (Fig. 5.4). Differences in the frequency distributions of EMG amplitudes with and without eEmc also were evident (Fig. 5.5). Higher EMG amplitudes were observed more frequently in both the TA and soleus in the presence of eEmc. There was greater evidence of reciprocal coordination between the TA and soleus muscles with than without eEmc across the 6-hr recording period (Fig. 5.6A). The level of EMG amplitude modulation was greater in the TA than the soleus; with the increased occurrence of higher amplitudes there was clearly a higher incidence of co-contraction between the TA and soleus muscles without eEmc. In addition,

instances showing apparent reciprocal activity without eEmc had fewer and less robust alternating patterns (Fig. 5.6B I) compared to those observed with eEmc (Fig. 5.6B II).

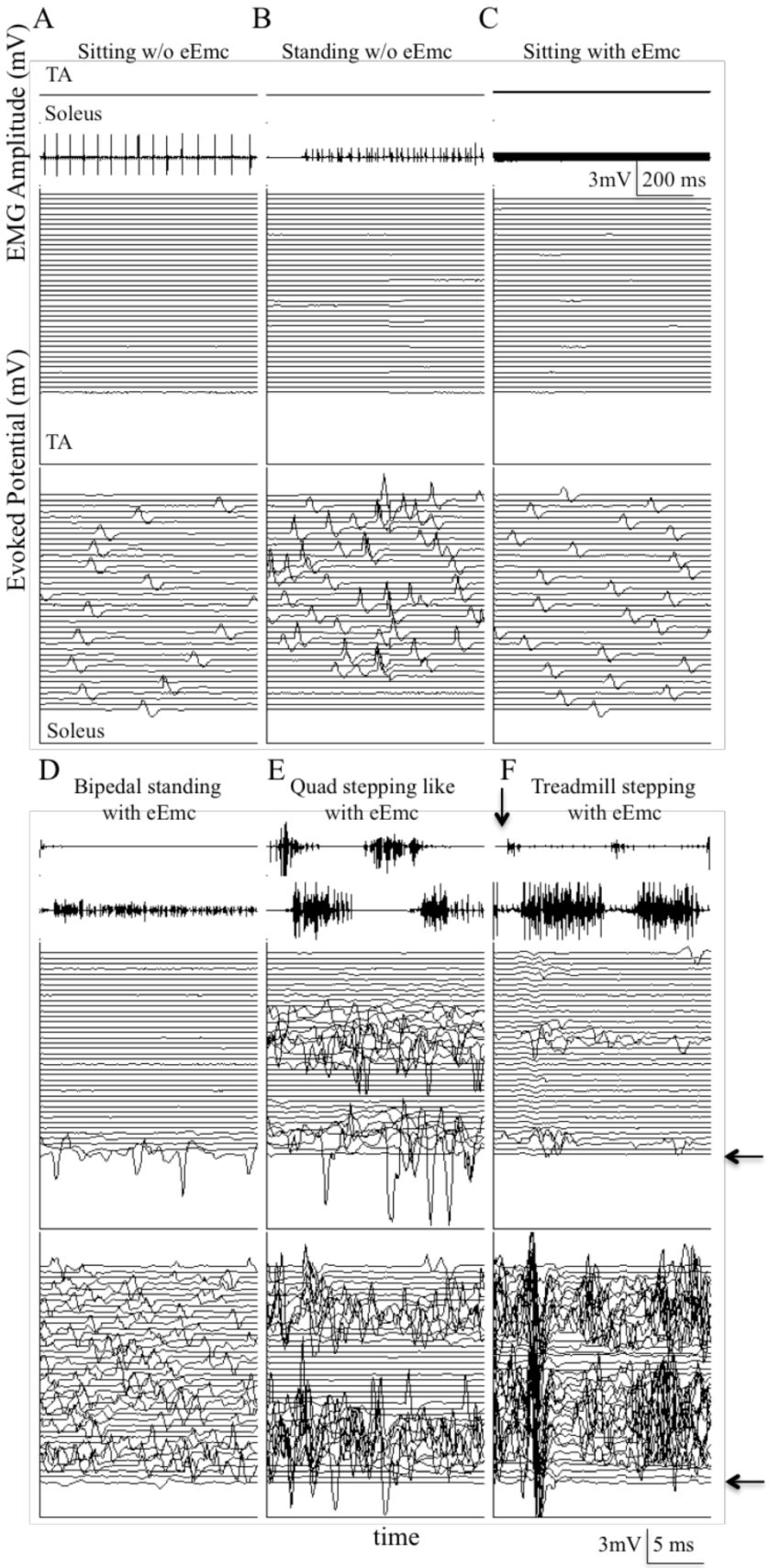
A
Sitting w/o eEmc
B
Standing w/o eEmc
C
Sitting with eEmc
EMG Amplitude (mV)
TA
Soleus
3mV
200 ms
Evoked Potential (mV)
TA
Soleus
D
Bipedal standing with eEmc
E
Quad stepping like with eEmc
F
Treadmill stepping with eEmc
time
3mV
5 ms

Figure 5.1: Representative raw EMG and evoked potentials from the soleus and tibialis anterior (TA) muscles without eEmc from one spinal rat during (A) sitting, (B) attempted bipedal standing, and with eEmc (1.5 V, 40 Hz between L2 and S1) during (C) sitting, (D) bipedal standing, and (E) quadrupedal (Quad) stepping like movement during the 6-hour recording period. (F) Representative EMG and evoked potential from soleus and TA from the same rat during body weight supported treadmill stepping facilitated by eEmc (2.5 V, 40 Hz between L2 and S1). The start of each trace with eEmc is synchronized with the initiation of the eEmc pulse. Each trace is 25 ms, i.e., the time between successive eEmc pulses. The arrow placed on the EMG signals demonstrates the time of the initial 25 msec scan.

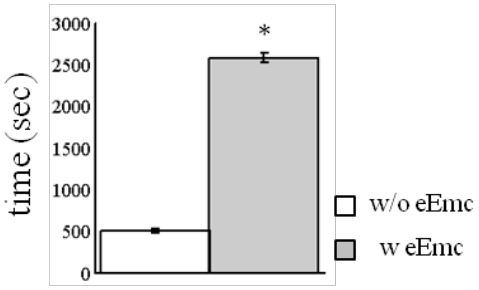

Figure 5.2: Mean (±SEM, n = 4) duration of spontaneous cage activity during the 6-hr recording period with and without eEmc. *, significantly different from without eEmc at $P < 0.05$.

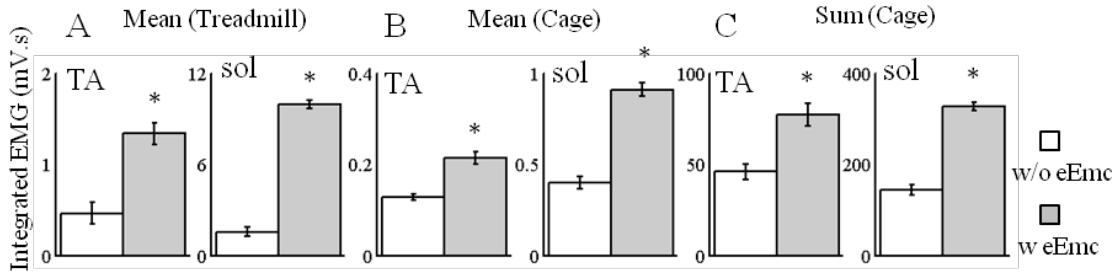

Figure 5.3: (A) Integrated EMG during body weight supported treadmill stepping at 13.5 cm/sec for 1 min. (B) Integrated EMG per min during the 6-hr recording period in the cage. (C) The sum of the mean integrated EMG during the 6-hr recording period in the cage for the TA and soleus muscles without and with eEmc. Values are mean ± SEM for 4 rats. *, significantly different from without eEmc at P< 0.05).

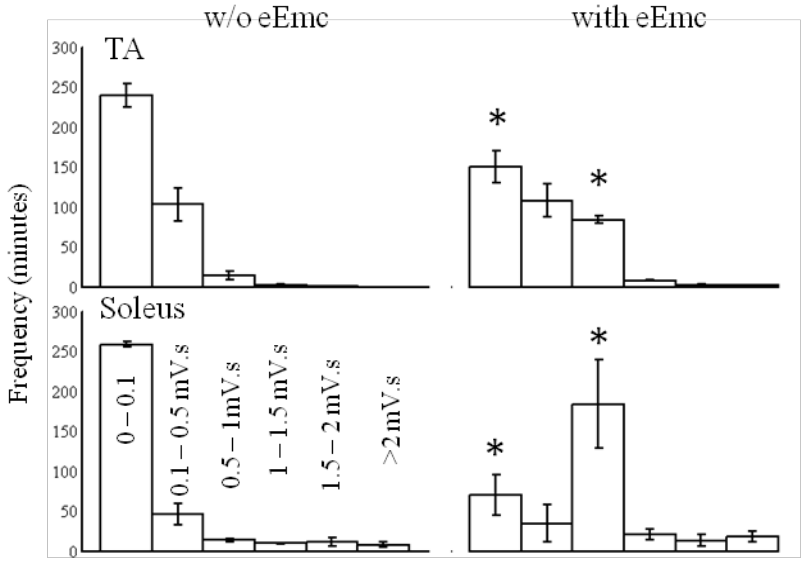

Figure 5.4: Mean (±SEM, n = 4 rats) integrated EMG for the TA and soleus with and without eEmc during the 6-hr recording period in the cage expressed in minute bins.

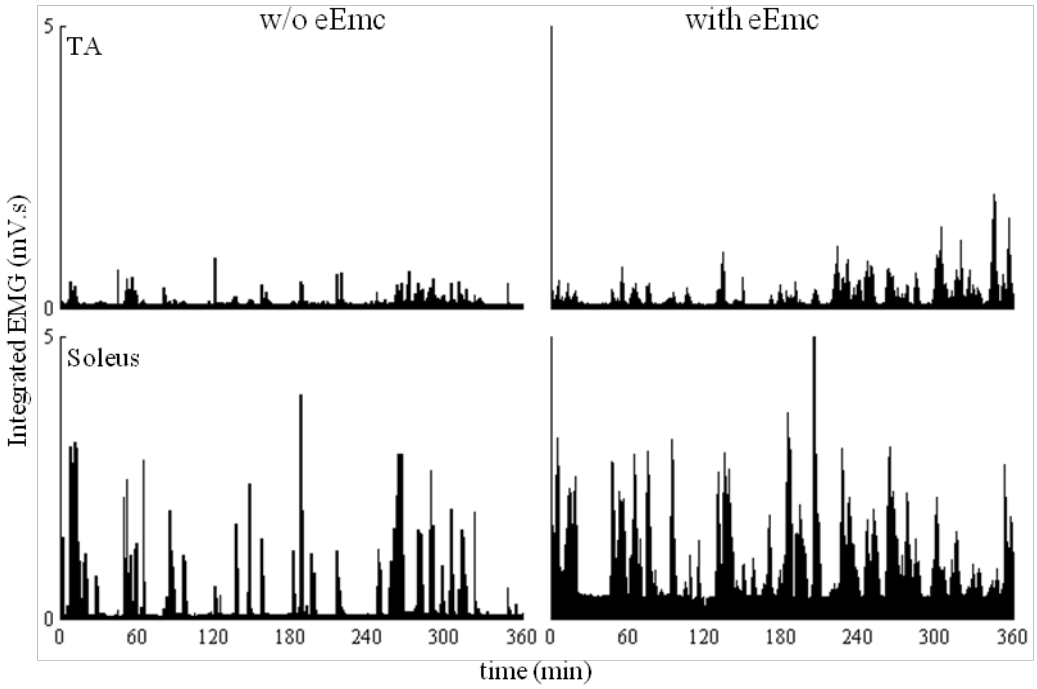

Figure 5.5: Mean (±SEM) frequency of occurrence of different ranges of integrated EMG amplitudes with and without eEmc. *, significantly different from the corresponding bin without eEmc at $P < 0.05$.

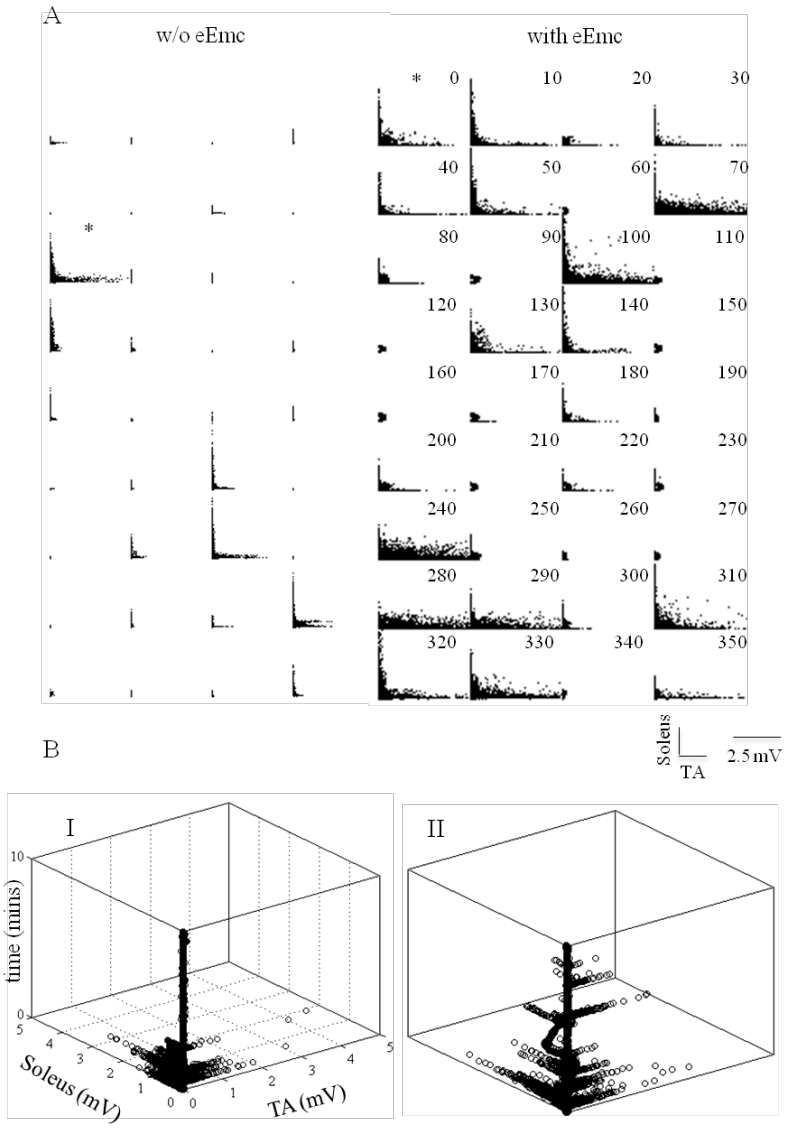

Figure 5.6: (A) Joint probability distribution plots showing the relationship between the soleus and TA activity in 10 min bins during the 6-hr recording period for a representative spinal rat. The 6-hr recording occurred during the dark period (8:00 pm to 2:00 am), i.e., the active period of the rats. (B) The incidence of occurrence of different joint probability distributions for 10 min of activity without (I) and with (II) eEmc. The asterisks identify the two bins being compared. Note the lack of consistent alternating flexor-extensor activation without compared to with eEmc.

Discussion

Spinal circuits controlling stepping and standing after a spinal cord injury can be improved by increasing the activity of those circuits (Roy et al., 2012; Rossignol and Frigon 2011). In the present study we show that there is a minimal amount of spontaneous activity in the sensorimotor circuits that generate and control standing and stepping after a mid-thoracic spinal cord transection in adult rats. eEmc below the level of the lesion, however, enhanced the amount of spontaneous activity several-fold and resulted in more robust stepping-like and partial weight-bearing standing activity. In effect, this enhanced spontaneous activity results in a 'self-training' phenomenon. This is consistent with the observation that independent, full weight-bearing standing can be initiated "voluntarily" and sustained in humans with complete paralysis in the presence of eEmc at an intensity that, in itself, induces little or no direct motor responses (Harkema et al., 2011).

Does the elevated motor activity observed with sub-threshold spinal cord stimulation reflect some level of "voluntary" control? The report that a completely paralyzed human subject can regain the ability to stand under the influence of eEmc (Harkema et al., 2011) raises the question as to whether this can be considered to be "voluntarily" initiated, at least indirectly, or is the result of some "reflex" mechanism, There are no "reflexes" described, however, that have the motor output features performed by the paralyzed subject noted above. While there are no widely accepted criteria for describing if a task is performed 'voluntarily' the subject acquired the ability to initiate and sustain standing on command. This could be viewed as being either a "voluntary" or an "automated" response. For instance, after a critical level of eEmc, the subject was able to volitionally position the upper body in a manner that increased weight bearing on the lower limbs that, in turn, engaged the proprioceptive input to the spinal cord from the hindlimbs

resulting in more weight-bearing activity. To what extent can one routinely and voluntarily engage proprioception to perform a motor task? We propose that the observations in the spinal rats in the present study parallel the human data in that the rats increased their cage activity levels in the presence of sub-motor threshold stimulation intensities. They were more active and mobile because the spinal networks were placed in a state of higher "readiness", making it more feasible to volitionally engage the postural and locomotor circuits when the rat chose to be mobile. Given that proprioception can initiate and control a wide range of postural and locomotor tasks, it seems feasible that the elevated activity in the presence of eEmc occurred as a result of the intent of the rats to be mobile as reported by Gad et al. (2012).

In both rats (van der Brand et al., 2012) and humans (Harkema et al., 2011; Angeli et al., 2012) the experiments were designed to engage the "paralyzed circuits" during a specific training-rehabilitation time period in the presence of stimulation. Since the level of stimulation necessary to achieve the results noted above appeared to have little or no recognizable direct motor or behavioral effects on the animal or human subjects, we tested the hypothesis that sustained sub-threshold levels of activity in the normal cage environment would result in greater amounts of spontaneous activity among those spinal circuits that generate and control standing and stepping in rats. The implications of these observations are that the training effects induced via formal motor rehabilitation sessions could be greatly amplified during periods of routine daily activity enhanced by eEmc. The question remains, however, whether a general increase in activity will result in improved standing and stepping ability, given the issue of the specificity of training. Recent findings by Garcia-Alias et al (2009) demonstrate that rats that are housed in an enriched environment after a spinal cord injury are more active and perform significantly better in reaching and locomotor tasks than those housed in standard cages.

The spinal rats in the present study were more spontaneously active with than without eEmc, even though they were housed in standard cages. It seems likely that a combination of eEmc and an enriched housing environment would result in even greater levels of spontaneous activity, particularly in rats that are completely paralyzed. Issues related to the type and intensity of the activity performed by a spinal cord injured patient (or animal) during the prolonged daily periods without any formal rehabilitation treatment (most likely >23 hrs) have come to the forefront only recently. Even in normal humans (Finni et al., 2012) and animals (Hodgson et al., 2005) 80-90% of the daily activity occurs at very low levels of activation of almost all motor pools. With the ability to carefully quantify muscle and body activity, surprising results have been reported in how daily activity levels change when uninjured individuals begin physical training (Finni et al., 2012).

The critical questions raised now are whether the effect of epidural stimulation alone or in combination with an enriched environment would result in improved performance of reaching, standing, and locomotion and how much and what type of spontaneous activity is sufficient to enhance each of these motor tasks. An answer to these questions would have significant clinical implications in humans. For example, can motor performance be improved after severe paralysis by enabling the spinal circuitry during routine daily activities in the home in addition to the specific training that occurs during structured rehabilitation sessions? The spontaneous activity that may occur in a wide range of sensorimotor pathways may result in progressive improvement in specific tasks requiring fine motor control of the hands or in postural and locomotor functions, particularly if the same motor pathways are engaged as they are during scheduled rehabilitative sessions.

Spinal circuits controlling stepping and standing after a spinal cord injury can be improved by increasing the activity of those circuits (Roy et al 2012, Rossignol S and Frigon A, 2011). In the present study we show that there is a minimal amount of spontaneous activity in the sensorimotor circuits that generate and control standing and stepping after a mid-thoracic spinal cord transection in adult rats. eEmc below the level of the lesion, however, enhanced the amount of spontaneous activity several-fold and resulted in more robust stepping-like and standing activity. In effect, this enhanced spontaneous activity results in a 'self-training' phenomenon. This is consistent with the observation that independent, full weight-bearing standing can be initiated voluntarily and sustained in humans with complete paralysis in the presence of eEmc at an intensity that, in itself, induces little or no direct motor responses (Harkema et al., 2011).

In both rats (van der Brand et al., 2012) and humans (Harkema et al.,2011, Angeli , 2012) the experiments engaged the "paralyzed circuits" during a specific training-rehabilitation time period in the presence of stimulation. Since the level of stimulation necessary to achieve the results noted above seemed to have little or no recognizable direct motor or behavioral effects on the animals or human subjects, we tested the hypothesis that sustained sub-threshold levels of activity in the normal cage environment would result in greater amounts of spontaneous activity among those spinal circuits that generate and control standing and stepping in rats. The implications of these observations are that the training effects induced via formal motor rehabilitation sessions could be greatly amplified during periods of routine daily activity enhanced by eEmc. The question remains, however, whether a general increase in activity will result in improved standing and stepping ability, given the issue of the specificity of training. Recent findings by Garcia-Alias (2009) demonstrate that rats that are housed in an enriched

environment after a spinal cord injury are more active and perform significantly better in reaching and locomotor tasks than those housed in standard cages.

The rats in our study were more spontaneously active due to the eEmc although their housing environment was a standard cage. It seems likely that a combination of eEmc and an enriched housing environment would result in even greater levels of spontaneous activity, particularly in rats that are completely paralyzed. Issues related to the type and intensity of the activity of the patient (or animal) for the ~23 hours outside of formal rehabilitation treatment have come to the forefront only recently. In normal humans (Finni et al., 2012) and animals (Hodgson et al., 2005) 80-90% of the daily activity occurs at very low levels of activation of almost all motor pools . With the ability to carefully quantify muscle and body activity, surprising results have been reported in how daily activity levels change when uninjured individuals begin physical training (Finni et al., 2012).

The critical questions raised now are whether the effect of epidural stimulation alone or in combination with an enriched environment would result in improved performance of reaching, standing, and locomotion and how much and what type of spontaneous activity is sufficient to enhance each of these motor tasks. With respect to humans these results would have significant clinical implications. For example, can motor performance be improved after severe paralysis by enabling the spinal circuitry during routine daily activities in the home in addition to the specific training that occurs during structured rehabilitation sessions? The spontaneous activity that may occur in a wide range of sensorimotor pathways may result in progressive improvement in specific tasks requiring fine motor control of the hands or in postural and locomotor functions, particularly if the same motor pathways are engaged as they are during scheduled rehabilitative sessions.

Chapter 6

Forelimb EMG-based trigger to control an electronic spinal bridge to enable hindlimb stepping after a complete spinal cord lesion in rats

Abstract

A complete spinal cord transection results in loss of all supraspinal motor control below the level of the injury. The neural circuitry in the lumbosacral spinal cord, however, can generate locomotor patterns in the hindlimbs of rats and cats with the aid of motor training, epidural stimulation and/or administration of monoaminergic agonists. We hypothesized that there are patterns of EMG signals from the forelimbs during quadrupedal locomotion that uniquely represent a signal for the "intent" to step with the hindlimbs. These observations led us to determine whether this type of "indirect" volitional control of stepping can be achieved after a complete spinal cord injury. The objective of this study was to develop an electronic bridge across the lesion of the spinal cord to facilitate hindlimb stepping after a complete mid-thoracic spinal cord injury in adult rats.

We developed an electronic spinal bridge that can detect specific patterns of EMG activity from the forelimb muscles to initiate eEmc of the lumbosacral spinal cord to enable quadrupedal stepping after a complete spinal cord transection in rats. A moving window detection algorithm was implemented in a small microprocessor to detect biceps brachii EMG activity bilaterally that then was used to initiate and terminate epidural stimulation in the lumbosacral spinal cord. We found dominant frequencies of 180-220 Hz in the EMG of the

forelimb muscles during active periods, whereas these frequencies were between 0-10 Hz when the muscles were inactive.

Once the algorithm was validated to represent kinematically appropriate quadrupedal stepping, we observed that the algorithm could reliably detect, initiate, and facilitate stepping under different pharmacological conditions and at various treadmill speeds.

Introduction

Functionally complete spinal cord injury is a severe debilitating condition and leads to paralysis. Numerous approaches have been attempted to recover function after paralysis, e.g., facilitation of axon regeneration including methods to suppress growth inhibitory molecules, modulation of the levels of neurotrophic factors, cell transplantation, and the use of activity-dependent mechanisms (Thuret et al., 2006, Edgerton et al., 2004,2008). These techniques, however, have not resulted in dramatic improvements of motor function after motor complete paralysis. A technique that has shown promise is Brain-Computer Interface. This approach has been successfully developed in integrating activity from the functionally unaffected sites, such as the motor cortex, to control robotic devices or muscle stimulating devices to generate the desired movement in paralyzed muscle groups (Muller et al., 2004).

Recent *in vivo* studies in rats and cats show that networks of neurons in the lumbosacral region of the spinal cord retain an intrinsic capability to generate coordinated rhythmic motor outputs in the hindlimbs (Edgerton et al., 2004, Ivashko et al., 2003, Gerasimenko et al., 2003). Several strategies have been tested to tap into these neural circuits and activate them to induce oscillatory motions in the hindlimbs. For example, pharmacologically enabling motor control strategies (fEmc) using serotonergic agonists of 5-$HT_{1A,2A}$ and 5-HT_7 receptors in combination with epidural stimulation, i.e., electrical-enabling motor control (eEmc) (Gerasimenko et al., 2007, Courtine et al., 2009), have been used to recover considerable function after paralysis. These two interventions combined with the availability of sensory information in real time have been used to induce full weight-bearing stepping in complete spinal rats (Lavrov et al., 2008). Gerasimenko et al., 2007) have shown that eEmc (at 40 Hz with monopolar stimulation)

between the L2 and S1 spinal cord levels facilitates bilateral stepping of spinal rats on a moving treadmill belt. In contrast, the spinal rats did not step when the treadmill was turned on but no eEmc was provided, indicating that the stimulation was necessary for the spinal rats to step.

These observations led us to ask whether 'indirect' volitional control of eEmc (by forelimb EMG activity) could be used to facilitate stepping in the hindlimbs and provide a new and stable level of control of motor function in spinal rats. Therefore, the purpose of this study was to determine whether 'indirect' volitional control via an electronic spinal bridge could be accomplished. In human subjects, this volitional control could avoid the use of an external switch to activate an electrode array by using EMG signals as occurs during normal locomotion. As importantly the present experiments provide a testbed for development of a Brain-Machine-Spinal Cord Interface (BMSCI) that allows for motor control with minimal conscious attention. In addition, it provides a potential mechanism for exerting finer motor control than could be accomplished using on a simple on/off system. To design and test such a 'Brain-Machine-Spinal Cord Interface', we used EMG signals from the forelimbs as a trigger to initiate spinal cord stimulation to facilitate movement of the hindlimbs. We used the forelimb EMG because these signals are part of the natural gait cycle in quadrupedal stepping.

The objectives of this study were to develop an effective pattern of step detection from the uninjured forelimb muscles and to use this pattern to control the on/off state of the eEmc of the spinal cord to facilitate quadrupedal stepping under different experimental conditions in spinal rats. We observed that voluntary signals from the forelimbs during stepping can be used as a control mechanism for generating signals to the spinal cord to facilitate hindlimb stepping. The underlying assumption is that when the rat "intends" to step the forelimbs will be activated in a

pattern that reflects this “voluntary” intent that will initiate eEmc to facilitate stepping of the hindlimbs.

Methods

Adult female Sprague-Dawley rats (n=5, ~300 g body weight) were used. Pre- and post-surgical animal care has been described previously (Roy et al., 1992). The rats were housed individually with food and water provided *ad libitum*. All survival surgical procedures were conducted under aseptic conditions and with the rats deeply anesthetized (isoflurane gas administered via facemask as needed). All procedures described below are in accordance with the National Institute of Health Guide for the Care and Use of Laboratory Animals and were approved by the Animal Research Committee at UCLA.

Experimental design

The rats underwent two separate surgeries. The first surgery was to implant the EMG electrodes. The rats were allowed to recover from this implant surgery for one week and then recordings (pre-transection) were made while the rats stepped on the treadmill. After completing these recordings, the rats underwent a second surgery during which the spinal cord was completely transected at a mid-thoracic level and epidural electrodes were implanted at spinal levels L2 and S1. The rats were allowed to recover for one week and then the training sessions were initiated. Recordings were performed to test the electronic bridge at 5 weeks post-transection. The pre-transection EMG recordings provided a baseline for comparison with the recordings post-transection. All of these procedures are performed routinely in our laboratory (Courtine et al., 2009, Gerasimenko et al., 2005). Details of each step are given below.

Head connector implantation

A small incision was made at the midline of the skull. The muscles and fascia were retracted laterally, small grooves were made in the skull with a scalpel, and the skull was dried thoroughly. Two amphenol head connectors with Teflon-coated stainless steel wires (AS632, Cooner Wire, Chatsworth CA) were securely attached to the skull with screws and dental cement as described previously (Roy et al., 1991, Ichiyama et al., 2005).

Intramuscular EMG electrode implantation

Selected hindlimb (tibialis anterior, TA; and soleus, Sol) and forelimb (biceps brachii, BB; and triceps brachii, TB) muscles were implanted bilaterally with EMG recording electrodes as described by Roy et al (1992). Skin and fascial incisions were made to expose the belly of each muscle. Two wires extending from the skull-mounted connector were routed subcutaneously to each muscle. The wires were inserted into the muscle belly using a 23-gauge needle and a small notch (~0.5-1.0 mm) was removed from the insulation of each wire to expose the conductor and form the electrodes. The wires were secured in the belly of the muscle via a suture on the wire at its entrance into and exit from the muscle belly. The wires were looped at the entrance site to provide stress relief. The proper placement of the electrodes was verified during the surgery by stimulating through the head connector and post-mortem via dissection.

Spinal cord transection

A partial laminectomy was performed at the T8-T9 vertebral level and a longitudinal cut was made in the dura to expose the spinal cord. A complete spinal cord transection to include the dura was performed at ~T8 spinal level using microscissors. Two surgeons verified the

completeness of the transection by lifting the cut ends of the spinal cord and passing a glass probe through the lesion site. Gel foam was inserted into the gap created by the transection as a coagulant and to separate the cut ends of the spinal cord.

Epidural electrode implantation

Epidural electrodes were coiled and left in the back region of the animal after the EMG surgery. The epidural electrodes were implanted during the second surgery. Partial laminectomies were performed to expose the spinal cord at spinal levels L2 and S1. Two Teflon-coated stainless steel wires from the head connector were passed under the spinous processes and above the dura mater of the remaining vertebrae between the partial laminectomy sites. After removing a small portion (~1 mm notch) of the Teflon coating and exposing the wire on the surface facing the spinal cord, the electrodes were sutured to the dura mater at the midline of the spinal cord above and below the electrode sites using 8.0 Ethilon suture **(**Ethicon, New Brunswick, NJ**)**. A common ground (indifferent) wire (~1 cm of the Teflon coating removed distally) was inserted subcutaneously in the mid-back region. All wires were coiled in the back region to provide stress relief.

All incision areas were irrigated liberally with warm, sterile saline. All surgical sites were closed in layers, i.e., muscle and connective tissue layers with Vicryl (Ethicon, New Brunswick, NJ) and the skin incision on the back with Ethilon and in the limbs with Vicryl. All closed incision sites were cleansed thoroughly with saline solution. Analgesia was provided by buprenex (0.5–1.0 mg/kg, s.c., 3 times/day). The analgesics were initiated before completion of the surgery and continued for a minimum of 2 days. The rats were allowed to fully recover from anesthesia in an incubator. The rats were housed individually, and the bladders of the spinal rats

were expressed manually 3 times/day for the first 2 weeks after surgery and 2 times per day thereafter. The hindlimbs of the spinal rats were moved passively through a full range of motion once per day to maintain joint mobility. All of these animal care procedures have been described in detail previously (Roy et al., 1992).

Stimulation and training procedures

All rats were trained to step quadrupedally using a body weight support system under the influence of quipazine administration (0.3 mg/kg, i.p.) and eEmc (40 Hz, between L2 and S1 with the current flowing from L2 to S1) (Courtine et al., 2009, Ichiyama et al., 2008). The maximum stimulation voltage used was 3 V and was modulated to produce maximum stepping performance. The rats stepped on a specially designed motor-driven rodent treadmill. The treadmill belt had an anti-slip material that minimized slipping while stepping. The rat was suspended in a jacket such that all four limbs were in contact with the treadmill and that there was enough room for all 4 limbs to carry out the swing and stance phases of the step cycle. This was a critical component of the design as it was important to engage the forelimbs in stepping to produce robust, high quality EMG signals from the forelimb muscles.

Testing procedures

Pre-transection the rats were stepped quadrupedally on the treadmill at varying speeds (13.5 to 21 cm/s) without the use of the body weight support system. These baseline recordings were compared to post-transection recordings. Five days post-transection, the rats were fitted with a jacket and secured to the body weight system for a period of 2-3 min initially and then the time was progressively increased to about 10 min by day 7. This was an acclimation period and

the rats were not stepped during this period. Training began one-week post-transection. Stepping ability was tested once a week pre-quipazine and 15 min post-quipazine administration. Quipazine (a serotoninergic agonist) administered intraperitoneally (0.3 mg/kg) improves stepping performance of spinal animals when receiving eEmc (Gerasimenko et al., 2007, Ichiyama et al., 2008). We used quipazine in the present study to produce robust stepping in the spinal rats. Kinematics and EMG data were collected on a weekly basis from all rats. The algorithm for detection of forelimb stepping was based on these data.

Data acquisition and post-processing

EMG recordings from the forelimb and hindlimb muscles were band-pass filtered (1 Hz to 1 KHz), amplified using an A-M Systems Model 1700 differential AC amplifier (A-M Systems, Carlsborg, WA), and sampled at a frequency of 10 KHz using a custom data acquisition program written in the LabView development environment (National Instruments, Austin, TX) as described previously (Courtine et al., 2009). The EMG signals from the forelimbs also are sent to the TI MSP430 where it went through a ADC to be processed for step detection. Raw analog EMG signals were collected, filtered, digitized, and processed in real time by the microprocessor (Fig. 6.1).

Kinematics recording parameters

Video recordings of the hip, knee, ankle, shoulder, elbow, and wrist joints were obtained to study the segmental and joint angle kinematics during stepping. A four-camera system was calibrated and then used to track reflective markers placed on bony landmarks on the iliac crest, greater trochanter, lateral condyle, lateral malleolus, the distal end of the fifth metatarsal of both

hindlimbs, and the head of the humerus, olecranon process, radial process, and tips of the paw of both forelimbs. The video footage was processed using SIMI Motion analysis software (SIMI, Unterschleissheim, Germany) to produce the 3-D reconstruction of the hindlimb and forelimb movements, as well as the 2-D ball-and-stick diagrams and hindlimb trajectory plots (Courtine et al., 2009). The 3-D coordinates for a given marker were calculated using a triangulation procedure that partially accounts for the movement of the skin. This is a technique that has been used successfully and implemented in many labs and has the precision necessary for the present study.

Electronic bridge schematic

Figure 6.1A shows the schematic of the electronic bridge and the experimental setup. The EMG signals from the forelimb muscles were fed to the electronic bridge. The output of the electronic bridge was connected to wire electrodes implanted at specific levels on the spinal cord. Figure 1B shows an expanded view of the electronic bridge. We used an 8:1 MUX (MAX14752, Maxim) that is controlled by a microcontroller (MSP EZ430, Texas Instruments). The electronic bridge has 2 input channels (RBB and LBB) and one output channel (Stim 1) while 5 other channels are reserved for future use. The EZ430 contains 10 I/O channels and 5 of these channels are used for this system (3 control lines, 1 input and 1 output).

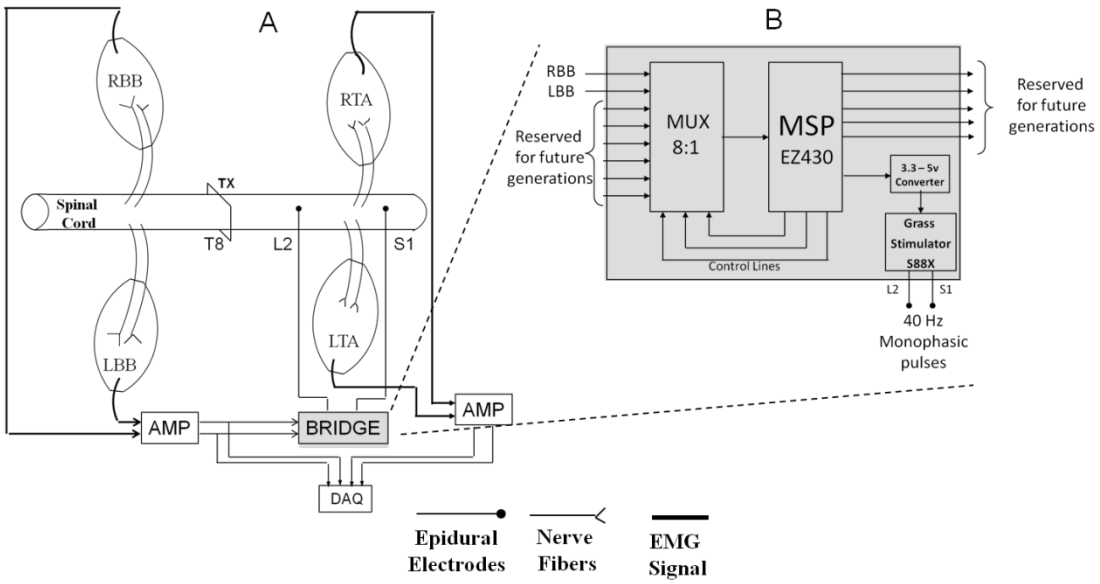

Figure 6.1: A) Schematic diagram showing the design of the electronic bridge. EMG signals from the right biceps brachii (RBB) and left BB (LBB) are sent to the bridge. Forelimb stepping is detected at the bridge that then generates electrical pulses (40 Hz monopolar) in the lumbosacral spinal cord to generate stepping in the hindlimbs. EMG from the forelimb and hindlimb muscles are amplified and stored using the DAQ. B) Expanded view of the electronic bridge circuitry.

The MSP EZ430 has an inbuilt 10-bit ADC with a maximum sampling rate of 200 kHz. It consists of 10 general-purpose analog I/O lines that allow the design to be flexible along with potential additions to the design in the future. The MSP EZ430 is powered by a DC source that provides a maximum output of 3.3 V. The minimum voltage required to trigger the Grass stimulator is 5 V. The 3.3 V output is converted to a 5 V output using a simple NE555 timer that is synchronized with the output of the MSP EZ430 to provide 40 Hz pulses.

EMG detection techniques

Two strategies were attempted for detecting stepping in the forelimbs. The first attempt at an electronic bridge involved the detection of the reciprocity of the EMG activity of the BB and TB (Fig. 6.2) using a moving window standard deviation technique. We calculated the standard deviation using a window of 20 consecutive data points and assigned the calculated value to the first data point. This procedure was repeated by moving the window across the length of the signal. The resultant plot of the standard deviation calculation forms a positive linear envelope around the raw EMG signals (Figs. 6.2 and 6.3iii and iv). Using the resultant signal we applied an optimum threshold to digitize the signals bilaterally from the BB and TB. Our objective was to achieve antagonistic action in the BB and TB and a finite phase difference between the left and right sides. This technique was effective and was successful in detecting stepping, but was limited in two ways: 1) it was dependent on the burst duration of all muscles involved; and 2) different thresholds were needed for each muscle. These thresholds vary from animal to animal and change over time. Accounting for these changes requires human intervention.

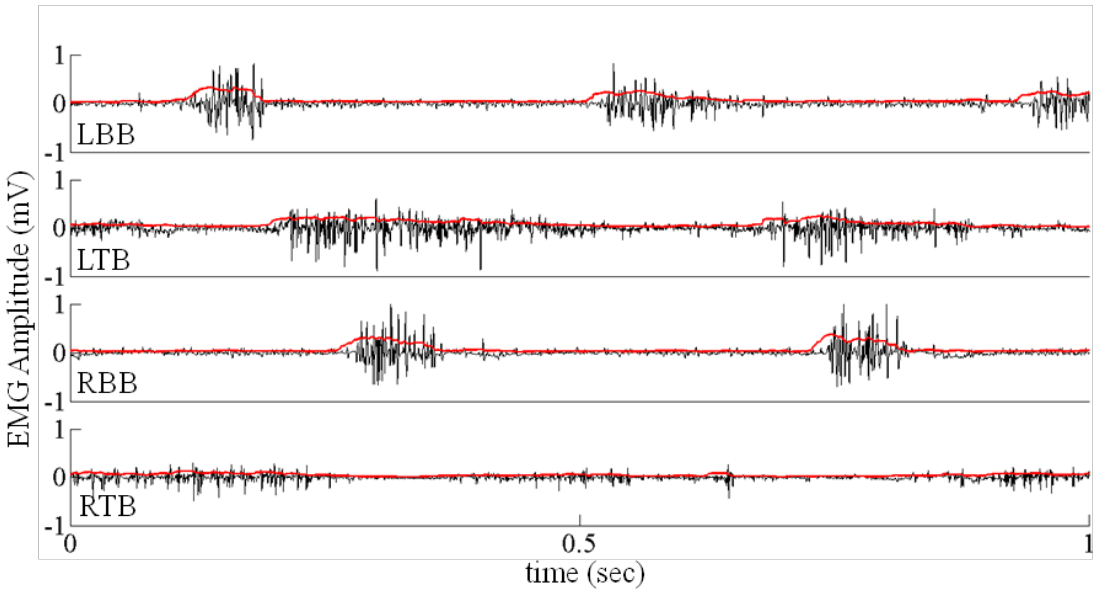

Figure 6.2: Sequence of strategies used to detect stepping in the first generation included: i) calculating the linear envelope (shown by the red lines) of each signal using a moving window standard deviation technique, ii) reciprocal activity between the BBs and TBs bilaterally, and iii) a constant phase difference between the left and right forelimbs.

Due to the problems faced by the first technique, we developed a second technique that would require little or no need for setting thresholds for detection of activity and calibration of the system. Such a step detection algorithm must exhibit low complexity with both memory and processing. Calibrating an EMG system can be an extremely time-consuming process. Another disadvantage is that, EMG must be calibrated often for each animal as well as physiological changes during recovery from an injury. To avoid requirements of calibration, this electronic bridge step-detection algorithm converts EMG signals to the frequency domain using a Fourier transform. We found the absolute value of each frequency to determine the overall frequency power curve (Fig. 6.3v and vi). Exact timing of movements, however, is required to efficiently

detect stepping patterns as well as to stimulate the rats properly. For this reason, we computed the 128-point Fourier transform at each point in time. In this scenario, a sliding window discrete fourier transform (DFT) as described by Jacobsen and Lyons (2003) is more computationally efficient than using the standard fast fourier transform (FFT) as described by Cooley et al., (1969). The following underlying principles are followed in the step detection algorithm: 1) calculation of a 128-point sliding window DFT at each time point; 2) rhythmic activity in both BBs during stepping; and 3) an alternating phase difference between the left and right BBs. An alternating phase is present when the EMG burst in one limb begins after 30% of the contralateral cycle period has been completed. Once these three conditions are met, a counter is initialized and continued to the completion of two steps at which time the signals to initiate eEmc are sent to the spinal cord (Figs. 6.4 and 6.5).

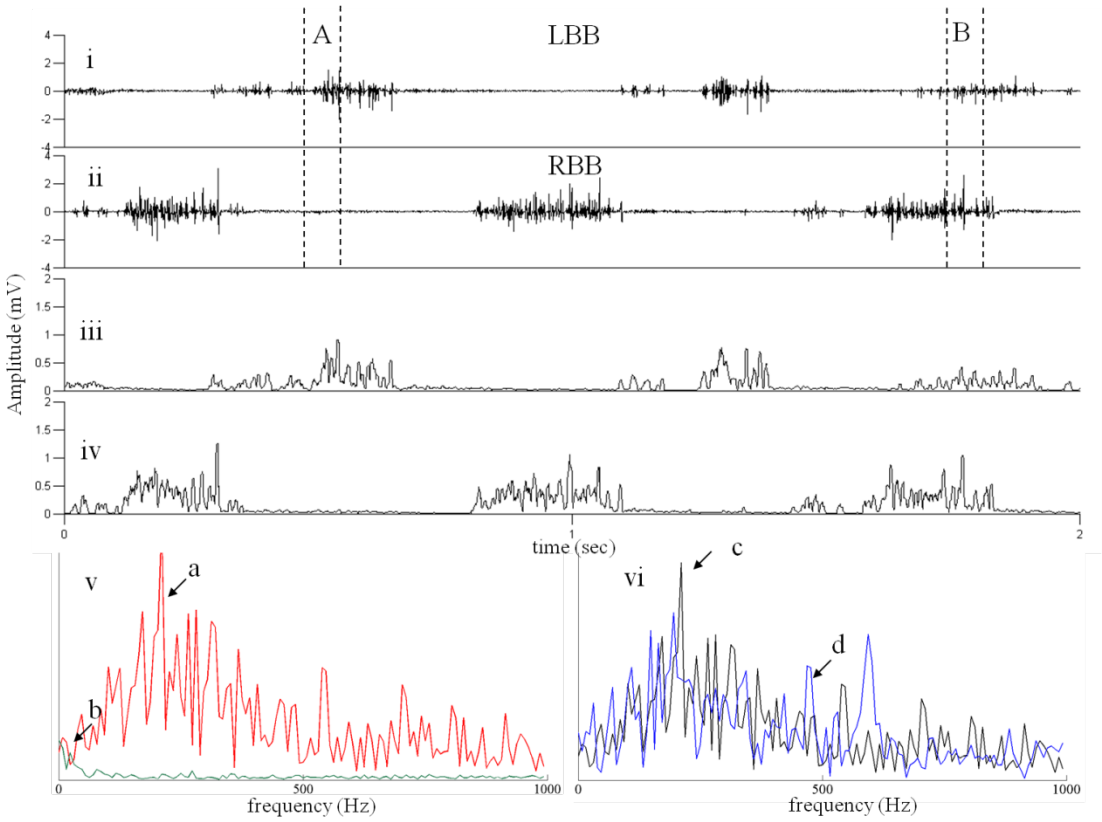

Figure 6.3: Raw EMG (i and ii), moving window standard deviation used in the first generation (iii and iv) and frequency spectrum used in the second generation (v) for the LBB (red) and RBB (green) for region marked by A and (vi) for the LBB (black) and RBB (blue) for region marked by B. during stepping. In v the frequency spectrum of the signals shown in A when there is reciprocal activity and in vi the frequency spectrum shown in B when there is co-activation.

Figure 6.4 represents the result of the frequency analysis technique. We observe that the RBB has higher baseline noise as compared to the LBB. Using the frequency response we were able to successfully define the bursts even in the case of large baseline noise. The use of the second technique allowed us to detect stepping based on the variation in the EMG frequency spectrum between the active phase and the inactive phase independent of the amplitude of the EMG signals.

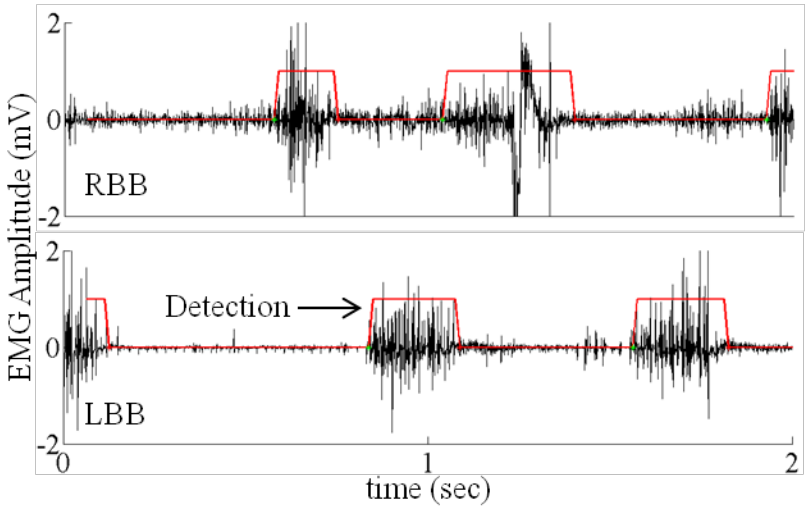

Figure 6.4: EMG activity from RBB and LBB superimposed with activity detection (shown by the red lines) using the frequency analysis algorithm (also see Fig. 3v and vi). This algorithm detects the start and end of each EMG burst. These data show examples of a period during which there is continuous stimulation through the bridge.

We tested the stability of the detection algorithm of the bridge 5 weeks post-transection at treadmill speeds of 13.5 and 21 cm/s and with and without quipazine. This enabled us to test the stability of the detection algorithm under different conditions (better hindlimb stepping with than without quipazine administration at both speeds). All rats were tested for a total of 5 trials under each condition and the 3 best trials were chosen for analysis. The efficiency of the electronic bridge was tested by measuring t_{on} and t_{off} for the various test conditions. t_{on} was defined as the time between the treadmill turning on and the stimulation turning on (time needed for the bridge to detect stepping). t_{off} was defined as the time between the treadmill turning off and the stimulation turning off (time needed for the bridge to detect the end of stepping).

We also tested the stepping ability of the rats at two treadmill speeds with and without quipazine with direct stimulation (without the electronic bridge) where the experimenter turned on the stimulation manually. This enabled us to compare the stepping ability with and without the electronic bridge.

Algorithm validation

Having identified three criteria based on FFT analysis of EMG as described above it was also necessary to validate whether these criteria resulted in kinematics characteristics associated with and without forelimb weight bearing. This validation was performed with respect to the speed of locomotion and with different pharmacological interventions. The single kinematics criteria reflecting successful stepping was a change in elbow angle bilaterally of at least 50^{o} for five consecutive steps.

Statistical analyses

All data are reported as mean ± SEM. Statistically significant differences were determined using a two-way (t_{on} and t_{off} under 4 experimental conditions) analysis of variance (ANOVA). The criterion level for determination of statistical significance was set at $P < 0.05$ for all computations.

Results

Voluntarily induced stepping.

We assessed the effectiveness of the algorithm for the electronic bridge when the rats were stepping consistently at 13.5 and 21 cm/s on a treadmill. Figure 4 shows a typical EMG recording using the electronic bridge. The EMG recording was divided into 5 phases to better understand the EMG of the forelimbs and hindlimbs and the state of the stimulation pulses. Phase I: prior to the first manual pulse and with the treadmill turned off, there is some random motion in the forelimbs that is not detected by the electronic bridge as stepping. Phase II: the treadmill is turned on and moving at a constant speed, resulting in forelimb stepping. Alternating EMG in the forelimb muscles is detected and triggers a counter that, on reaching a pre-determined threshold (two steps), sends pulses to the spinal cord at a preset frequency at the end of Phase II. The counter is designed to avoid false positives. Phase III: the treadmill is moving at the same speed and the EMG from the forelimb muscles continues to be detected. eEmc results in oscillatory weight-bearing movements in the hindlimbs. Phase IV: the treadmill is turned off (second manual pulse) and movements in the forelimbs are reduced progressively. In this phase, the detection of the forelimb muscle EMG ends, and this triggers a downcounter. Once the downcounter reaches zero, stimulation stops. In this phase, even though the treadmill is turned

off some motion in the hindlimbs remains due to a residual effect of stimulation. Phase V: this phase is identical to Phase I where the microprocessor is looking for detection of EMG in the forelimb muscles. There were no significant differences for either t_{on} or t_{off} across the 4 conditions tested at the P = 0.05 level (Fig. 6). The lack of a difference in ton and toff across the four conditions demonstrates the robustness of the algorithm.

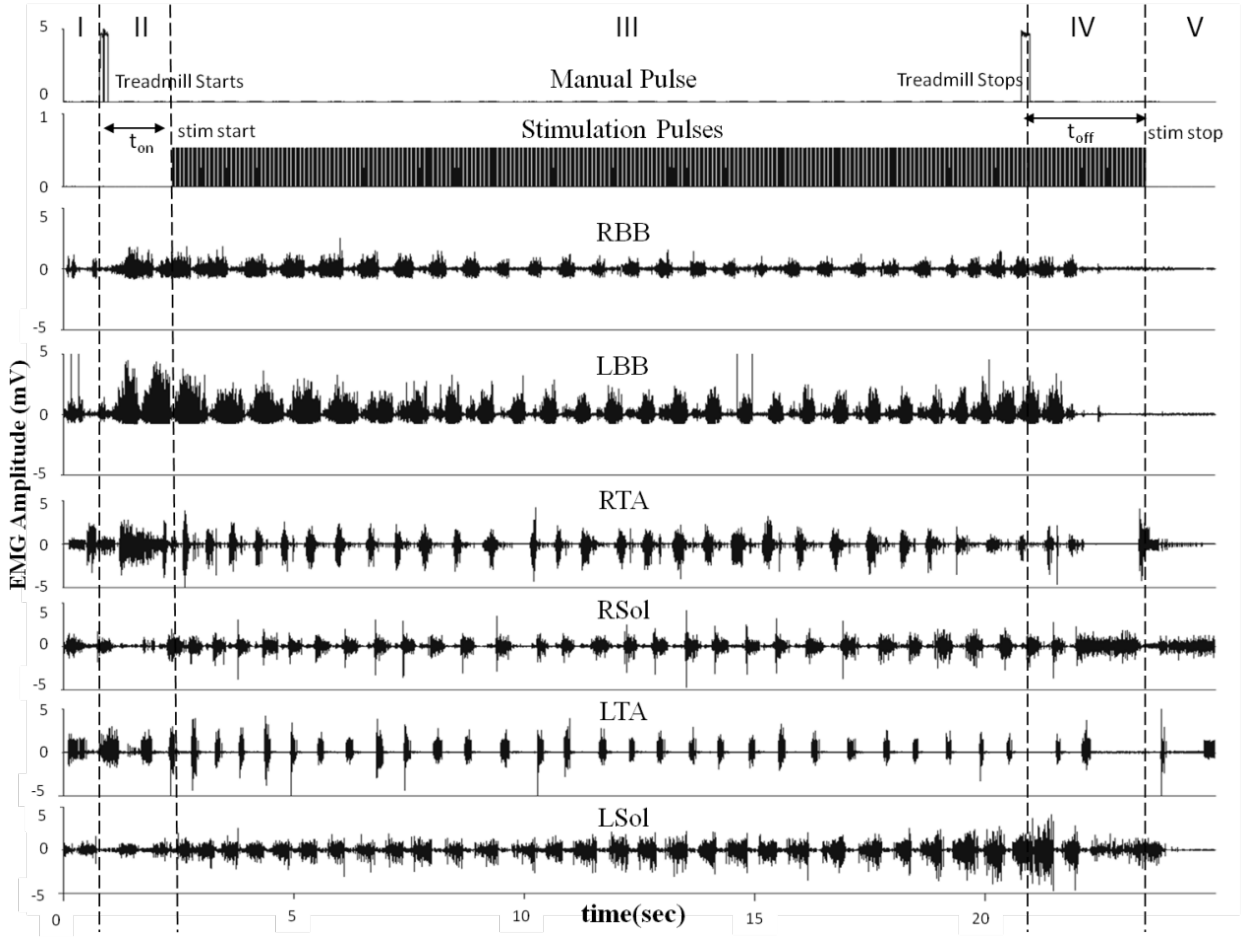

Figure 6.5: EMG recorded during stimulation through the second generation electronic bridge. Manual pulse indicates the turning on (first manual pulse at the beginning of Phase II) and turning off (second manual pulse at the end of Phase III) of the treadmill. Alternating RBB and LBB EMGs are read by the microcontroller to detect forelimb stepping. Electrical pulses are generated in the lumbosacral spinal cord resulting in hindlimb stepping. Alternating EMG bursts in the tibialis anterior (TA, ankle flexor) and soleus (Sol, ankle extensor) muscles of each leg indicate rhythmic movements of the hindlimbs.

Does the electronic bridge have a detrimental effect on stepping performance?

We used quipazine in the present study to produce robust stepping in the spinal rats as reported previously for bipedal stepping (Gerasemenko et al., 2007). The mean EMG burst durations and amplitudes for selected forelimb and hindlimb muscles during the 4 conditions tested while being stimulated via the bridge are shown in Figure 6.7. There was a significant decrease in the RBB EMG burst duration between pre- and post-quipazine stepping at 13.5 cm/s. Regardless of this difference, the response time of the electronic bridge was similar with and without quipazine, i.e., quipazine did not affect the detection protocol. The EMG burst characteristics of the hindlimb muscles were not different with direct stimulation (no electronic bridge) and with the electronic bridge, indicating that the electronic bridge does not affect the stepping performance (Fig. 6.8). With increasing treadmill speeds, the ankle flexors had a relatively constant burst duration, whereas the ankle extensors had a shorter burst duration (Fig. 7), consistent with that reported previously in control adult rats (Roy et al., 1991).

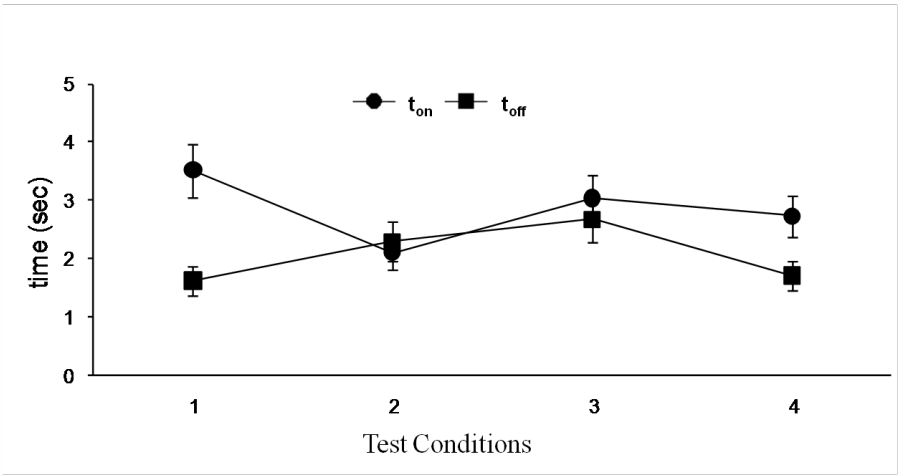

Figure 6.6: Mean response times (mean ± SEM, n=5 rats) calculated by the algorithm to start (t_{on}) and stop (t_{off}) stimulation under four test conditions of quadrupedal stepping on a treadmill: 1) 13.5 cm/s pre-quipazine; 2) 13.5 cm/s post-quipazine; 3) 21 cm/s pre-quipazine; and 4) 21 cm/s post-quipazine administration. Note that there are no significant differences between t_{on} and t_{off} for any test condition or across all test conditions.

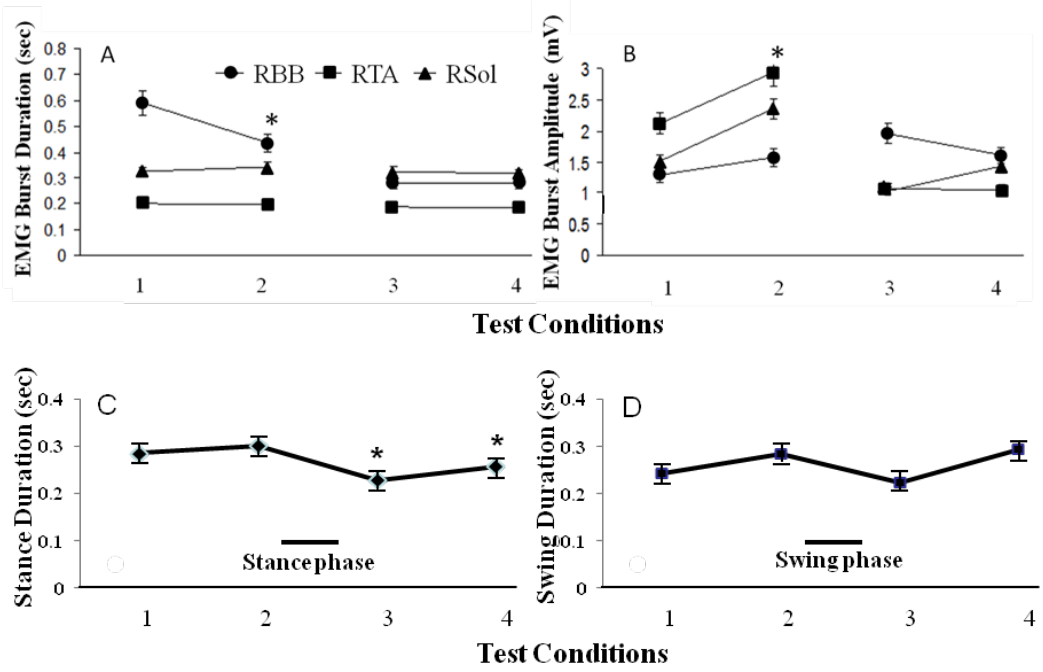

Figure 6.7: A and B: Mean EMG burst durations and amplitudes (mean ± SEM, n=5 rats) for hindlimb and forelimb muscles during stimulation via the bridge under the same four. *, RBB in test condition 2 is significantly different from test condition 1. C and D: mean duration of stance phase and swing phase (mean ±SEM, n=5 rats) during stimulation via the bridge under the same four conditions tested in Figure 6.6. *, duration of stance phase is significantly lower for condition 3 compared to condition 1 and for case 4 compared to case 2

Algorithm validation: determining the detection threshold for stepping

We compared the kinematics and the effectiveness of the detection algorithm in the presence and the absence of stepping (Fig. 6.9A).Using the forelimbs as a reference, the step cycle began when the forelimb touched the treadmill belt and ended when it touched the treadmill belt again. The kinematics were derived from the angles of the elbow during stepping using 3-D coordinates. Figure 6.9B shows the variation in the angle of the right elbow in the same step cycle as shown in Figure 6.9A. The black trace represents the angle of the elbow when the forelimbs stepping, whereas the red trace represents the angle of the elbow when there was no forelimb stepping. Figure 6.9C and D show the scatterplots between the amplitude of the BB EMG envelope and the elbow angle for the same data shown in Figure 6.9A and B. BB EMG amplitudes were minimal and the elbow angle decreased during the stance phase (when the paw was on the treadmill), whereas the BB EMG amplitude increased and the elbow angle increased during the swing phase (when the paw was off the treadmill). The relationship between the elbow angle and the BB EMG frequency is illustrated in Figure 6.9E, demonstrating a clear dichotomy of the presence of stepping vs. no stepping based the frequency spectrum.

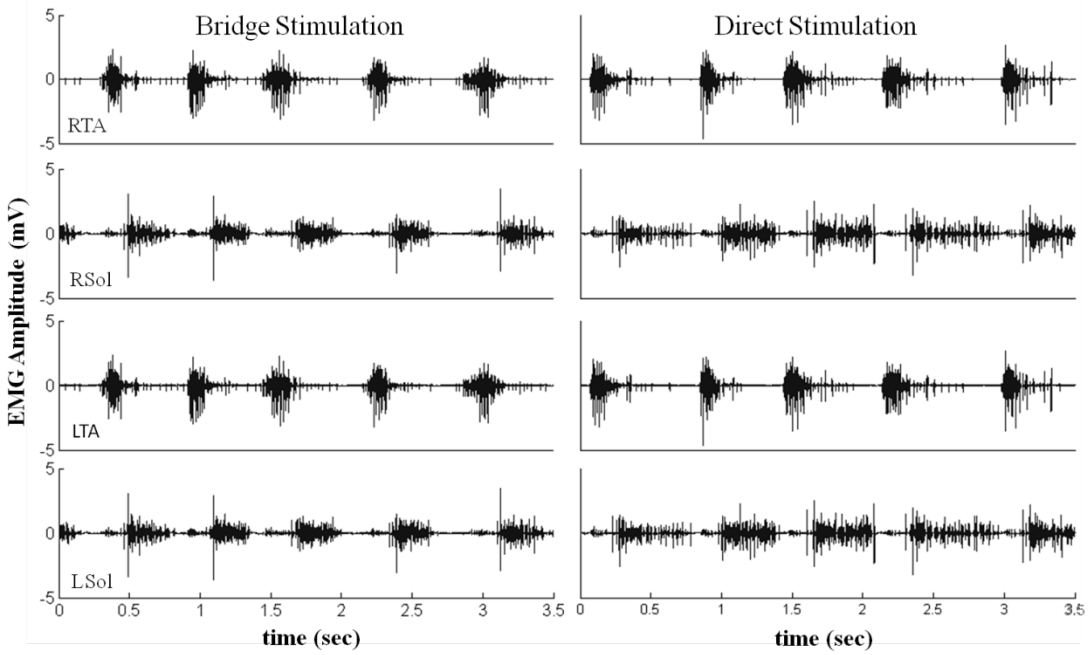

Figure 6.8: Raw EMG activity from hindlimb muscles bilaterally during quadrupedal stepping on a treadmill at 13.5 cm/s with stimulation via the bridge and with direct stimulation (stimulation without the use of the bridge).

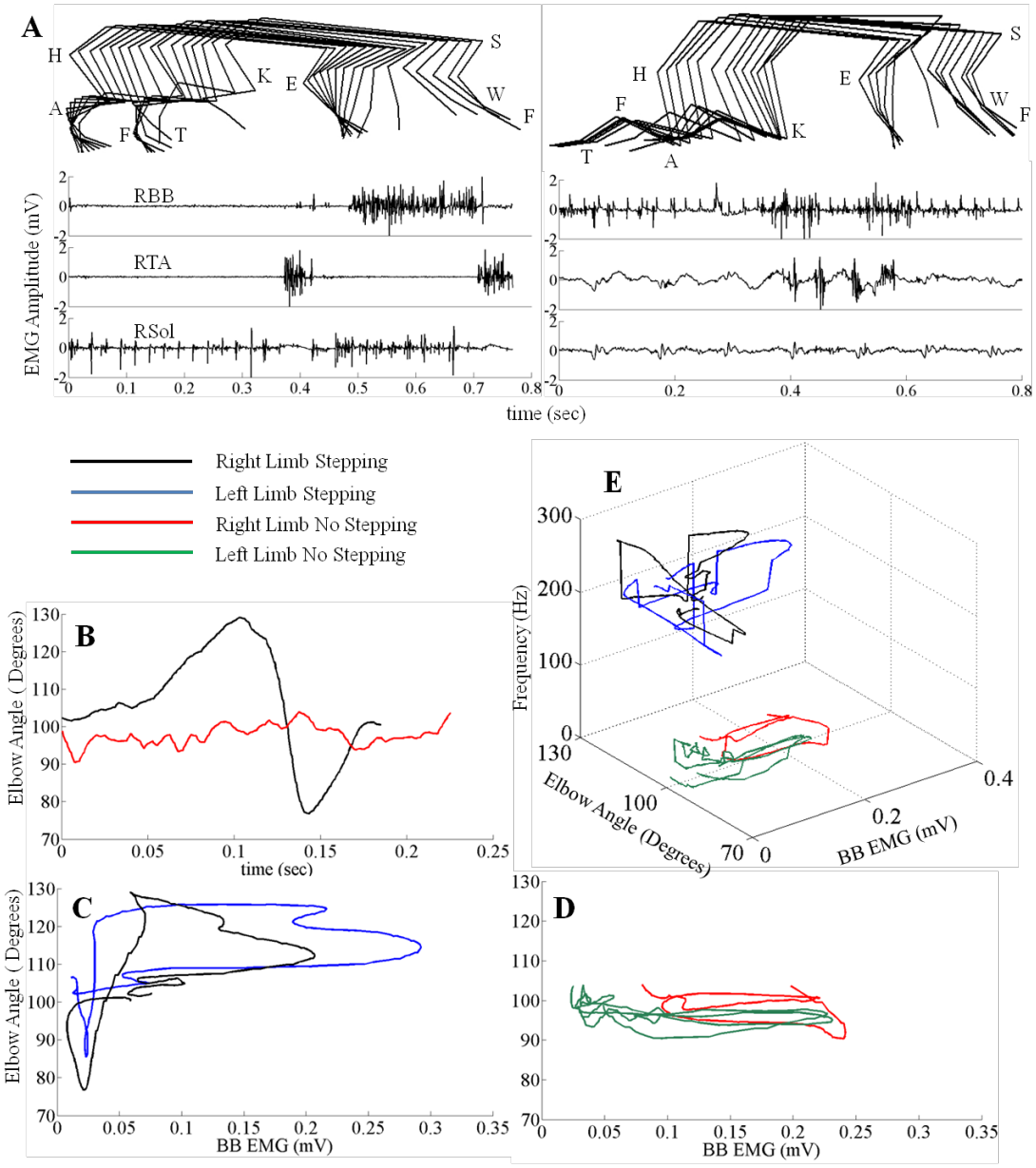

Figure6. 9: EMG and kinematics responses when the forelimbs were stepping or not stepping. (A) 2-D stick diagrams (50 ms between sticks) of the limbs observed when the forelimbs were stepping or not stepping with the corresponding EMG. (B) Changes in the elbow angle for the data shown in (A). (C) Scatterplot between the linear envelope of the BB EMG and the elbow angle during stepping. (D) Scatterplot between the linear envelope of the BB EMG and the

elbow angle when the forelimbs were not stepping. (E) 3-D plot representing the elbow angle, BB EMG, and peak frequency (see Fig. 3v and vi and Fig. 4).

Discussion

We have developed a BMSCI having a pattern recognition algorithm that can use EMG from the forelimb muscles to trigger the initiation and termination of the stimulation of the spinal cord below the level of a complete spinal cord injury. This algorithm (second generation) detects stepping with little or no calibration and thus provides an advantage over the system (first generation) we tested initially that needs constant monitoring. Our logic for using the EMG signals from the forelimb muscles as a trigger was that these signals reflect the "intent to step" quadrupedally. The point was to use naturally generated EMG signals from the forelimbs to control an electronic bridge that would facilitate hindlimb stepping in spinal rats. Our results from multiple test conditions demonstrate that this system is capable of adapting to different pharmacological and stepping conditions. Results from the first generation showed us that it is possible to develop a real time EMG detection system on the MSP430, but this generation was cumbersome to run due to calibration of the multiple channels and the variability between animals. The technique used in the second generation allowed us to reduce the calibration and to accommodate the variability between animals. Given the variability in the conditions under which the step detection algorithm was tested on the MSP430, the time taken to detect the beginning of stimulation (ton) and the time taken to detect the stopping of stimulation (toff) had about the same consistency and demonstrated the algorithm's ability to detect EMG signals and to adapt to different conditions and different animals (Fig. 6.6).

To further enhance the utility of spinal stimulation, the control system must go beyond an on/off control as shown in the present experiments. In paraplegic humans any set of muscles that can be voluntarily controlled could be used as a trigger. Generating and controlling the EMG in muscles such as the deltoid or pectoralis to control prosthetic devices has been shown to be

feasible in humans.. Harkema et al., (2011) demonstrated in a single human subject the importance of varying stimulation parameters in obtaining the most effective standing and voluntary control of the legs in a subject with a motor complete injury. Similarly, Ichiyama et al., (2005) reported the variation in stimulation voltage at different time points after injury: the stimulation intensity needed to generate locomotor activity in spinal rats was 3.39 ± 0.2V at 2 weeks and 7.55 ± 1.2 V at 4 weeks post-ST using 40 Hz stimulation monopolar stimulation at L2.

Dutta et al., (2009) reported a system to detect EMG during stepping to trigger muscles in the contralateral limb to initiate stepping in patients with an incomplete spinal cord injury. A training data set was derived from patients with a switch-based functional electrical stimulation (FES) system to assist the patients in stepping and a feature extraction was performed on the EMG. A threshold-based binary classifier was trained to distinguish a set of feature templates in the EMG linear envelopes indicating the intention to trigger the next step. These authors report that during online testing the intention to trigger the next step was detected using analyses between features extracted from real time EMG linear envelopes and feature templates derived from the training data set.

The ultimate objective of the present study was to use EMG from multiple muscles in the forelimb to detect stepping and fine variations in forelimb and hindlimb stepping and to modulate the stimulation of the spinal cord to generate optimum stepping movements in the hindlimbs. We also have developed a simulated test bench in MATLAB (Mathworks) to test the EMG signals for offline step detection. This testbench is an exact replica of the algorithm run on the MSP430. Using this simulated test bench, we can validate the recordings seen in real time as well as test the detection algorithm at different time points during recovery after an injury.

Further simulations could be used to develop a 'self-learning' or 'threshold-adjusting' algorithm that could be animal specific as well as being applicable for different stages of recovery after an injury.

Conclusions

We have developed a novel technique for detecting stepping of the forelimbs and neuromodulating the spinal circuitry in real time to control hindlimb movements in rats with complete paralysis. This detection algorithm can accommodate the variations in EMG amplitudes that normally occur during spontaneous functional recovery after a spinal cord injury. This neuromodulatory approach also is likely to have the potential to improve the control of movements in other neuromotor disorders, such as stroke and Parkinson Disease.

Chapter 7

Volitional control of bladder voiding after a complete spinal cord injury in adult female rats

Abstract

The primary function of the lower urinary tract is to store and expel urine in a coordinated manner without leakage. After a spinal cord injury, the coordinated function of the lower urinary tract is lost and manual voiding of the bladder several times per day is required. Electrical enabling motor control (eEmc) has been shown to improve locomotor and postural function after a spinal cord injury in several animal models and in humans. In the present study we demonstrate the ability of eEmc to control bladder function. eEmc applied to the lumbosacral spinal cord at a low frequency (1 Hz) results in an increase in bladder pressure and a bursting pattern in the external urethral sphincter muscle similar to that in intact animals, thus partially overcoming destrusor EUS co-contraction and enabling volitional bladder voiding. The result is self-expression of the bladder in complete spinal animals.

Introduction

The two main functions of the lower urinary tract, which is comprised of the bladder and urethra, are to store urine without leakage and to expel urine in a coordinated, controlled manner (de Groat et al., 1998). In the normal adult rat, storage is dependent on the inhibition of parasympathetic action on the smooth bladder muscle (detrusor) and on the sympathetic tonic activation of the internal urethral sphincter for outflow resistance. During micturition, efficient voiding is dependent on synchronous activation of the detrusor for contraction, relaxation of the internal urethral sphincter, and bursting activity of the striated external urethral sphincter (EUS) for enhanced urine flow (Maggi et al., 1986; Kruse et al., 1993). Normal control of bladder function involves a complex interaction between the the cerebral cortex, pontine micturition center, sympathetic and parasympathetic nervous systems, and somatic motoneurons in the lumbar spinal cord.

The level and extent of a spinal cord lesion determines the extent of loss of bladder function (Potter 2006). A mid-thoracic spinal cord transection in adult rats results in complete loss of bladder function (D'Amico et al., 2011). In individuals with a spinal cord injury at either the thoracic or cervical level, however, descending projections from supraspinal centers are severed and their axons degenerate. In many such individuals, the reflex pathways mediating continence remain intact, but micturition cannot be initiated in a normal manner (Barrington 1931), The most common form of this condition is detrusor-sphincter dyssynergia (de Groat 1998) in which both the detrusor and EUS tend to be activated together rather than reciprocally. When the bladder becomes distended, both muscles contract and, while some urine may be voided, bladder emptying is usually incomplete. de Groat et al., (2011) reported in rats, afferents

originating in the bladder and EUS projecting to the lumbosacral region of the spinal cord with changes in roles of these projections after a mid-thorascc spinal cord injury. The overlap in the lumbosacral region of the spinal cord controlling bladder function (De Groat et al., 2011, and locomotor function (Grillner et al., 1973; Edgerton et al., 2001; Ichiyama et al., 2005) could represent two separate sets of circuits with potential overlap or a single circuit being tuned differently by eEmc at different frequencies of stimulation. Therefore the purpose of the present study was to assess the effect of eEmc on volitional control on bladder voiding using a range of frequencies after a complete mid-thoracic spinal cord transection in adult female rats.

Methods

Animal care procedures

Data were obtained from 4 adult female Sprague Dawley rats (270-300 g body weight). Pre- and post-surgical animal care procedures have been described in detail previously (Roy et al., 1992). The rats were housed individually with food and water provided *ad libitum*. All survival surgical procedures were conducted under aseptic conditions and with the rats deeply anesthetized with isoflurane gas administered via facemask as needed. All procedures described below are in accordance with the National Institute of Health Guide for the Care and Use of Laboratory Animals and were approved by the Animal Research Committee at UCLA.

Head connector and intramuscular EMG electrode implantation

A small incision was made at the midline of the skull. The muscles and fascia were retracted laterally, small grooves were made in the skull with a scalpel, and the skull was dried thoroughly. Two amphenol head connectors with Teflon-coated stainless steel wires (AS632, Cooner Wire, Chatsworth CA) were securely attached to the skull with screws and dental cement as described previously (Roy et al., 1992; Ichiyama et al., 2005). Selected hindlimb muscles, i.e., the tibialis anterior (TA) and soleus, were implanted bilaterally with EMG recording electrodes as described by Roy et al. (1991). Skin and fascial incisions were made to expose the belly of each muscle. Two wires extending from the skull-mounted connector were routed subcutaneously to each muscle. The wires were inserted into the muscle belly using a 23-gauge needle and a small notch (~0.5-1.0 mm) was removed from the insulation of each wire to expose

the conductor and form the electrodes. The wires were secured in the belly of the muscle via a suture on the wire at its entrance into and exit from the muscle belly. The proper placement of the electrodes was verified during the surgery by stimulating through the head connector and post-mortem via dissection.

After a midline incision in the lower abdomen, the pubic symphysis was removed exposing the underlying EUS muscle. Two fine wire electrodes (A-M Systems; 50 μm insulated stainless steel) were inserted bilaterally into the EUS to measure EMG activity.

Spinal cord transection and ES electrode implantation procedures and post-surgical animal care

A complete spinal cord transection to include the dura was performed at approximately the T8 spinal level using microscissors. Two surgeons verified the completeness of the transection by lifting the cut ends of the spinal cord and passing a glass probe through the lesion site. Gel foam was inserted into the gap created by the transection as a coagulant and to separate the cut ends of the spinal cord.

For ES electrode implantation, partial laminectomies were performed to expose the spinal cord at spinal levels L2 and S1. Two Teflon-coated stainless steel wires from the head connector were passed under the spinous processes and above the dura mater of the remaining vertebrae between the partial laminectomy sites. After removing a small portion (~1 mm notch) of the Teflon coating and exposing the conductor on the surface facing the spinal cord, the electrodes were sutured to the dura mater at the midline of the spinal cord above and below the electrode sites using 8.0 Ethilon suture (Ethicon, New Brunswick, NJ). Two common ground (indifferent EMG and stimulation grounds) wires (~1 cm of the Teflon removed distally) were inserted

subcutaneously in the mid-back region. All wires (for both EMG and ES) were coiled in the back region to provide stress relief. All incision areas were irrigated liberally with warm, sterile saline. All surgical sites were closed in layers using 5.0 Vicryl (Ethicon, New Brunswick, NJ) for all muscle and connective tissue layers and for the skin incisions in the hindlimbs and 5.0 Ethilon for the back skin incision. All closed incision sites were cleansed thoroughly with saline solution. Analgesia was provided by buprenex (0.5–1.0 mg/kg, s.c. 3 times/day). The analgesics were initiated before completion of the surgery and continued for a minimum of 3 days. The rats were allowed to fully recover from anesthesia in an incubator. The rats were housed individually in cages that had ample CareFresh bedding, and the bladders of the spinal rats were expressed manually 3 times daily for the first 2 weeks after surgery and 2 times daily thereafter. The hindlimbs of the spinal rats were moved passively through a full range of motion once per day to maintain joint mobility. All of these procedures have been described in detail previously (Courtine et al., 2009).

Training, stimulation, and acute testing procedures

The rats were trained to step bipedally on a specially designed motor-driven rodent treadmill using a body weight support system (de Leon et al., 2002) under the influence of eEmc at 40 Hz between L2 and S1 (Lavrov et al., 2006; Gerasimenko et al., 2008; Ichiyama et al., 2008; Courtine et al., 2009). The animals were tested 6 weeks post-injury. The rats were suspended using the same body weight support used for training but with their feet not touching the treadmill. A PE50 catheter was inserted into the bladder via the urethral opening as described by (rD'Amico et al.,2011). A solid-state pressure transducer (SPR 524, Millar instruments) was inserted adjacent to the catheter. EMG and pressure recordings were band-pass filtered (1 Hz to 5 KHz), amplified using an A-M Systems Model 1700 differential AC amplifier (A-M Systems,

Carlsborg, WA), and sampled at a frequency of 10 KHz using a custom data acquisition program written in the LabView development environment (National Instruments, Austin, TX) as described previously (Courtine et al., 2009).

Using a syringe, 1 cc of saline was infused into the bladder at a steady rate. No saline leaked out through the catheter during or after the infusion. Three stimulation frequencies (1, 5, and 40 Hz) were tested with stimulation consistently between L2 and S1. Three trials were performed at each frequency with each trial lasting at least 90 sec in random order to check for consistency. The stimulation intensity at each frequency was maintained at 1-2 V above the threshold for evoking a response in the hindlimb muscles. The saline voided during the stimulation was collected using a weigh boat and the volume measured. The bladder was manually emptied before and after each trial to account for any residual urine in the bladder.

Statistical analyses

All data are reported as mean ± SEM. Statistically significant differences were determined using paired t-tests. The criterion level for the determination of a statistical difference was set at $P < 0.05$ for all computations.

Results

The rats were tested at 6 weeks post-transection and after xx weeks of step training. At this time, all rats were able to perform plantar steps with partial body weight support under the influence of eEmc at 40 Hz between L2 and S1. Infusion of 1 cc of saline into the bladder via the urethral catheter at a steady rate did not result in any leakage of saline, whereas volumes greater than 1cc resulted in visible leakage. Stimulation at 40 Hz resulted in rhythmic bilateral air stepping as reflected by the alternating EMG bursting pattern in a flexor (TA) and extensor (soleus) muscle (Fig. 1). Similar patterns of air stepping were observed during infusion of saline (Fig. 1) and with tail pinching (data not shown), but with greater amplitudes in the flexors and extensors but shorter cycle durations compared to 40Hz eEmc.

Although a rhythmic alternating bilateral locomotor pattern was observed in the hindlimbs.with eEmc at 40 Hz, only a small amount of voiding of saline (~5%) was observed (Fig. 7.2), Interestingly ~30% of the saline was voided after the stimulation was turned off with no movements or evoked potentials in the hindlimbs. Stimulation at 5 Hz resulted in strong vibratory movements in both hindlimbs but only ~10-20% of the saline was voided, with no saline being voided immediately after the stimulation was turned off. The most efficient voiding occurred at 1-Hz stimulation with ~90-95% of the volume voided within the 90 sec stimulation duration. Hindlimb evoked potentials (Fig. 3) monitored during 1-Hz stimulation demonstrates a marginal increase (not significant) in MR (latency ~5ms) amplitude in the extensors (soleus) during voiding compared to during not voiding. No such change was seen in the flexor-evoked potentials. The lack of significant changes in the evoked potentials may suggest consistent pattern of tuning in the lumbosacral networks during both bladder voiding and non voiding,

suggesting that the networks are primed for bladder voiding at 1Hz stimulation and when the right afferent input is provided, the bladder would be emptied.

Lower frequencies of stimulation (1 and 5Hz) resulted in substantial contractions of the bladder and EUS as demonstrated by the changes in bladder pressure and evoked potentials corresponding to each stimulation pulse (Fig. 4A and B), whereas the EUS demonstrates bursting activity between the 200ms and 1000ms duration post 1Hz stimulation pulse (Figure 4D) which was not seen in the case of higher frequencies. On the other hand, 40Hz eEmc generates minimal change in bladder pressure while maintaining a constant state of pressure higher than 1 and 5 Hz. (Figure 4B and C).

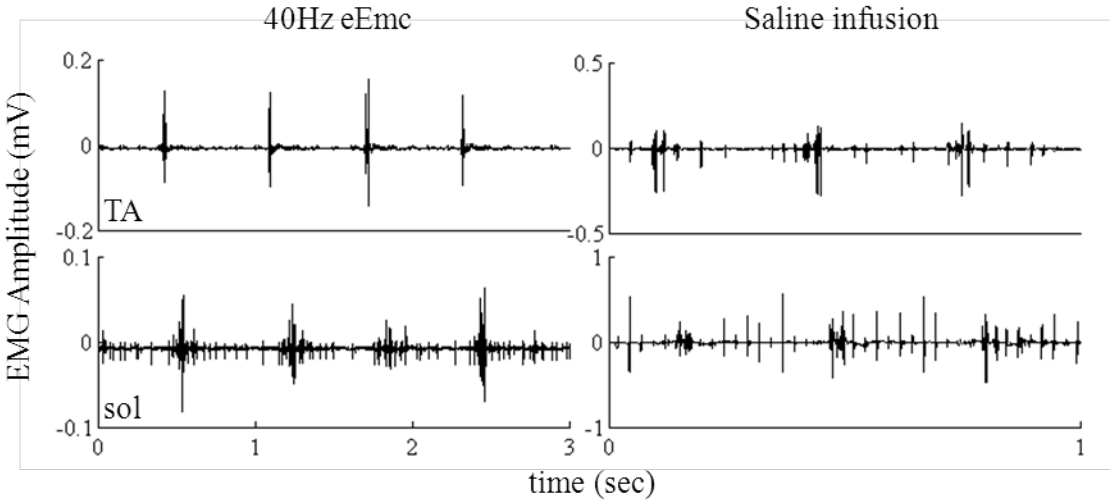

Figure 7.1: Representative recording of locomotor like patterns of EMG from ankle flexor (TA) and extensors (sol) with the animal suspended in the air during 40Hz eEmc and saline infusion

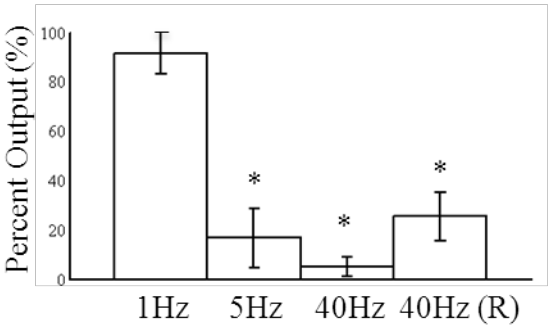

Figure 7.2: mean (+/- SEM, n = 3 animals, 3 trials each animal, each frequency) percentage saline output.

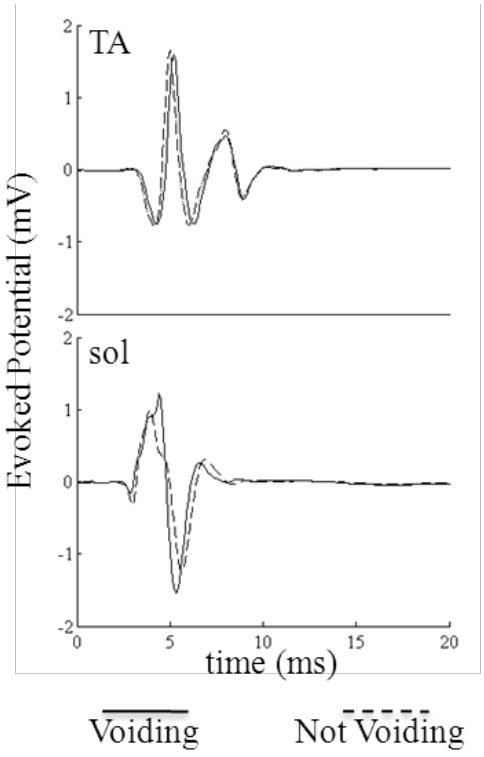

Figure 7.3: Motor evoked potential from TA and sol during voiding and during **not voiding** from the same animal at the same intensity.

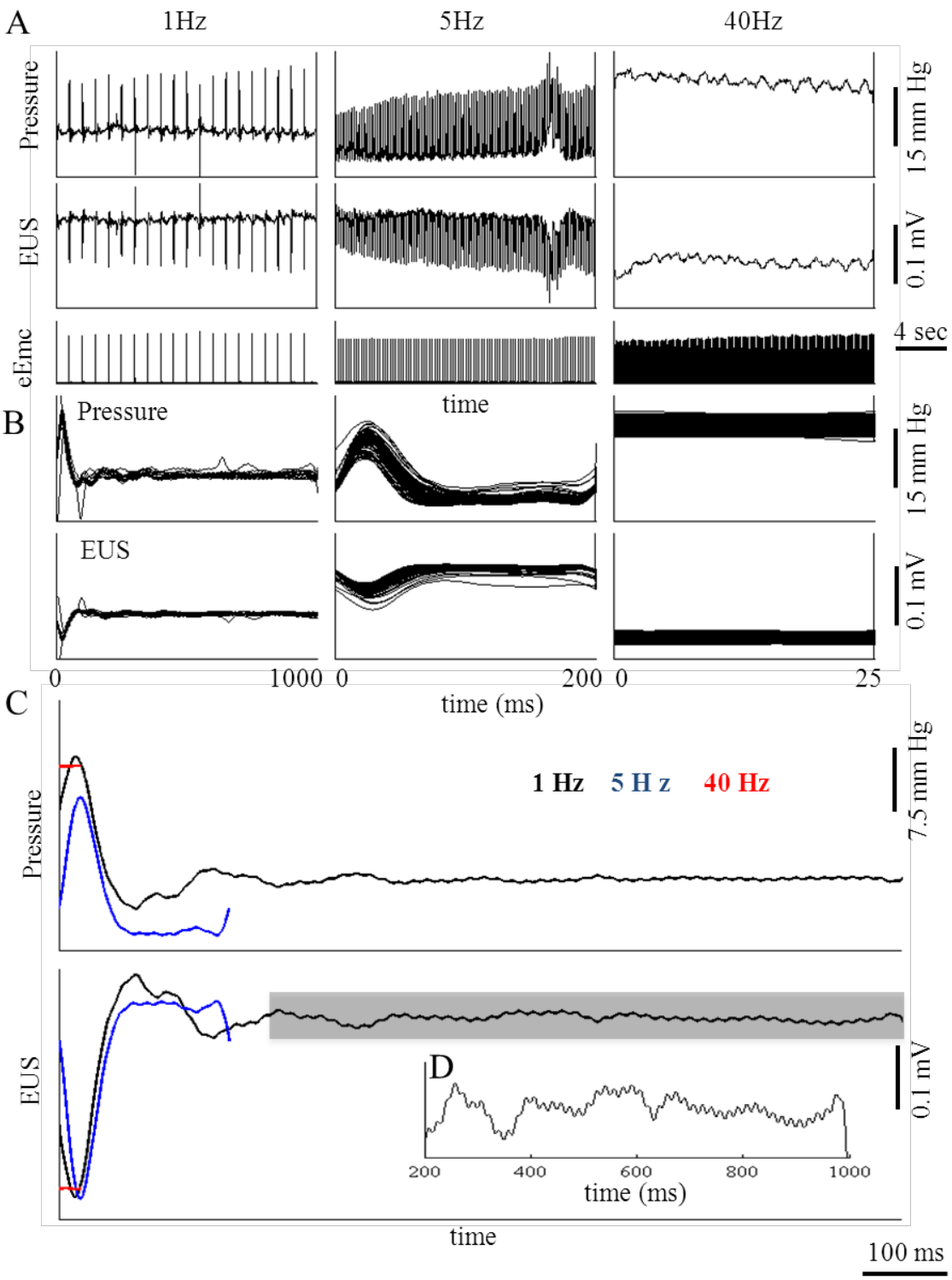
A
1Hz
5Hz
40Hz
Pressure
EUS
eEmc
15 mm Hg
0.1 mV
4 sec
B
Pressure
EUS
time
15 mm Hg
0.1 mV
0
1000
0
200
0
25
time (ms)
C
1 Hz
5 H z
40 Hz
Pressure
EUS
7.5 mm Hg
0.1 mV
D
200
400
600
800
1000
time (ms)
time
100 ms

Figure 7.4: A) Internal bladder pressure and EMG amplitude from external urethral sphincter (EUS) muscle at 1,5 and 40 Hz. B) Individual responses to each stimulation pulse in the bladder pressure and EUS muscle. C) Average pressure and EUS evoked potential. D) Zoomed in section of EUS activity between the 200ms and 1000ms duration highlighted in C.

Discussion

Stimulation of the spinal cord (eEmc) has been shown to be effective in restoring locomotor function in animal models (Iwahara et al., 1991, Gerasimenko et al., 2003, Edgerton et al.,2004), and in human subjects (Harkema et al., 2011) after a spinal cord injury. One of the hypothesized mechanisms suggests that the stimulation raises the excitability of the neural networks (interneurons and motoneurons) and combined with locomotor training results in improvement in locomotor function (Ichiyama et al., 2008, Courtine et al., 2009). Harkema et al. (2011) reported an improvement in locomotor function and voluntary control of the hindlimbs in a subject with motor complete paralysis using spinal cord stimulation at a caudal level (~S1). They also reported an improvement in autonomic function such as bladder, sexual, and thermoregulatory activity. More recently Chang et al. (2012, SFN abstracts) demonstrated an inhibition in EUS tonic activity via stimulation of L2-L3 spinal segments in rats. The present data demonstrate the ability to overcome detrusor-sphincter dyssynergia and facilitate efficient voiding of the bladder of awake rats with a complete spinal cord transection.

Possible mechanism to explain volitional control of bladder after SCI via eEmc

There is a bursting pattern (4-8 Hz) in the EUS in concert with bladder contractions in intact rats during efficient voiding (D'Amico et al., 2011, 2012). This bursting pattern in the EUS, however, changes to tonic activity after a SCI resulting in asynchronous activity of the bladder and EUS and inefficient voiding.

Based on the results seen thus far, we could hypothesize that a partially filled bladder (with 1CC saline) activates specific projections to the lumbosacral spinal cord 'sensing' the feeling of a filled bladder. eEmc at 1 Hz produces immediate contractions of the bladder and EUS. The interpulse duration allows sufficient latent time for the EUS to start 'bursting'. The EUS bursting activates afferents projecting to the spinal cord along with afferents from the bladder 'sensing a filled state' and triggers a feedforward loop to reinforce the action of the stimulation on the neural networks to generate voiding. Further investigation into the exact mechanism is needed including the identification of specific interneurons responsible for the coordinated working of the detrusor and EUS muscles.

Plasticity in neural networks

The rats were successful in voiding via 1-Hz stimulation between L2 and S1 after 3 weeks of locomotor training using eEmc at L2 and S1 at 40 Hz (Ichiyama et al., 2005, Courtine et al., 2009). It appears that locomotor training along with eEmc allows us to engage the neural networks, which when stimulated at 1 Hz get tuned differently to facilitate bladder voiding. Note that the earliest time point that the animals started voiding via 1-Hz epidural stimulation was three weeks and that this coincided with the time point at which the spinal animals recovered partial locomotor ability (Lavrov et al., 2006). Efficient bladder voiding was observed from weeks 3 to 6 while the animals continued to be trained to step on a treadmill. When training was stopped for 2 weeks (between weeks 6 to 8), the animals failed to void the bladder via eEmc at 1 Hz. Thus it appears that there is a need to constantly engage the neural circuits via locomotor training to generate functional voiding responses.

Neural networks controlling bladder function and

Stimulation at higher frequencies (40 Hz) while maintaining the sites of stimulation constant resulted in consistent air stepping bilaterally. Similar responses were seen in the hindlimbs during infusion of saline, suggesting an overlap in the neural networks controlling both the hindlimb locomotor activity and bladder control. A phenomenon that is seen often during locomotor testing under the influence of eEmc in spinal rats is that locomotor ability is lost when the animals spontaneously void their bladders (unpublished data). The alternating nature of the neural networks controlling bladder function and locomotor function are realized via epidural stimulation at different frequencies, i.e.., 1 and 40 Hz respectively.

Conclusion

Thus, the data demonstrates that eEmc is capable of restoring volitional control of bladder voiding after spinal cord injury, but requires constant engagement of the circuit and tuning in a specific fashion to facilitate voiding.

Chapter 8

Concluding remarks and future directions

In this thesis we used the rat spinal cord transection model to explore the effect of spinal cord epidural stimulation in improving the locomotor ability. For the first time we have defined the "footprint" of locomotion after spinal cord injury under the influence of epidural stimulation and the variations under different pharmacological conditions and loading. Thus, we could use this technique to define rehabilitation strategies based on the pathological conditions.

We then explored the effect of varying stimulation sites and frequencies using a parylene based microelectrode array. For the first time we identified the effect of parameters of stimulation on facilitation of standing and stepping after a complete spinal cord transection as early as 8 days after injury.

These studies lead us to ask questions regarding the chronic effects of stimulation. We studied the locomotor ability of freely moving rats with a complete spinal cord injury over a 6 hour period with and without epidural stimulation. We observed that animals with stimulation showed greater mobility and performed tasks such as standing and stepping compared to animals without stimulation that couldn't. The last study on locomotion after spinal cord injury involved, designing a device that would allow us to trigger epidural stimulation during quadrupedal locomotion based on movements in forelimbs with little or no calibration. This would allow us to stimulate the spinal cord when the forelimbs would indicate an intent to move.

Lastly, we started studying the highly complicated but relevant area of physiology after spinal cord injury, bladder control. We identified stimulation parameters that would enable

partial volitional control of the bladder after spinal cord injury via epidural stimulation of the spinal cord.

The major contribution of this thesis work was to define rehabilitation strategies for rats after spinal cord injury with the aim to adapt them to human subjects and clinical trials. Using the animal model, we have been partially successful in designing spinal implants which will enable in the design of implants to be used in human subjects. Another longterm goal would be to apply the learnings of this model to other pathological conditions such as stroke, Parkinson's disease and partial paralysis.

Bibliography

Alaimo, M. A., Smith, J. L., Roy, R. R., & Edgerton, V. R. (1984). EMG activity of slow and fast ankle extensors following spinal cord transection. *Journal of Applied Physiology*, *56*(6), 1608-1613.

Angeli CA, Edgerton VR, Gerasimenko YP , Harkema SJ. Improvements in level of recovery of task specific voluntary control of lower limbs with lumbosacral epidural stimulation and training after chronic complete paralysis. *SFN Abstracts 2012*; 475.26/JJ12, 2012.

Barrington, F. J. F. (1931). THE COMPONENT REFLEXES OF MICTURITION IN THE CAT PARTS I AND II. *Brain*, *54*(2), 177-188.

Barbeau, H., & Rossignol, S. (1991). Initiation and modulation of the locomotor pattern in the adult chronic spinal cat by noradrenergic, serotonergic and dopaminergic drugs. *Brain research*, *546*(2), 250-260.

Bitzer, S., & van der Smagt, P. (2006, May). Learning EMG control of a robotic hand: Towards active prostheses. In *Robotics and Automation, 2006. ICRA 2006. Proceedings 2006 IEEE International Conference on* (pp. 2819-2823). IEEE.

Brown, T. G. (1911). The intrinsic factors in the act of progression in the mammal. *Proceedings of the Royal Society of London. Series B, Containing Papers of a Biological Character*, *84*(572), 308-319.

Calancie, B., Broton, J. G., John Klose, K., Traad, M., Difini, J., & Ram Ayyar, D. (1993). Evidence that alterations in presynaptic inhibition contribute to segmental hypo-and hyperexcitability after spinal cord injury in man.*Electroencephalography and Clinical Neurophysiology/Evoked Potentials Section*, *89*(3), 177-186.

CHANG H, ICHIYAMA R, HAVTON L. Epidural stimulation induces voiding and external urethral sphincter (EUS) bursting activity in intact rats, SFN Abstracts 2012,

Chiba, A., Oshio, K. I., & Inase, M. (2003). Magnetically evoked EMGs in rats.*Neurological research*, *25*(1), 87-91.

Cooley, J. W., Lewis, P. A., & Welch, P. D. (1969). The fast Fourier transform and its applications. *Education, IEEE Transactions on*, *12*(1), 27-34.

Courtine, G., Harkema, S. J., Dy, C. J., Gerasimenko, Y. P., & Dyhre-Poulsen, P. (2007). Modulation of multisegmental monosynaptic responses in a variety of leg muscles during walking and running in humans. *The Journal of Physiology*,*582*(3), 1125-1139.

Courtine, G., Gerasimenko, Y., van den Brand, R., Yew, A., Musienko, P., Zhong, H., ... & Edgerton, V. R. (2009). Transformation of nonfunctional spinal circuits into functional states after the loss of brain input. *Nature neuroscience*,*12*(10), 1333-1342.

D'Amico, S. C., Schuster, I. P., & Collins, W. F. (2011). Quantification of external urethral sphincter and bladder activity during micturition in the intact and spinally transected adult rat. *Experimental neurology*, *228*(1), 59-68.

D'Amico, S. C., & Collins, W. F. (2012). External urethral sphincter motor unit recruitment patterns during micturition in the spinally intact and transected adult rat. *Journal of Neurophysiology*.

de Groat, W. C. (1998). Anatomy of the central neural pathways controlling the lower urinary tract. *European urology*, *34*(1), 2-5.

de Groat W. C. , (2011). Autonomic Regulation of the Urinary Bladder and Urethra. *Central Regulation of Autonomic Functions*, 345.

de Leon, R. D., Hodgson, J. A., Roy, R. R., & Edgerton, V. R. (1998). Full weight-bearing hindlimb standing following stand training in the adult spinal cat.*Journal of neurophysiology*, *80*(1), 83-91.

de Leon, R. D., Hodgson, J. A., Roy, R. R., & Edgerton, V. R. (1999). Retention of hindlimb stepping ability in adult spinal cats after the cessation of step training. *Journal of neurophysiology*, *81*(1), 85-94.

de Leon, R. D., Tamaki, H., Hodgson, J. A., Roy, R. R., & Edgerton, V. R. (1999). Hindlimb locomotor and postural training modulates glycinergic inhibition in the spinal cord of the adult spinal cat. *Journal of neurophysiology*,*82*(1), 359-369.

de Leon, R. D., Reinkensmeyer, D. J., Timoszyk, W. K., London, N. J., Roy, R. R., & Reggie Edgerton, V. (2002). Use of robotics in assessing the adaptive capacity of the rat lumbar spinal cord. *Progress in brain research*, *137*, 141-149.

Deliagina, T. G., Beloozerova, I. N., Zelenin, P. V., & Orlovsky, G. N. (2008). Spinal and supraspinal postural networks. *Brain research reviews*, *57*(1), 212-221.

Dietz, V., & Harkema, S. J. (2004). Locomotor activity in spinal cord-injured persons. *Journal of Applied Physiology*, *96*(5), 1954-1960.

Dutta, A., Kobetic, R., & Triolo, R. J. (2009). Gait initiation with electromyographically triggered electrical stimulation in people with partial paralysis. *Journal of biomechanical engineering*, *131*(8), 81002.

Edgerton, V. R., Tillakaratne, N. J., Bigbee, A. J., de Leon, R. D., & Roy, R. R. (2004). Plasticity of the spinal neural circuitry after injury*. *Annu. Rev. Neurosci.*, *27*, 145-167.

Edgerton, V. R., Courtine, G., Gerasimenko, Y. P., Lavrov, I., Ichiyama, R. M., Fong, A. J., ... & Roy, R. R. (2008). Training locomotor networks. *Brain research reviews*, *57*(1), 241-254.

Etlin, A., Blivis, D., Ben-Zwi, M., & Lev-Tov, A. (2010). Long and short multifunicular projections of sacral neurons are activated by sensory input to produce locomotor activity in the absence of supraspinal control. *The Journal of Neuroscience*, *30*(31), 10324-10336.

Finni, T., Haakana, P., Pesola, A. J., & Pullinen, T. (2012). Exercise for fitness does not decrease the muscular inactivity time during normal daily life.*Scandinavian journal of medicine & science in sports*.

Fong, A. J., Cai, L. L., Otoshi, C. K., Reinkensmeyer, D. J., Burdick, J. W., Roy, R. R., & Edgerton, V. R. (2005). Spinal cord-transected mice learn to step in response to quipazine treatment and robotic training. *The Journal of neuroscience*, *25*(50), 11738-11747.

Grillner, S. (1974). Locomotion in the spinal cat. In *Control of posture and locomotion* (pp. 515-535). Springer US.

Forssberg, H. (1979). Stumbling corrective reaction: a phase-dependent compensatory reaction during locomotion. *Journal of Neurophysiology*, *42*(4), 936-953.

García-Alías, G., Barkhuysen, S., Buckle, M., & Fawcett, J. W. (2009). Chondroitinase ABC treatment opens a window of opportunity for task-specific rehabilitation. *Nature neuroscience*, *12*(9), 1145-1151.

Gerasimenko, Y. P., Avelev, V. D., Nikitin, O. A., & Lavrov, I. A. (2003). Initiation of locomotor activity in spinal cats by epidural stimulation of the spinal cord. *Neuroscience and behavioral physiology*, *33*(3), 247-254.

Gerasimenko, Y. P., Lavrov, I. A., Courtine, G., Ichiyama, R. M., Dy, C. J., Zhong, H., ... & Edgerton, V. R. (2006). Spinal cord reflexes induced by epidural spinal cord stimulation in normal awake rats. *Journal of neuroscience methods*, *157*(2), 253-263.

Gerasimenko, Y. P., Ichiyama, R. M., Lavrov, I. A., Courtine, G., Cai, L., Zhong, H., ... & Edgerton, V. R. (2007). Epidural spinal cord stimulation plus quipazine administration enable stepping in complete spinal adult rats. *Journal of neurophysiology*, *98*(5), 2525-2536.

Gerasimenko, Y., Roy, R. R., & Edgerton, V. R. (2008). Epidural stimulation: comparison of the spinal circuits that generate and control locomotion in rats, cats and humans. *Experimental neurology*, *209*(2), 417-425.

Grillner, S. (1975). Locomotion in vertebrates: central mechanisms and reflex interaction. *Physiological reviews*, *55*(2), 247-304.

Grillner, S. (2003). The motor infrastructure: from ion channels to neuronal networks. *Nature Reviews Neuroscience*, *4*(7), 573-586.

Harkema, S., Gerasimenko, Y., Hodes, J., Burdick, J., Angeli, C., Chen, Y., ... & Edgerton, V. R. (2011). Effect of epidural stimulation of the lumbosacral spinal cord on voluntary movement, standing, and assisted stepping after motor complete paraplegia: a case study. *The Lancet*, *377*(9781), 1938-1947.

Harkema, S. J., Hurley, S. L., Patel, U. K., Requejo, P. S., Dobkin, B. H., & Edgerton, V. R. (1997). Human lumbosacral spinal cord interprets loading during stepping. *Journal of Neurophysiology*, *77*(2), 797-811.

Hodgson, J. A., Roy, R. R., de Leon, R., & Dobkin, B. (1994). Can the mammalian lumbar spinal cord learn a motor task?. *Medicine & Science in Sports & Exercise*.

Hodgson, J. A., Roy, R. R., Higuchi, N., Monti, R. J., Zhong, H., Grossman, E., & Edgerton, V. R. (2005). Does daily activity level determine muscle phenotype?. *Journal of experimental biology*, *208*(19), 3761-3770.

Ichiyama, R. M., Gerasimenko, Y. P., Zhong, H., Roy, R. R., & Edgerton, V. R. (2005). Hindlimb stepping movements in complete spinal rats induced by epidural spinal cord stimulation. *Neuroscience letters*, *383*(3), 339-344.

Ichiyama, R. M., Courtine, G., Gerasimenko, Y. P., Yang, G. J., van den Brand, R., Lavrov, I. A., ... & Edgerton, V. R. (2008). Step training reinforces specific spinal locomotor circuitry in adult spinal rats. *The Journal of Neuroscience*, *28*(29), 7370-7375.

Ivashko, D. G., Prilutsky, B. I., Markin, S. N., Chapin, J. K., & Rybak, I. A. (2003). Modeling the spinal cord neural circuitry controlling cat hindlimb movement during locomotion. *Neurocomputing*, *52*, 621-629.

Iwahara, T., Atsuta, Y., Garcia-Rill, E., & Skinner, R. D. (1991). Locomotion induced by spinal cord stimulation in the neonate rat in vitro. *Somatosensory & Motor Research*, *8*(3), 281-287.

Jacobs, B. L., & Fornal, C. A. (1993). 5-HT and motor control: a hypothesis.*Trends in neurosciences*, *16*(9), 346-352.

Jacobsen, E., & Lyons, R. (2003). The sliding DFT. *Signal Processing Magazine, IEEE*, *20*(2), 74-80.

Jankowska, E., Jukes, M. G. M., Lund, S., & Lundberg, A. (1967). The Effect of DOPA on the Spinal Cord 6. Half-centre organization of interneurones transmitting effects from the flexor reflex afferents. *Acta Physiologica Scandinavica*, *70*(3-4), 389-402.

Kiehn, O., & Butt, S. J. (2003). Physiological, anatomical and genetic identification of CPG neurons in the developing mammalian spinal cord.*Progress in neurobiology*, *70*(4), 347.

Kjaerulff, O., & Kiehn, O. (1996). Distribution of networks generating and coordinating locomotor activity in the neonatal rat spinal cord in vitro: a lesion study. *The Journal of Neuroscience*, *16*(18), 5777-5794.

Kruse, M. N., Belton, A. L., & De Groat, W. C. (1993). Changes in bladder and external urethral sphincter function after spinal cord injury in the rat. *American Journal of Physiology-Regulatory, Integrative and Comparative Physiology*,*264*(6), R1157-R1163.

Lavrov, I., & Cheng, J. (2004). Activation of NMDA receptors is required for the initiation and maintenance of walking-like activity in the mudpuppy (Necturus Maculatus). *Canadian journal of physiology and pharmacology*, *82*(8-9), 637-644.

Lavrov, I., & Cheng, J. (2008). Methodological optimization of applying neuroactive agents for the study of locomotor-like activity in the mudpuppies (< i> Necturus maculatus</i>). *Journal of neuroscience methods*, *174*(1), 97-102.

Lavrov, I., Dy, C. J., Fong, A. J., Gerasimenko, Y., Courtine, G., Zhong, H., ... & Edgerton, V. R. (2008). Epidural stimulation induced modulation of spinal locomotor networks in adult spinal rats. *The Journal of Neuroscience*, *28*(23), 6022-6029.

Lavrov, I., Gerasimenko, Y. P., Ichiyama, R. M., Courtine, G., Zhong, H., Roy, R. R., & Edgerton, V. R. (2006). Plasticity of spinal cord reflexes after a complete transection in adult rats: relationship to stepping ability. *Journal of neurophysiology*, *96*(4), 1699-1710.

Lavrov, I., Courtine, G., Dy, C. J., Van Den Brand, R., Fong, A. J., Gerasimenko, Y., ... & Edgerton, V. R. (2008). Facilitation of stepping with epidural stimulation in spinal rats: role of sensory input. *The Journal of Neuroscience*, *28*(31), 7774-7780.

Maegele, M., Müller, S., Wernig, A., Edgerton, V. R., & Harkema, S. J. (2002). Recruitment of spinal motor pools during voluntary movements versus stepping after human spinal cord injury. *Journal of neurotrauma*, *19*(10), 1217-1229.

Maggi, C. A., Santicioli, P., & Meli, A. (1986). The nonstop transvesical cystometrogram in urethane-anesthetized rats: a simple procedure for quantitative studies on the various phases of urinary bladder voiding cycle.*Journal of pharmacological methods*, *15*(2), 157-167.

Manzano, G., & McComas, A. J. (2004). Longitudinal structure and innervation of two mammalian hindlimb muscles. *Muscle & nerve*, *11*(11), 1115-1122.

Pfurtscheller, G., Müller, G. R., Pfurtscheller, J., Gerner, H. J., & Rupp, R. (2003). 'Thought'–control of functional electrical stimulation to restore hand grasp in a patient with tetraplegia. *Neuroscience letters*, *351*(1), 33-36.

Musienko, P. E., Bogacheva, I. N., & Gerasimenko, Y. P. (2007). Significance of peripheral feedback in the generation of stepping movements during epidural stimulation of the spinal cord. *Neuroscience and behavioral physiology*, *37*(2), 181-190.

Musienko, P., van den Brand, R., Märzendorfer, O., Roy, R. R., Gerasimenko, Y., Edgerton, V. R., & Courtine, G. (2011). Controlling specific locomotor behaviors through multidimensional monoaminergic modulation of spinal circuitries. *The Journal of Neuroscience*, *31*(25), 9264-9278.

Musienko, P., Courtine, G., Tibbs, J. E., Kilimnik, V., Savochin, A., Garfinkel, A., ... & Gerasimenko, Y. (2012). Somatosensory control of balance during locomotion in decerebrated cat. *Journal of neurophysiology*, *107*(8), 2072-2082.

Nandra, M. S., Lavrov, I. A., Edgerton, V. R., & Tai, Y. C. (2011, January). A parylene-based microelectrode array implant for spinal cord stimulation in rats. In *Micro Electro Mechanical Systems (MEMS), 2011 IEEE 24th International Conference on* (pp. 1007-1010). IEEE.

Nelson, S. G., & Mendell, L. M. (1978). Projection of single knee flexor Ia fibers to homonymous and heteronymous motoneurons. *Journal of neurophysiology*,*41*(3), 778-787.

Peyronnard, J. M., & Charron, L. (1983). Decreased horseradish peroxidase labeling in deafferented spinal motoneurons of the rat. *Brain research*, *275*(2), 203-214.

Potter, P. J. (2006). Disordered control of the urinary bladder after human spinal cord injury: what are the problems?. *Progress in brain research*, *152*, 51-57.

Rivero-Melián, C. (1998). Organization of hindlimb nerve projections to the rat spinal cord: a choleragenoid horseradish peroxidase study. *The Journal of comparative neurology*, *364*(4), 651-663.

Rodger, D. C., & Tai, Y. C. (2005). Microelectronic packaging for retinal prostheses. *Engineering in Medicine and Biology Magazine, IEEE*, *24*(5), 52-57.

Rodger, D. C., Weiland, J. D., Humayun, M. S., & Tai, Y. C. (2006). Scalable high lead-count parylene package for retinal prostheses. *Sensors and Actuators B: Chemical*, *117*(1), 107-114.

Rossignol, S., Chau, C., Brustein, E., Giroux, N., Bouyer, L., Barbeau, H., & Reader, T. A. (1998). Pharmacological Activation and Modulation of the Central Pattern Generator for Locomotion in the Cata. *Annals of the New York Academy of Sciences*, *860*(1), 346-359.

Rossignol, S., & Frigon, A. (2011). Recovery of locomotion after spinal cord injury: some facts and mechanisms. *Annual review of neuroscience*, *34*, 413-440.

Roy, R. R., Hutchison, D. L., Pierotti, D. J., Hodgson, J. A., & Edgerton, V. R. (1991). EMG patterns of rat ankle extensors and flexors during treadmill locomotion and swimming. *Journal of Applied Physiology*, *70*(6), 2522-2529.

Roy, R. R., Hodgson, J. A., Lauretz, S. D., Pierotti, D. J., Gayek, R. J., & Edgerton, V. R. (1992). Chronic spinal cord-injured cats: surgical procedures and management. *Laboratory animal science*, *42*(4), 335.

Roy, R. R., Harkema, S. J., & Edgerton, V. R. (2012). Basic concepts of activity-based interventions for improved recovery of motor function after spinal cord injury. *Archives of Physical Medicine and Rehabilitation*, *93*(9), 1487-1497.

Shah, P. K., Gerasimenko, Y., Shyu, A., Zhong, H., Roy, R. R., & Edgerton, V. R. (2012). Variability in step training enhances locomotor recovery after a spinal cord injury. *European Journal of Neuroscience*.

Shik, M. L., & Orlovsky, G. N. (1976). Neurophysiology of locomotor automatism. *Physiological reviews*, *56*(3), 465-501.

Thuret, S., Moon, L. D., & Gage, F. H. (2006). Therapeutic interventions after spinal cord injury. *Nature Reviews Neuroscience*, *7*(8), 628-643.

van den Brand, R., Heutschi, J., Barraud, Q., DiGiovanna, J., Bartholdi, K., Huerlimann, M., ... & Courtine, G. (2012). Restoring voluntary control of locomotion after paralyzing spinal cord injury. *science*, *336*(6085), 1182-1185.

Vejsada, R., & Hnik, P. (1980). Radicular innervation of hindlimb muscles of the rat. *Physiologia Bohemoslovaca*, *29*(5), 385.

Viitasalo, J. H., & Komi, P. V. (1977). Signal characteristics of EMG during fatigue. *European journal of applied physiology and occupational physiology*,*37*(2), 111-121.

Whiting, W. C., Gregor, R. J., Roy, R. R., & Edgerton, V. R. (1984). A technique for estimating mechanical work of individual muscles in the cat during treadmill locomotion. *Journal of biomechanics*, *17*(9), 685-694.

Wolgemuth, L. (2000). Assessing the performance and suitability of parylene coating. *Medical Device and Diagnostic Industry*, *22*(8), 42-49.

Zecca, M., Micera, S., Carrozza, M. C., & Dario, P. (2002). Control of multifunctional prosthetic hands by processing the electromyographic signal.*Critical Reviews in Biomedical Engineering*, *30*(4-6), 459.